Electrochemical Investigations of Ruthenium-Substituted Heteropolytungstate Anions: Catalytic Studies of an Inorganic Oxometalloporphyrin Analog

Thesis by

John C. Bart

In Partial Fulfillment of the Requirements

for the Degree of

Doctor of Philosophy

California Institute of Technology

Division of Chemistry and Chemical Engineering

Pasadena, California

1995

(Defended August 3, 1994)

This thesis is dedicated

in memory of

Ruth Springsteen

and

Ramon Bart

Acknowledgements

There are a number of people who need to be mentioned here for their constant help and support during the past five years. First and foremost among these are my parents; without their love, support, and prayers I would not have ever made it this far. I am truly blessed to have such a loving (and fun!) family. Thanks for all the IU basketball newspaper clippings which kept me from getting homesick. Have we ever figured out how my love of science grew out of a family led by a professional musician and an English teacher? Special thanks also to my grandparents, brother, and aunts and uncles for all the mail which made it seem like I was a lot closer than 2000 miles from home.

Three teachers in my life deserve most of the credit for getting me to where I am today. The first is my high school chemistry teacher, Robert Watson. His particularly bizarre and energetic approach to teaching chemistry was entirely responsible for focusing my general interest in science towards chemistry (well, my Aunt Carol deserves some of the credit for a Christmas chemistry set given long ago). The day he retired from teaching was a sad day for Indianapolis because he was such a positive influence on many future scientists. The second person is Professor Dennis Peters, who was my advisor through 3.5 years (!!) of undergraduate research. To this day I still have no idea how he could pick one person out of a freshman chemistry class of hundreds and turn him or her into a future Ph.D. chemist, but he seems to be able to do it all the time. Without his guidance and constant encouragement, I probably never would have pursued a Ph.D. and would still think that electrochemistry was limited to a piece of zinc and copper stuck in a lemon! Finally, Professor Fred Anson deserves much credit for keeping me motivated during those hard times that occur in every project and gently pointing me in the right direction whenever my research would start wandering. I am not sure how he was able to be both an advisor to a lab full of enthusiastic students and the chairman of the largest division on campus, but he performed each job admirably, which is a testament to his hard work and dedication to Caltech.

I would be remiss if I didn't acknowledge all my peers down in the trenches who helped me out through the years. Dr. David Conrad was one of the most valuable of these. During my early Caltech years, he taught me all the inorganic chemistry that I know and never grew tired of my questions, and in the past few months he has taught me the value of "networking." Thanks Dave! David's right-hand man during my first two years was Dr.

Bryan Balazs, a fellow graduate student who was not only a big help in the lab, but was also a great cook for those weekend "feed sessions" and generally a great guy that wouldn't allow chemistry to stand in the way of a good time. Dr. Beat Steiger was a valuable asset anytime I attempted to exercise my weak synthetic abilities; he was always ready with advice on which of the hundreds of details I failed to incorporate into my prep (they are *never* in the literature because "everyone knows that"). He is also responsible for my having been to nearly every hamburger joint within a ten mile radius of campus. Without the help I received from Dr. Chaoying Rong concerning the synthesis heteropolytungstates, I'd probably still be back in the lab trying to figure out how to make my catalyst, so he deserves many thanks. Mark Fraley got me interested in mountain biking as an escape from lab (very important!), and then would shame me by getting out for rides while I slept. I hope we can stay friends as we head for our respective jobs. Very special kudos go out to David Hall, my best friend since junior high. Thanks to the miracle of e-mail, we have been able to keep each other going by swapping "horror" stories from the lab. I'm still not sure who had the most traumatic experience, but they all seem worth it now (C'mon Dave, I've done it. You can too!).

In this limited space, I must now thank all the staff of the Chemistry Department. Everyone deserves credit for their indispensable aid, but a couple really stand out. Dian Buchness for walking me through the mounds of paperwork needed to get a Ph.D. and for calling with all those offers of free dinners and lunches. Tom Dunn should get a medal for keeping all the equipment and computers in our lab running. I'm sure that few people think to mention Paul Carroad and Chris Smith, but without their talents the entire department would come to a crashing halt. Finally, Fenton Harvey was a godsend (Hallelujah!!!) with helping us teach all the youngsters in Chem 15. We sure had a special group of TA's last year. By the way, you're still trailing Marilena in my polls, but it's a close race. Too bad we never got a chance to go out into the desert so I could show you how a true Hoosier goes "muddin'" in his truck! You are an OK guy for a biologist who never saw Jimi Hendrix live in concert.

Well, I should wrap this up and get down to business, so I'll close by expressing my apologies to everyone that didn't get mentioned specifically above. I am in debt to every past and present member of the Anson Group for their insightful comments that were so helpful in bringing my project to a fruitful completion. A heartfelt "Thanks" to you all!

Abstract

Ruthenium-substituted heteropolytungstate anions (Ru-HPAs), such as $Cs_4PRu(OH_2)W_{11}O_{39}$, are expected to be catalytically active for reactions such as the oxidation of alcohols. Since little is known about this compound, several studies were undertaken so as to better understand its chemical and electrochemical properties.

Ligand exchange of nitrogen bases like pyridine for the water molecule bound to the ruthenium center confirmed an earlier report that the polyoxotungstate cage acts as a weak π-electron acceptor. When this action is taken into account, the physical properties of the ruthenium-nitrogen base complexes and the rate constants for their formation are comparable to other Ru^{II} species such as $Ru(NH_3)_5(OH_2)^{2+}$.

Electron transfer studies between Ru^{II}-HPA and $Co(C_2O_4)_3^{3-}$ are complicated by the fact that the cage species does not act as a point charge, and thus rate constant calculations based on simple ionic strength equations are not accurate. Switching the oxidant to a neutral compound like dioxygen greatly simplifies the reaction conditions, so that the Marcus equation for outer sphere electron transfer can be used to precisely predict the electron transfer rate constant.

Rate constants for the catalytic oxidation of various alcohols by Ru^{V}-HPA have been measured. The magnitude of these rate constants was much smaller than initial expectations, but not unusually so compared to other oxoruthenium (V) catalysts which have been described in the literature since this project began. Work in which Ru-HPA was used to catalyze the oxidation of non-alcoholic substrates is also discussed. Lessons learned from this project are analyzed in the context of general catalysis of oxidation reactions and thoughts on the next generation of catalysts are presented.

Table of Contents

List of Figures

Chapter 1

Chapter 2

List of Figures (cont'd)

Chapter 3

Chapter 4

List of Figures (cont'd)

List of Tables

Chapter 2

Chapter 3

Chapter 4

Chapter One

Introduction to Heteropolytungstates

1.1 *Introduction*

The search for efficient, non-polluting sources of energy is becoming increasingly important as society begins to understand the negative effects that burning fossil fuels has on the environment. Nuclear power promised to provide a source of clean, cheap electricity, but that technology is potentially quite hazardous to the environment too, as witnessed by well-publicized reactor accidents in the United States[1] and the former Soviet Union.[2] Furthermore, the problem of disposing of or recycling tons of highly radioactive waste is still one of the main drawbacks of this technology. One of the more promising sources of "pollution-free" electricity for the next century is the fuel cell, an electrochemical device which efficiently converts chemical energy into electrical energy.[3] There are many different variations on the fuel cell currently being investigated, including the solid oxide fuel cell (SOFC),[4] the phosphoric acid fuel cell (PAFC),[5] the molten carbonate fuel cell (MCFC),[6] and the alkaline fuel cell (AFC).[7] Each has certain qualities which make it attractive, but all of these proposed fuel cells also have areas where much improvement is needed before widespread commercialization of this technology is possible. For the purposes of this study, we will concentrate solely on catalysts applicable to the PAFC. The general requirements needed for a catalyst to be effective in a PAFC are long-term stability in 85% phosphoric acid and tolerance of temperatures up to 200 ^{o}C. Beyond these simple needs, the catalyst must be capable of running at a high turnover rate for months without any significant poisoning or deactivation, convert the fuel to its most oxidized form, be easily immobilized on a high surface area electrode so loss of catalyst can be minimized, and do all of this under the mildest of conditions so that the chemical-to-electrical energy conversion proceeds as efficiently as possible.

In order to produce an efficient fuel cell, there are many problems which must be overcome. The two main ones which concern chemists are: the large overpotentials often needed to drive a reaction (for example: dioxygen is reduced at a Nafion-coated edge-plane graphite electrode at about -0.45 V vs. SCE, nearly 1.5 V more negative than the theoretical reduction potential)[8] and slow reaction kinetics. One way to overcome these problems is to employ noble metals,[9] or alloys which contain noble metals,[10] as electrodes. These electrodes can offer either high catalytic activity or good resistance towards poisoning, but rarely both. Another strategy is to employ a transition metal complex which will be used to both shuttle electrons between the electrode and substrate and to activate the fuel so that the reaction goes more quickly than at bare electrodes. Over the past 15 years, great effort has been expended to create catalysts which will convert dioxygen to water as close to the theoretical limit as possible.[8,11] These catalysts, especially the ones based on transition metal porphyrins, are becoming rather successful and may soon find use in the cathodic compartment of a fuel cell. Unfortunately, research has not progressed as quickly on the development of oxidation catalysts.[12]

1.2 *Historical Background*

12-Phosphotungstic acid ($H_3PW_{12}O_{40}$) is a nearly spherical tungsten-oxo cluster which is assembled around a central phosphate anion (Figure 1.1) in a structure known as a Keggin ion.[13] If one of the tungsten atoms in 12-phosphotungstic acid is removed from the cage, along with its terminally-bound oxo group, a similar compound called a "lacunary ion"[14] ($K_7PW_{11}O_{39}$) is produced. This lacunary ion has five oxides which used to be bound to the tungsten atom, but which are now uncoordinated and are conveniently in the proper geometry to form 5/6^{ths} of an octahedron (Figure 1.2). In

Figure 1.1 Stick model[33] of a compound having the general formula $XM_{12}O_{40}^{n-}$ (Keggin ion) showing the individual metal-oxo octahedra (solid lines) and the central XO_4 tetrahedron (dashed lines).

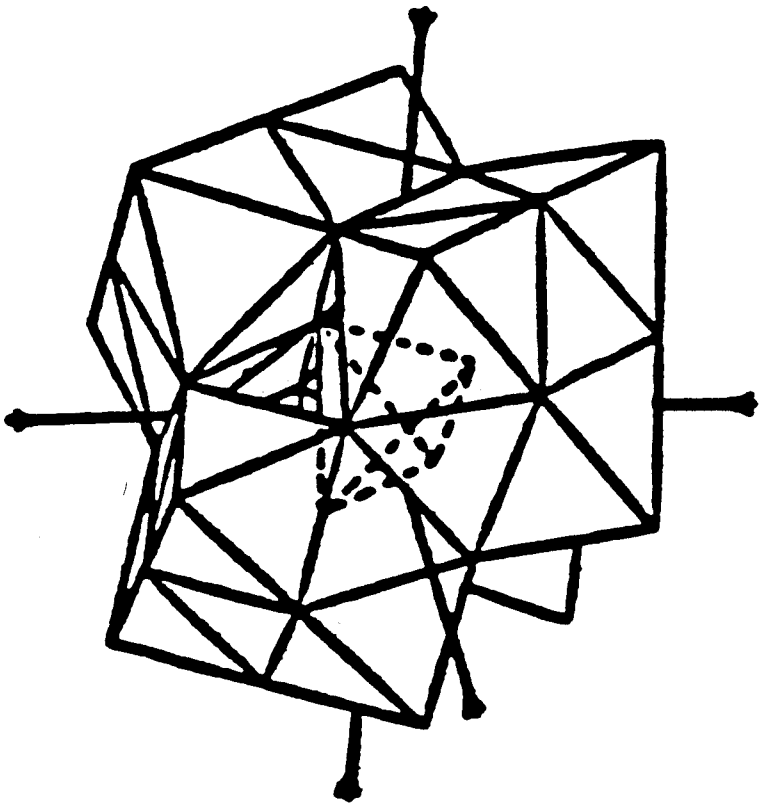

Figure 1.2 Lacunary ion ($XW_{11}O_{39}^{n-}$) structure. The large open circles are the tungsten atoms, the small open circles the oxygens, the filled circle is the heteroatom, X, and the hatched circles are the oxides which form the open binding site. Artwork taken from ref. 30b with minor modifications.

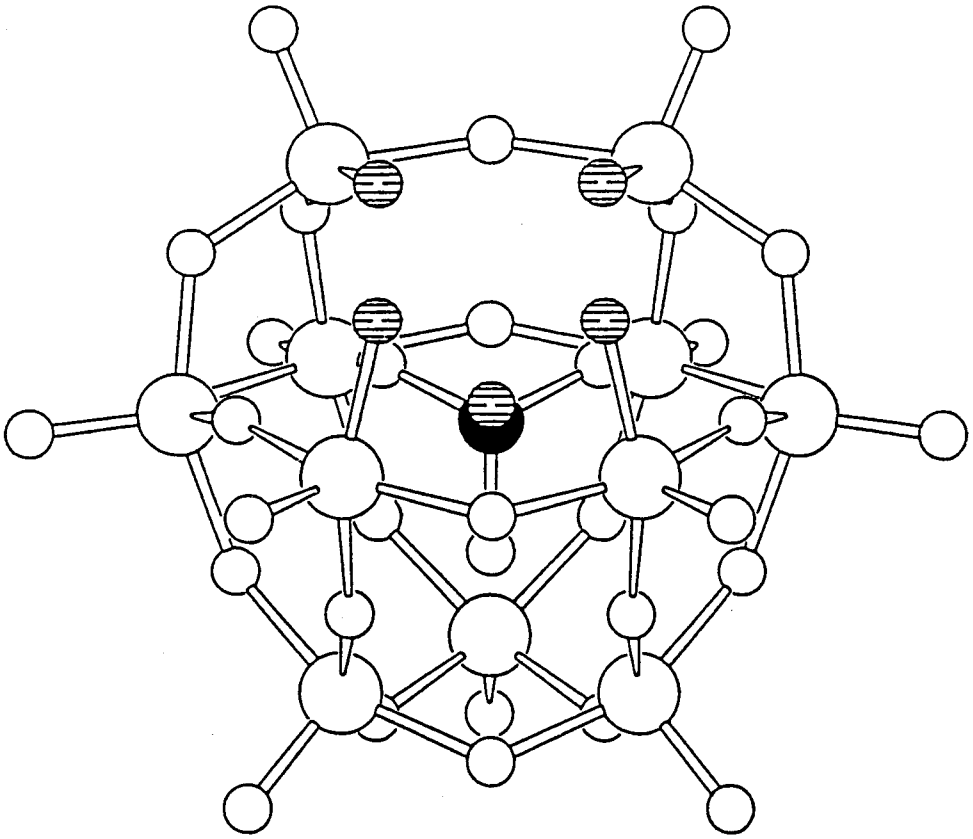

1966, Baker *et al.*[15] first reported the synthesis of a Keggin ion in which the "hole" of the lacunary ion was filled by a transition metal other than tungsten. Soon, procedures were published for a variety of these transition metal-substituted heteropolytungstate anions (HPA's), including metals such as Fe,[16,17] Rh,[17] Co,[18] Ni,[18] Cu,[19] Mn,[19] Re,[20] and Cr.[21] Unfortunately, these compounds were little more than synthetic novelties until the mid-1980's when it was discovered that the unsubstituted $PW_{12}O_{40}^{3-}$ and its lacunary ion (and related compounds where the central phosphorus atom is replaced by another tetrahedral heteroatom such as Si, As, or Ge) were active both as photocatalysts[22] and as electrocatalysts.[23] During this same period of time, it became evident that the transition metal catalysts containing organic ligands such as porphyrins or macrocyclic amines, which had been developed over the past decade as man-made models of very efficient biochemical systems, had a potentially fatal flaw. Although these systems often possessed excellent catalytic properties, they occasionally suffered from problems of decomposition. If during the course of catalysis there is a pathway by which radicals are produced, even if only a tiny fraction of the overall product yield, these high-energy intermediates eventually attack the organic ligand(s) surrounding the metal center and destroy the complex. People soon began to realize that transition metal-substituted HPA's were similar to these organometallic compounds, but with the important difference being that they are very resistant to oxidative attack by radicals since they are completely inorganic and all of the tungsten atoms are already fully oxidized. Some went as far as to christen transition metal-substituted HPA's as inorganic "porphyrin analogs."[24]

1.3 *Transition Metal-substituted Heteropolytungstate Catalysts*

The robust nature of HPA-based catalysts was proven by Toth and co-workers,[25] who demonstrated that $SiFeW_{11}O_{39}^{5-}$ could catalyze the reduction of hydrogen peroxide

(by a mechanism where hydroxyl radicals are known to be produced) without any detectable decomposition of the tungsten-oxo framework. Another advantage that these catalysts have is that they will readily perform multielectron transfers. This is due to the fact that the transition metal center is not the only electroactive element of the catalyst; the tungsten-oxo cage itself can also be electrochemically reduced by up to four electrons. Thus the metal center can act as a bridge between the substrate and the cage, binding the reactant and then either reducing it with electrons stored in the cage, or perhaps oxidizing it by funneling electrons into the polyoxotungstate "electron sink." Toth and Anson[26] illustrated this property in their investigation of the electrocatalytic reduction of nitrite by $SiFeW_{11}O_{39}^{5-}$. They found that the Fe-HPA catalyzed the production of ammonia (a net six electron reduction) from nitrite by a mechanism which involves concerted, multielectron transfer(s). The byproduct hydroxylamine, which arises from the incomplete reduction of the substrate, was not detected as it is for other catalysts,[27] even though the Fe-HPA system operates at a more positive potential.

Heteropolytungstates also have several other beneficial properties, such as the ease in which they can be synthesized. The lacunary ion, for example, can be made by simply dissolving the heteroatom source (i.e., Na_2SiO_3 if the heteroatom is to be silicon) and sodium tungstate in hot water in a ratio of 1:11 and then adjusting the pH so that the proper number of protons are present to balance the equation (1). In an hour or two, the

$$Na_2SiO_3 + 11Na_2WO_4 + 16HCl \longrightarrow Na_8SiW_{11}O_{39} + 16NaCl + 8H_2O \quad (1)$$

cage has fully assembled itself and is ready for insertion of the catalytic transition metal into its cavity.[28] Because the synthesis of the heteropolyanion is pH driven, it is found that the cage is most stable in acidic solutions. This stability in strong acids makes transition metal-substituted heteropolytungstates good candidates for use in PAFC's, where the ability to withstand concentrated acids at elevated temperatures is a primary requirement. Finally, the electrochemical properties of the catalyst can be "fine-tuned"

without changing the exterior surface of the complex. This is accomplished by varying the nature of the heteroatom in the center of the cage. For example, the potential of the $Fe^{III/II}$ wave for $XFeW_{11}O_{39}^{n-}$ varies from -0.145 to -0.065 to 0.039 to 0.123 V when X = Si, Ge, P, and As, respectively. This could be a very attractive property in tailoring the catalyst for a particular substrate. Although transition metal substituted HPA's were first used as reduction catalysts, they have been tested in performing oxidations (and also in more novel areas such as an anti-viral agent against the AIDS virus[29]) in more recent times. The problem with these studies is that they have involved reactions which are not applicable for use in a fuel cell, such as the oxidation of activated alkenes[30,31] or in organic syntheses where an oxo transfer from the transition metal-substituted heteropolytungstate to a hydrocarbon substrate occurs.[24,32]

1.4 *Ruthenium-substituted Heteropolytungstate Background*

The goal of my research was to see if the success in our lab[25,26] using the Fe-HPA as a multielectron reduction catalyst could be carried over to oxidation catalysis by changing the catalytic center to a metal such as chromium or ruthenium which would be capable of being oxidized to a high-valent, metal-oxo state. At this time, there was only one brief communication[21] published about $XCrW_{11}O_{39}^{n-}$ and none concerning the Ru-HPA (see Figure 1.3). After nine months of study, the Cr-HPA was determined to be unworthy of further investigation since there were no electrochemically accessible oxidation states beyond Cr^{III}. This decision was also spurred by the fact that Neumann[30a] had just published a simple synthesis of $SiRuW_{11}O_{39}^{5-}$ and showed that it could catalyze the oxidation of alkenes by various chemical oxidants. Unfortunately, the electrochemistry of the Ru-HPA synthesized by the Neumann method[30a] was quite poor, consisting mainly of two irreversible oxidation waves and an irreversible reduction. No

Figure 1.3 The structure of $PRu(L)W_{11}O_{39}^{4-}$. The symbology is the same as in Figure 1.2 and L is generally a molecule of water.

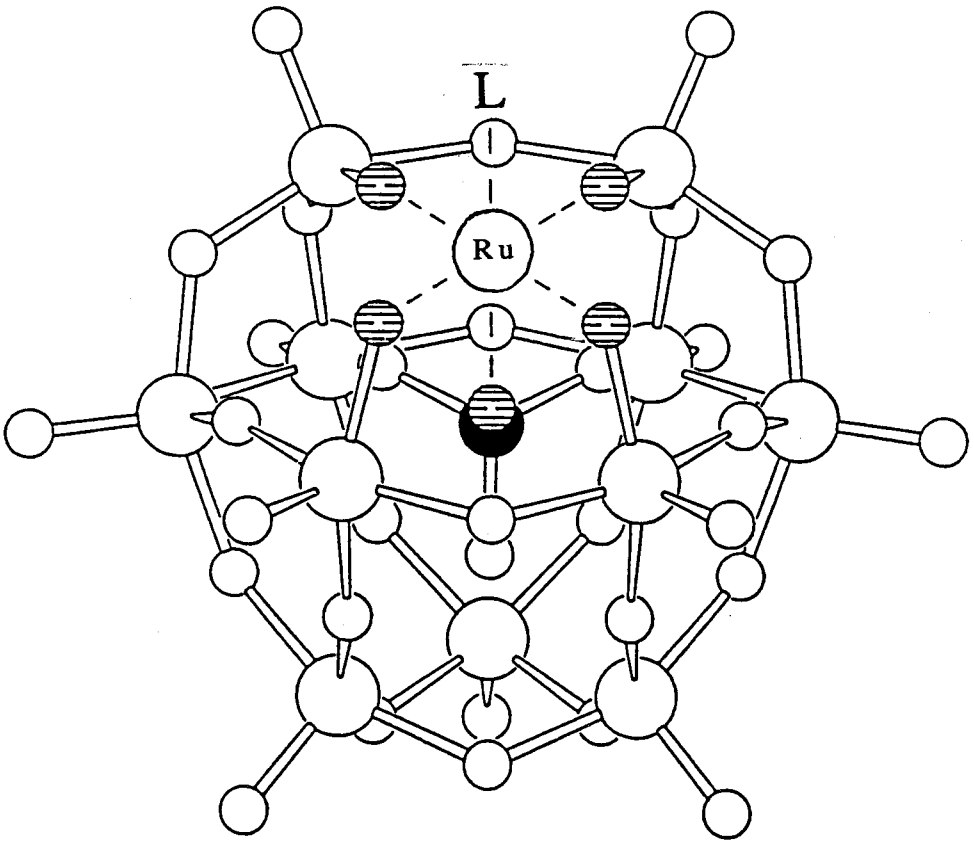

evidence of the reversible tungsten-oxo reduction peaks was ever observed, as the compound is apparently a decent proton reduction catalyst. By improving the synthesis, it was possible to isolate a compound which analyzed as $K_5SiRuW_{11}O_{39}$ and had reversible one electron waves in the potential range where we would expect the $Ru^{III/II}$ and $Ru^{IV/III}$ couples to occur. Again, the electrochemistry associated with the reduction of the tungsten-oxo cage was not seen as proton reduction occurred at more positive potentials. As studies progressed on this catalyst, it was learned that the Pope group at Georgetown was working on the phosphorus version, $PRuW_{11}O_{39}^{4-}$, and found that it had much better electrochemistry than the silicon compound: not only could both of the two electron cage reductions be seen, but also reversible $Ru^{III/II}$, $Ru^{IV/III}$, and $Ru^{V/IV}$ peaks (Figure 1.4). Since the phosphorus version of Ru-HPA had higher oxidation states electrochemically accessible, research on the silicon complex was soon dropped in favor of the phosphorus-based catalyst, and all the studies reported in this thesis were done using $PRuW_{11}O_{39}^{4-}$.

It is perhaps not surprising that in the trade-off for getting vastly improved electrochemistry, a more difficult synthesis is required. While the procedure used was the same as in the literature,[30b] it is quite a tricky reaction and there are some details worth mentioning here. Initially, the product is collected as the cesium salt because this counterion was determined to be the best at precipitating the HPA from the reaction mixture, and yet still being moderately soluble. Unfortunately, this compromise means that the product can only be redissolved to a concentration of about 1 mM in aqueous media. If a more concentrated solution is needed, it is best to stir the salt in the desired solvent containing a cation exchange resin (such as Amberlite IR-120, Li^+ form). The ruthenium heteropolytungstate seems to be most soluble when the counterion is lithium; even the sodium salt is much less soluble. In conjunction with the counterion identity, there are several ways in which the solubility can be seriously affected during the

Figure 1.4 A cyclic voltammogram of 0.68 mM $Cs_4PRu(OH_2)W_{11}O_{39}$ in pH = 2.0, sulfate buffer (μ = 0.90 M) at a scan rate of 50 mV s^{-1} using an edge-plane graphite electrode.

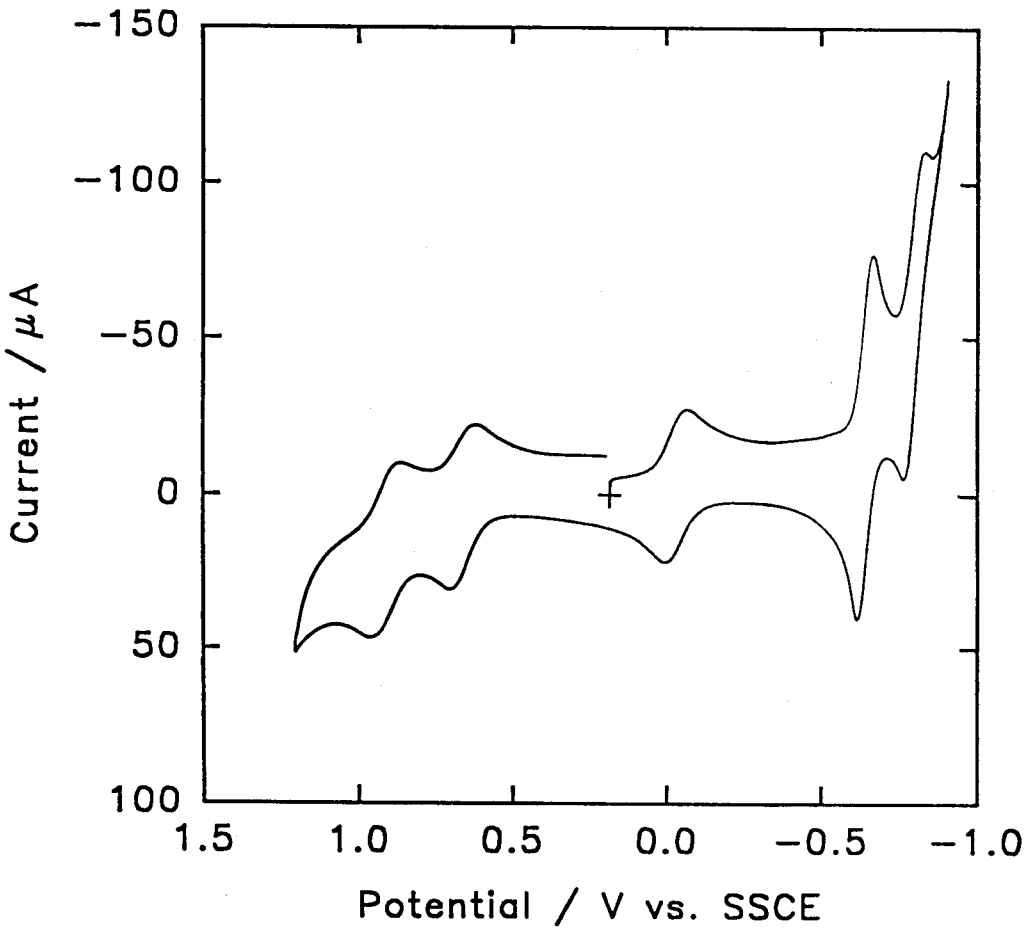

synthesis. Anything which dehydrates the product, such as washing the collected salt with ethanol and ether or drying the salt in a vacuum oven at elevated temperature, will have an extremely detrimental effect on the rate of dissolution of the heteropolyanion. The best way to collect the product is to filter off the reaction solution, wash the solid with water, and then cover the funnel with a watchglass and let the salt slowly dry over the next few days. It is also important to keep the reaction temperature at or above 100 ^{o}C, as it has been found that the yield of the reaction decreases with temperature. One of the most likely impurities in this synthesis is $Ru(OH_2)_6^{3+}$ which becomes oxidized before entering the lacunary cage. Since the Ru^{III} salt is considerably less substitutionally labile than the reduced species, this complex will remain in the reaction solution and not enter the lacunary ion. In order to remove this and other cationic impurities, the Rong[30b] procedure was modified slightly. After oxidation of the Ru-HPA by dioxygen, but before the precipitation of the product by addition of CsCl, the entire reaction mixture is passed down a column containing a cation exchange resin (SP-Sephadex C-25, Na^+ form). The anionic Ru-HPA passes quickly through the column, but any unreacted ruthenium salts are trapped.

Although electrochemistry is the most common method of analysis used in this thesis, it was occasionally beneficial to be able to monitor reactions spectroscopically. In its air-stable Ru^{III} state, the heteropolytungstate is dark brown and has no significant absorbance maxima in the visible spectrum. The one electron reduced species, $PRu^{II}W_{11}O_{39}^{5-}$, is dark pink-purple and has a d-d transition at 530 nm with an ε of 2200 M^{-1} cm^{-1} (Figure 1.5). Comparison of the Ru^{III} and Ru^{II} forms of the HPA clearly illustrate the presence of the broad underlying $Ru^{II} \longrightarrow W^{VI}$ charge transfer band described by Rong.[30b] This feature begins in the visible, but reaches well into the near-infrared spectrum. The spectra of the oxidized Ru^{IV} species is not distinguishable from that of Ru^{III}, even though the solution color appears different from the Ru^{III} compound.

Figure 1.5 The UV-visible spectra for 0.35 mM $PRu(OH_2)W_{11}O_{39}^{n-}$ in pH = 2 sulfate buffer (μ = 0.90 M) for the Ru^{III} and Ru^{II} oxidation states.

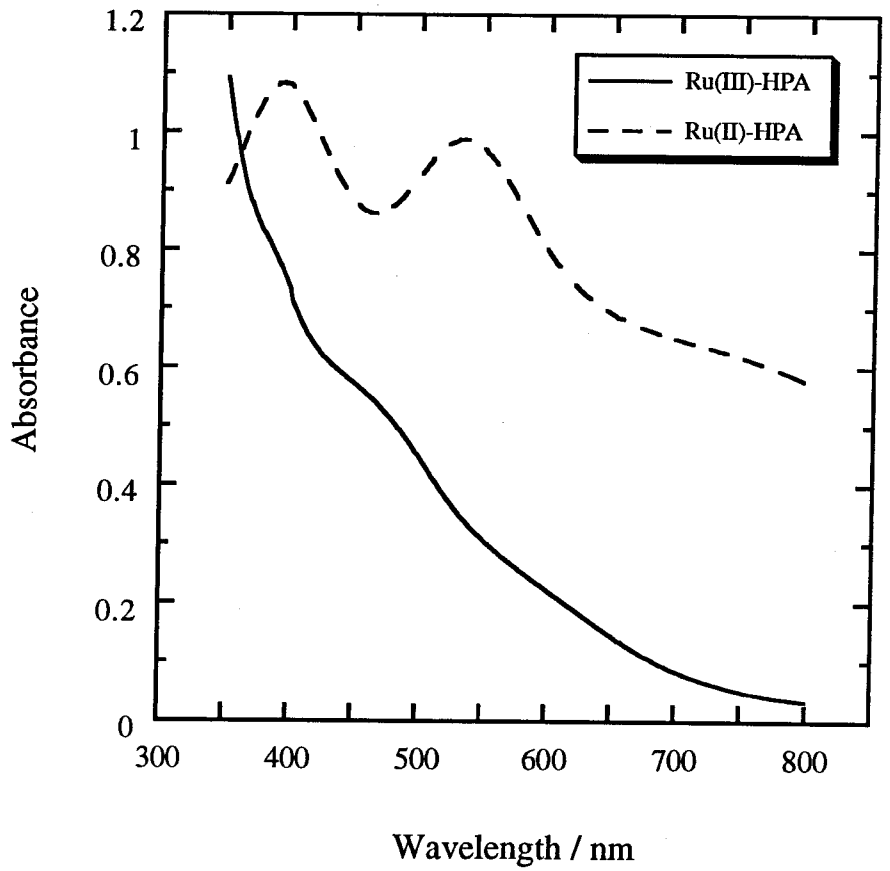

This may be because the Ru-HPA is not completely stable at oxidation states higher than Ru^{III}, so that over the course of time needed for a bulk electrolysis, some of the Ru^{IV} is probably reduced by water or some other adventitious reductants present as impurities in the buffer solution.

1.5 *Thesis Outline*

This thesis is organized into two main parts: the study of the chemistry of ruthenium bound inside the pentadentate $PW_{11}O_{39}^{7-}$ ligand, and the ability of this compound to act as an electrocatalyst for the oxidation of a variety of organic and inorganic substrates. Chapter 2 describes the ability of ruthenium in the cage to undergo coordination chemistry by exchanging the molecule of water in the sixth ligand site on the ruthenium metal center for a nitrogen base such as pyridine. Probing the chemistry of ruthenium and its bond to this ligand in the sixth coordination site should yield information which will be useful when studying the mechanism of substrate binding and catalysis. The topic of Chapter 3 concerns measuring the heterogeneous and homogeneous electron transfer rate constants for the oxidation of Ru^{II}-HPA. This study may help predict whether or not the ruthenium center will be a good catalytic site by providing details on the rate of electron transfer. All of the oxidation studies done using Ru-HPA as an electrocatalyst are detailed in Chapter 4. This work will include both model compounds (easily oxidized, but not feasible for use in a fuel cell) and actual fuel cell substrates such as methanol. Throughout this thesis, a common theme will continue to appear: that despite the fact that the ruthenium center is surrounded by this rather exotic metal-oxo cluster, its chemistry deviates from that of more common ruthenium compounds (such as $Ru(NH_3)_6^{3+}$ or $Ru(edta)(OH_2)^-$) in a simple, logical fashion.

References

1. a) *The Three Mile Island Nuclear Accident: Lessons and Implications*; Moss, T. H., Sills, D. L., Eds.; New York Academy of Sciences: New York, 1981.
   b) Stephens, M. *Three Mile Island*; Random House: New York, 1980.

2. a) Chernousenko, V. M. *Chernobyl, Insight from the Inside*; Springer-Verlag: Berlin, 1991.
   b) Marples, D. R. *Chernobyl and Nuclear Power in the USSR*; St. Martin Press: New York, 1986.

3. a) Appleby, A. J.; Foulkes, F. R. *Fuel Cell Handbook*; Van Nostrand Reinhold: New York, 1989.
   b) Anahara, R.; Yokokawa, S.; Sakurai, M. *Proc. IEEE* **1993,** *81,* 399.
   c) Fry, M. R. *IEE Proc.-A* **1993,** *140,* 40.

4. a) Liu, M. L.; Khandkar, A. *Solid State Ionics* **1992,** *52,* 3.
   b) Kirk, T. J.; Winnick, J. *J. Electrochem. Soc.* **1993,** *140,* 3494.

5. a) Mitsuda, K.; Murahashi, T. *J. Appl. Electrochem.* **1991,** *21,* 524.
   b) Stonehart, P. *Ibid.* **1992,** *22,* 995.
   c) Passalacqua, E.; Antonucci, P. L.; Vivaldi, M. *Electrochim. Acta* **1992,** *37,* 2725.

6. a) Yuh, C. Y.; Selman, J. R. *J. Electrochem. Soc.* **1992,** *139,* 1373.
   b) Plomp, L.; Veldhuis, J. B. J.; Sitters, E. F.; VanderMolen, S. B. *J. Power Sources* **1992,** *39,* 369.
   c) Tanimoto, K.; Miyazaki, Y.; Yanagida, M.; Tanase, S.; Kojima, T.; Ohtori, N.; Okuyama, H.; Kodama, T. *Ibid.* **1992,** *39,* 285.

7. a) Tomantschger, K.; Kordesch, K. V. *Ibid.* **1989,** *25,* 195.
   b) Ward, C. A.; Stanga, D.; Pataki, L. *Ibid.* **1993,** *41,* 335.
   c) Bjornbom, P.; Yang, S. C. *Electrochim. Acta* **1993,** *38,* 2599.

8. Shi, C.; Anson, F. C. *J. Am. Chem. Soc.* **1991,** *113,* 9564.

9. a) Sun, S. G.; Clavilier, J. *J. Electroanal. Chem.* **1987,** *236,* 95.
   b) Beden, B.; Juanto, S.; Leger, J. M.; Lamy, C. *Ibid.* **1987,** *238,* 323.

10. a) Beden, B.; Kadirgan, F.; Lamy, C.; Leger, J. M. *Ibid.* **1981,** *127,* 75.
    b) Hughes, V. B.; Miles, R. *Ibid.* **1983,** *145,* 87.

11. a) Kuwana, T.; Fujihara, M.; Sunakawa, K.; Osa, T. *Ibid.* **1978,** *88,* 229.
    b) Collman, J. P.; Denisevich, P.; Konai, Y.; Marrocco, M.; Koval, C.; Anson, F. C. *J. Am. Chem. Soc.* **1980,** *102,* 6027.
    c) Ni, C.-L.; Anson, F. C. *Inorg. Chem.* **1985,** *24,* 4754.
    d) Collman, J. P.; Kim, K. *J. Am. Chem. Soc.* **1986,** *108,* 1847.
    e) Toma, H. E.; Araki, K. *J. Chem. Res.* **1990,** 82.
    f) Steiger, B.; Shi, C.; Anson, F. C. *Inorg. Chem.* **1993,** *32,* 2107.

12. Parsons, R.; VanderNoot, T. *J. Electroanal. Chem.* **1988,** *257,* 9.

13. Pope, M. T. *Heteropoly and Isopoly Oxometallates*; Springer-Verlag: Berlin, 1983; p 59.

14. Ref. 13, p 93.

15. Baker, L. C. W.; Baker, V. E. S.; Eriks, K.; Pope, M. T.; Shibata, M.; Rollins, O. W.; Fang, J. H.; Koh, L. L. *J. Am. Chem. Soc.* **1966,** *88,* 2329.

16. Zonnevijlle, F.; Tourné, C. M.; Tourné, G. F. *Inorg. Chem.* **1983,** *22,* 1198.

17. Zonnevijlle, F.; Tourné, C. M.; Tourné, G. F. *Ibid.* **1982,** *21,* 2751.

18. Weakley, T. J. R.; Malik, S. M. *J. Inorg. Nucl. Chem.* **1967,** *29,* 2935.

19. Tourné, C. M.; Tourné, G. F.; Malik, S. A.; Weakley, T. J. R. *Ibid.* **1970,** *32,* 3875.

20. Ortéga, F.; Pope, M. T. *Inorg. Chem.* **1984,** *23,* 3292.

21. Katsoulis, D. E.; Pope, M. T. *J. Chem. Soc., Chem. Commun.* **1986,** 1186.

22. a) Akid, R.; Derwent, J. R. *J. Chem. Soc., Dalton Trans.* **1985,** 395.
b) Nomiya, K.; Miyazaki, T.; Maedak, M.; Miwa, M. *Inorg. Chim. Acta* **1987,** *127,* 65.
c) Combswalker, L. A.; Hill, C. L. *J. Am. Chem. Soc.* **1992,** *114,* 938.

23. a) Keito, B.; Nadjo, L. *J. Electroanal. Chem.* **1985,** *191,* 441.
b) Keito, B.; Nadjo, L. *Ibid.* **1987,** *227,* 265.
c) Keito, B.; Nadjo, L. *Ibid.* **1988,** *240,* 325.
d) Keito, B.; Nadjo, L. *Ibid.* **1990,** *287,* 149.
e) Keita, B.; Bouaziz, D.; Nadjo, L. *Electroanalysis* **1991,** *3,* 637.

24. Khenkin, A. M.; Hill, C. L. *J. Am. Chem. Soc.* **1993,** *115,* 8178.

25. Toth, J. E.; Melton, J. D.; Cabelli, D.; Bielski, B. H. J.; Anson, F. C. *Inorg. Chem.* **1990,** *29,* 1952.

26. Toth, J. E.; Anson, F. C. *J. Am. Chem. Soc.* **1989,** *111,* 2444.

27. a) Barley, M. H.; Takeuchi, K. J.; Meyer, T. J. *Ibid.* **1986,** *108,* 5876.
b) Taniguchi, I.; Nakashima, N.; Matshushita, K.; Yasukouchi, K. *J. Electroanal. Chem.* **1987,** *224,* 199.

28. Tézé, A.; Hervé, G. *J. Inorg. Nucl. Chem.* **1977,** *39,* 999.

29. Weeks, M. S.; Hill, C. L.; Shinazi, R. F. *J. Med. Chem.* **1992,** *35,* 1216.

30. a) Neumann, R.; Abu-Gnim, C. *J. Am. Chem. Soc.* **1990,** *112,* 6025.
b) Rong, C.; Pope, M. T. *Ibid.* **1992,** *114,* 2932.
c) Steckhan, E.; Kandzia, C. *Synlett.* **1992,** 139.

31. a) Kuznetsova, N. I.; Detusheva, L. G.; Kuznetsova, L. I.; Fedotov, M. A.; Likholobov, V. A. *Kinet. Catal.* **1992,** *33,* 415.
b) Mizuno, N.; Hirose, T.; Tateishi, M.; Iwamoto, M. *Chem. Lett.* **1993,** 1839.

32. a) Mizuno, N.; Tateishi, M.; Hirose, T.; Iwamoto, M. *Ibid.* **1993,** 2137.
b) Neumann, R.; Delavega, M. *J. Mol. Cat.* **1993,** *84,* 93.

33. Toth, J. E. Ph.D. thesis, California Institute of Technology, 1990.

Chapter Two

Ligand Exchange Reactions

2.1 *Introduction*

Initial studies of ruthenium-substituted heteropolytungstate anions (Ru-HPA's) were mainly concerned with characterization of the complexes and their subsequent use as oxidation and oxygen-atom transfer catalysts.[1-3] Only Rong and Pope[2] attempted any investigations into the chemical interaction between the ruthenium metal center and the pentadentate tungsten-oxo "ligand." They concluded that the HPA acts as a π-electron acceptor because: (1) the Ru^{II}-HPA $\longrightarrow$ pyridine (π^*) charge transfer band lies in between those for $Ru^{II}(NH_3)_5(py)$ (the ammine groups are not π-acceptors) and $Ru^{II}(CN)_5(py)$ (the cyanide groups are strong π-acceptors); (2) the ^{183}W NMR of the aquo version of Ru-HPA has two peaks which are shifted downfield *ca.* 300 ppm vs. other transition metal-substituted HPA's; these peaks shift upfield again when the aquo ligand is replaced by a ligand which can accept π-electron density; (3) the self-exchange rate for Ru^{II}-HPA is about five orders of magnitude greater than that for $Ru^{II}(OH_2)_6$ (where no π-backbonding is possible).[2]

There are many studies in the literature about ruthenium π-backbonding to a ligand. Some of the more well-understood complexes include $Ru^{II}(NH_3)_5L$[4] and $Ru^{II}(edta)L$[5] where L is a ligand capable of accepting π-electron density from the metal center and edta is the pentadentate ligand ethylenediaminetetraacetate (one of the carboxylate groups is not coordinated to the ruthenium center). These compounds will be used as models to which the chemistry of ruthenium which is bound to the heteropolytungstate cage can be compared. The topic of this chapter is a detailed investigation into how the HPA affects the coordination chemistry of the ruthenium center and the lability of the compound bound to its sixth coordination site.

2.2 *Experimental*

2.2.1 Syntheses

Potassium 11-tungstophosphate ($K_7W_{11}O_{39}\cdot xH_2O$) was synthesized based on the method of Tézé and Hervé[6] (for $K_8SiW_{11}O_{39}$) with the substitution of Na_2HPO_4 for Na_2SiO_3. Hexaaquoruthenium (II) *p*-toluenesulfonate, $Ru(OH_2)_6(C_7H_7SO_3)_2$, was prepared by the literature method.[7] Cesium undecatungstophospho(aqua)ruthenium (III), **1**, $Cs_4PRu(OH_2)W_{11}O_{39}\cdot 5H_2O$ was made by following the procedure of Rong and Pope[2] with the modification described in Chapter 1 of this thesis. Chloropentaammineruthenium chloride, $Ru(NH_3)_5Cl_3$, was synthesized following literature methods.[8] $Ru(Hedta)\cdot H_2O$ was prepared according to Mukaida *et al.*[9] The water used in the all of the experiments was house deionized water that had been passed through a Barnstead NANOpure purification system.

***N*-Methylpyrazinium Iodide**

A modified version of the standard literature synthesis was used to prepare this compound.[10] 4 g (49.9 mmol) of pyrazine (Aldrich) was dissolved in 5 mL (80.3 mmol) of iodomethane (Aldrich) in a 25 mL flask. A condenser capped with an argon-filled balloon was employed to avoid solvent evaporation. The flask contents were stirred constantly and the flask was kept in a thermostatted oil bath at 37 ± 1 °C. A yellow precipitate started to form almost immediately and soon the solution was so thick that stirring was inhibited, so another 5 mL portion of iodomethane was added. The reaction was allowed to proceed for one day, yielding a thick slurry of yellow product suspended in iodomethane. The excess solvent was suction filtered off using a medium glass fritted funnel and then washed with several portions of anhydrous diethyl ether to remove any residual pyrazine. The crude yellow powder was recrystallized from hot absolute ethanol

and then dried in a vacuum oven at room temperature for 2-3 hours yielding small yellow needles. Yield = 6.695 g (60.4 %).

Cesium Undecatungstophospho(pyridine)ruthenate(III)

60 mg (17.6 μmol) of **1** was dissolved in 20 mL of 0.2 M pH = 5.0 acetate buffer and electrolytically reduced by one electron per mole of complex at -0.2 V vs. SSCE. The resulting Ru(II) solution was transferred to an argon-flushed flask containing 0.3 mL (3.71 mmol) pyridine (Mallinckrodt). The flask was heated in an oil bath at *ca.* 65 °C while stirring and constantly bubbling argon through the solution. After 2-3 hours, the flask was removed from the bath and exposed to air. After the solution cooled to room temperature, the Ru^{II} center was oxidized by bubbling oxygen through the solution for 30 minutes. The product was collected by adding CsCl, cooling, and suction filtering (on a fine glass frit) the polyoxotungstate from the reaction solution. The solid was washed with water and then acetone and finally dried on the bench top. The purity was checked by cyclic voltammetry.

Cesium Undecatungstophospho(pyrazine)ruthenate(III)

72 mg (21.1 μmol) of **1** was dissolved in 35 mL of 0.2 M pH = 3.0 sulfate solution and electrolytically reduced by one electron per mole of complex at -0.2 V vs. SSCE. The resulting Ru(II) solution was transferred to an argon-flushed flask containing 0.3 g (3.75 mmol) pyrazine (Aldrich). The flask was heated in an oil bath at *ca.* 65 °C while stirring and bubbling argon through the solution. After 2-3 hours, the flask was removed from the oil bath and cooled. Dioxygen was bubbled through the solution for 30 minutes to oxidize the Ru^{II} center. The product was collected by adding CsCl to start the precipitation and then cooling the solution overnight in the refrigerator. The tan solid was separated from the solution by suction filtration (on a fine glass frit) and washed with water, acetone, and then air dried. The purity was checked by cyclic voltammetry and UV-vis spectroscopy.

Cesium Undecatungstophospho(*N*-methylpyrazinium)ruthenate(II)

This complex was prepared in a similar manner to the pyrazine complex, except for omitting the bubbling of dioxygen through the solution after the synthesis. The ruthenium center is unreactive towards oxidation by dioxygen when Mepyz is the ligand because the formal potential of the *N*-methylpyrazinium-substituted heteropolyanion is too positive.

2.2.2 Physical Measurements

Cyclic voltammetric experiments were performed using a Princeton Applied Research Corp. (PARC) Model 173 Potentiostat / Galvanostat with a PARC Model 176 current-to-voltage converter and a PARC Model 175 Universal Programmer to produce the desired waveforms. A Houston Instruments 2000-5-5 X-Y recorder was used to record the voltammograms. The working electrode was a home-built edge-plane pyrolytic graphite (EPG) electrode (Union Carbide), the auxiliary electrode was a platinum wire, and all potentials are quoted against the saturated sodium chloride calomel reference electrode (SSCE). All scan rates were 50 mV s^{-1} unless otherwise noted. All solutions were sparged with argon (5-10 minutes) before any measurements were taken and the solution was kept under a blanket of argon during the voltammetry. The argon was bubbled through two towers containing acidic vanadium(II) solutions to remove any residual dioxygen and then passed through a tower containing water before it reached the cell. Controlled potential electrolyses were done using either a Bioanalytical Systems BAS100 or BAS100B electrochemical analyzer. The working electrode was a piece of carbon cloth (Union Carbide, VCK grade) and the auxiliary electrode was a piece of platinum wire. The reference electrode was either an SSCE or a BAS Ag/AgCl reference electrode. A standard two-compartment cell was used to separate the working and auxiliary electrodes. Experiments involving oxygen-reactive Ru^{II} compounds were sometimes performed in a Vacuum Atmospheres Co. (VAC) glove box equipped with a

VAC Pedatrol pressure controller, a VAC AO 316-C oxygen analyzer, and a VAC HE-493 Dri-Train system for removal of dioxygen and water vapor from the inert gas (nitrogen) used as the atmosphere inside the box. The kinetic experiments, and all other spectroscopic measurements, were performed on a Hewlett-Packard HP8450A UV-visible spectrophotometer equipped with an HP89100A temperature controller. All experiments were done at ambient laboratory temperatures (22 ± 2 °C) unless otherwise specified.

The measurement of the ligand exchange rate constants involved the following procedure: all equipment needed to carry out the bulk electrolysis was brought into the glove box. A controlled-potential electrolysis was done to reduce the ruthenium center by one electron. The UV-vis cuvette used in these experiments is shown in Figure 2.1. The ligand, in the form of a concentrated aqueous solution, was syringed into the cuvette section while the auxiliary arm is used to contain the Ru^{II} solution. The cuvette was then sealed at the valve to keep the entire experiment under an atmosphere of virtually oxygen-free nitrogen. The cuvette was then removed from the box and a background spectrum of the glass cuvette was recorded. This was possible since the amount of ligand solution in the cuvette was generally 10-250 μL and thus was not analyzed by the spectrophotometer. The cuvette holder was thermostatted to the desired temperature for the ligand exchange and then the heteropolyanion solution was added to the ligand by tilting the cuvette. The cuvette was then placed into the holder and the kinetics monitored by watching the growth of absorbance at the proper wavelength for the product. The spectrophotometer automatically subtracted the background spectrum from each of the measurements during the experiment. The absorbance versus time curves were plotted using an HP7470A plotter and then digitized using a Logitech ScanMan Model 32 hand-held scanner, a Gateway 2000 386SX/16 computer, and Un-Scan-It (Silk Scientific Corp.). The digitized data were manipulated and graphed using SigmaPlot

Figure 2.1 Cartoon of the modified cuvette used in the ligand exchange experiments.

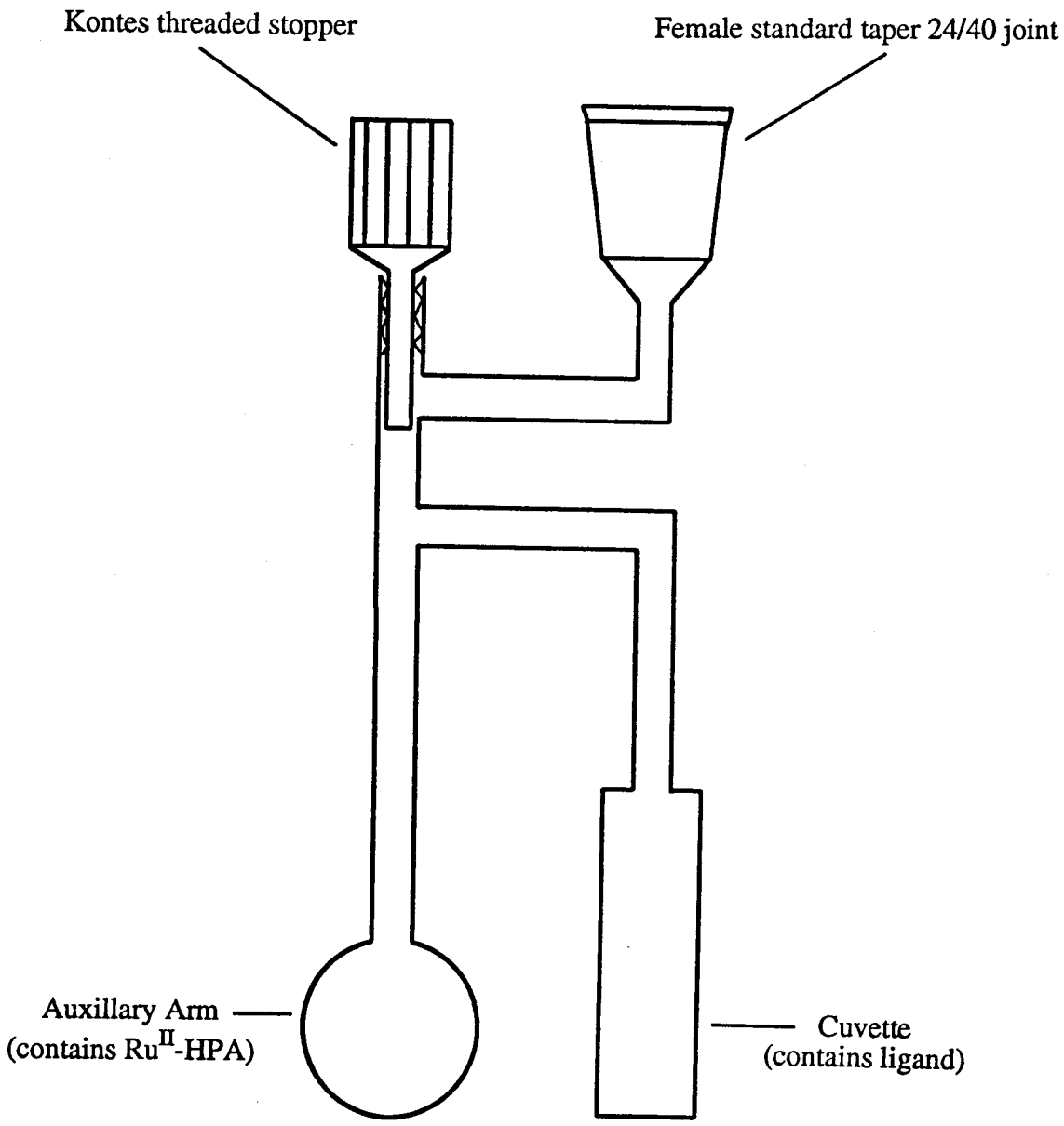

(version 5.0, Jandel Scientific). The value of the pseudo-first order rate constant, k_{obs}, was calculated from the slope of the plot of $-[\ln(A_\infty - A_{time})]$ vs. time.

2.3 *Results*

2.3.1 Ligand Exchange with Pyridine

In order to study the effect of the polyoxotungstate on the ligating properties of the ruthenium metal center, several compounds were made in which the water molecule occupying the sixth coordination site on the ruthenium was replaced by a nitrogen base. The pyridyl analogue of $PRu^{III}(OH_2)W_{11}O_{39}^{4-}$ had been previously synthesized,[2] so this seemed to be a good ligand to begin the study with. While the ligand exchange can be performed on the laboratory bench top if the proper precautions are taken to remove oxygen from the system, it was found that the kinetics experiments were more easily (and accurately) accomplished if the initial work was done in an oxygen-free glove box. The kinetic experiments were followed by monitoring the peak at 381 nm, corresponding to the formation of $PRu^{II}(py)W_{11}O_{39}^{5-}$. While this peak is only a few nanometers from the peak for the ruthenium aquo heteropolyanion (Figure 2.2), the increase in the ε upon coordination of pyridine is so large that the initial absorbance can be neglected in the evaluation of the rate constant. The kinetics experiments were performed under pseudo-first order conditions by employing a large (97 to 445) molar excess of the pyridine ligand. Plotting $\ln(A_\infty - A_t)$ versus time yielded a straight line over 4-7 half-lives with a slope of $-k_{obs}$. Figure 2.3 shows a plot of k_{obs} vs. pyridine concentration at 60 °C in pH = 5.0 acetate buffer. The slope of the line yields the second order rate constant for this ligand exchange reaction, $k = 1.1 \times 10^{-2}\ M^{-1}\ s^{-1}$. The temperature dependence of the rate constant was also investigated. An Arrhenius plot (Figure 2.4) of this data gives an activation energy of 107 kJ mol^{-1}.

Figure 2.2 UV-visible spectra (at various times) for the ligand exchange reaction of $PRu^{II}(OH_2)W_{11}O_{39}^{5-}$ with pyridine in pH = 5.0, sodium acetate buffer (μ = 0.2 M) at T = 40 °C.

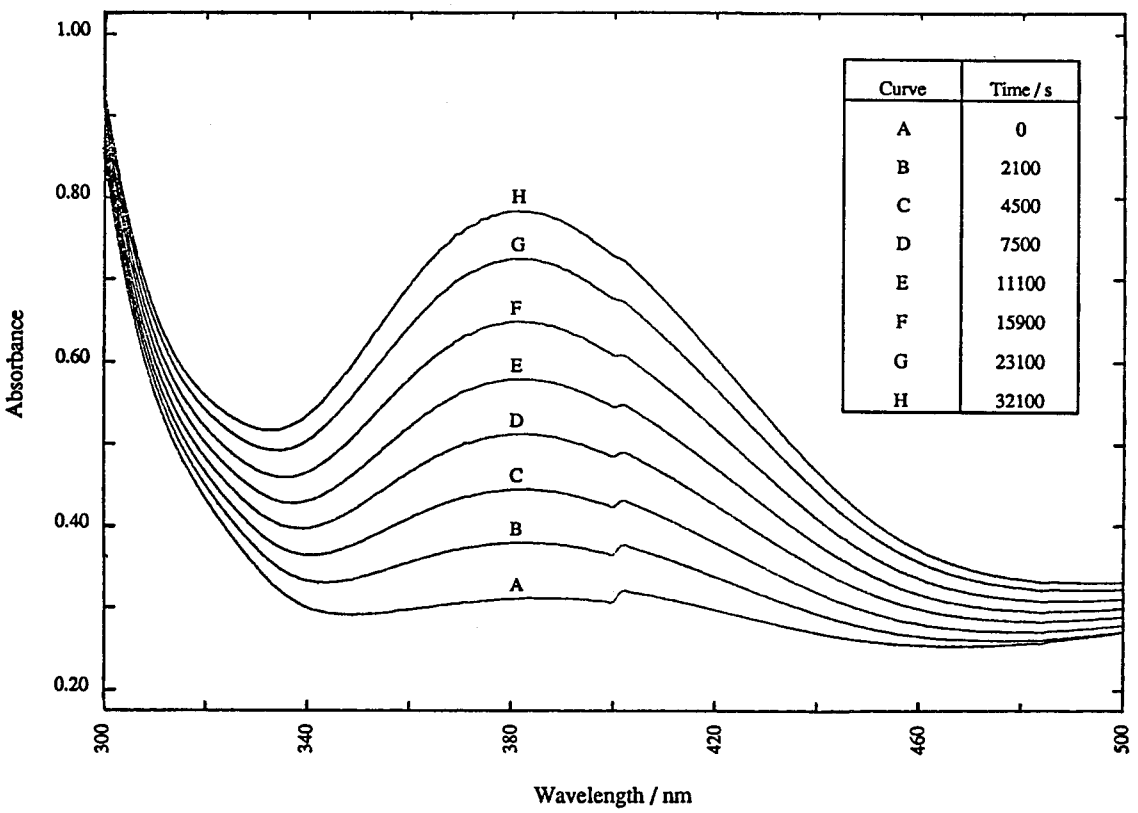

Figure 2.3 k_{obs} vs. the concentration of pyridine used in the ligand exchange experiments. All data collected in pH = 5.0, sodium acetate buffer (μ = 0.2 M) at T = 60 °C.

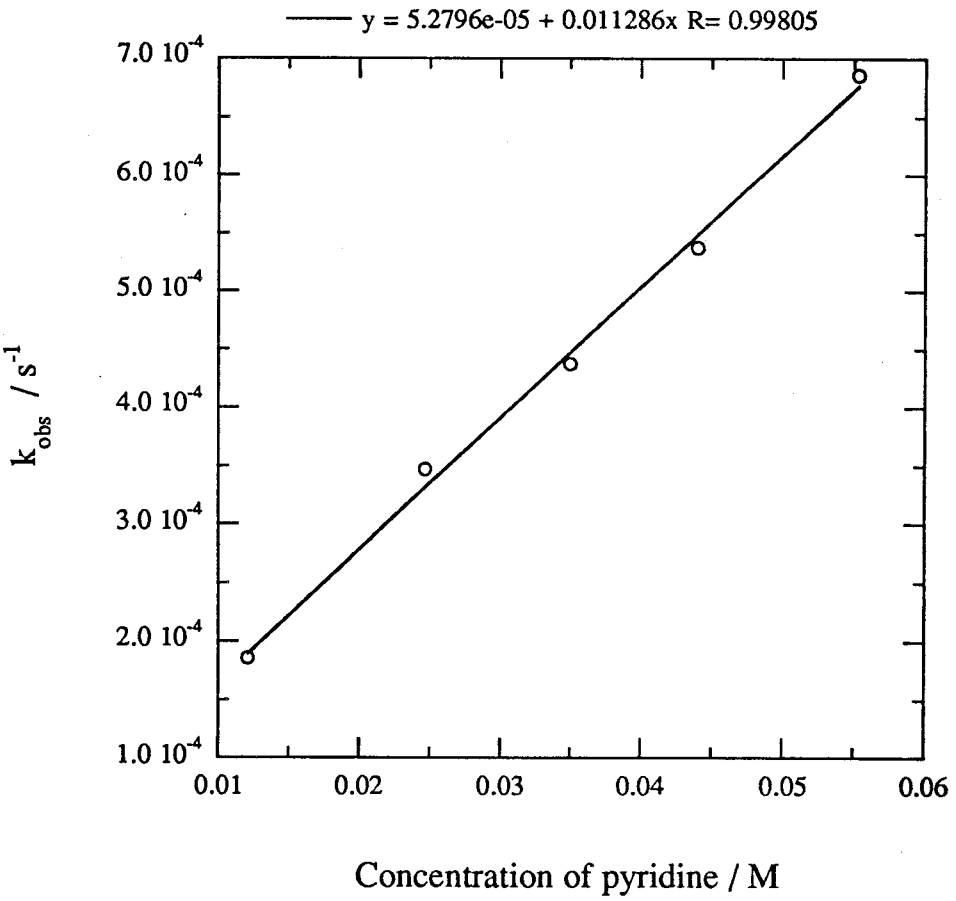

Figure 2.4 Arrhenius plot for the ligand exchange reaction of $PRu^{II}(OH_2)W_{11}O_{39}^{5-}$ with pyridine in pH = 5.0, sodium acetate buffer (μ = 0.2 M).

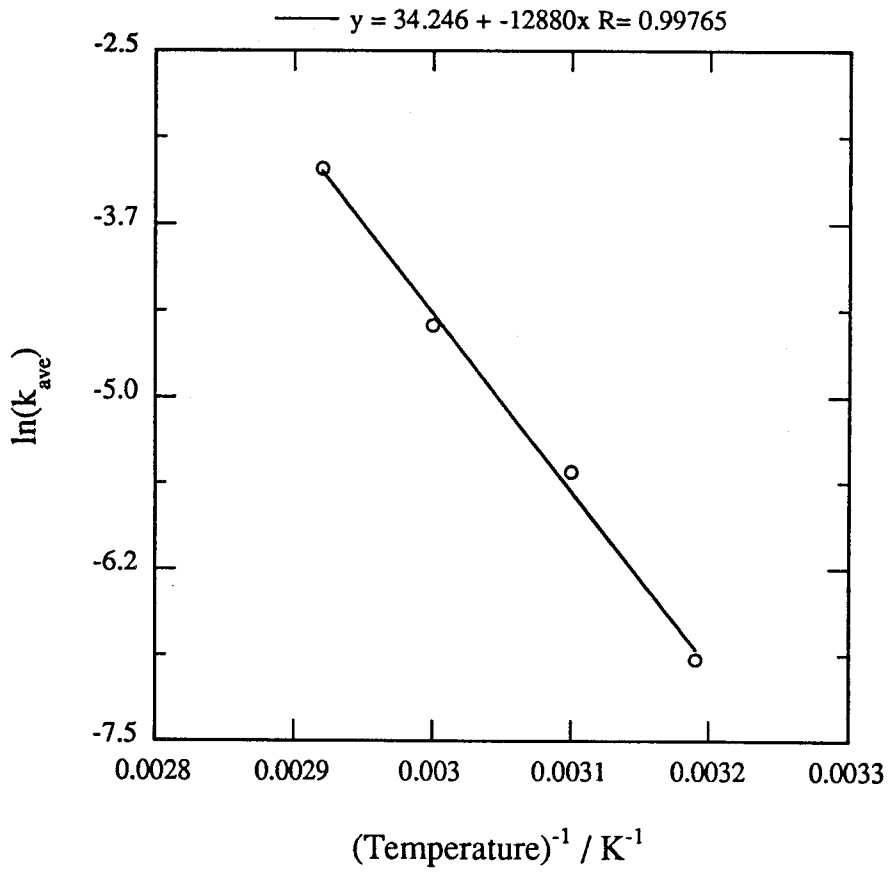

The cyclic voltammogram of $PRu(py)W_{11}O_{39}^{4-}$ shows only three waves, the $Ru^{III/II}$ couple and both of the two electron reductions of the tungsten-oxo cage. The $Ru^{IV/III}$ and $Ru^{V/IV}$couples seen in the aqua compound $PRu(OH_2)W_{11}O_{39}^{4-}$ are not observed within the potential window available. The aqua ligand of $PRu(OH_2)W_{11}O_{39}^{4-}$ has been reported to have a pK_a value of 5.1 and the formal potential of the $Ru^{III/II}$ couple changes by 60 mV per pH unit at pH values above 5.[2] The corresponding pyridyl complex should show no acidic properties. Figure 2.5 shows the plot of peak potential of the $Ru^{III/II}$ couple as a function of the pH of the solution. As expected, there is no significant change in the formal potential over a wide range of solution pH.

2.3.2 Ligand Exchange with Pyrazine

The second ligand studied was pyrazine, which presents several opportunities that pyridine did not. Although it is a nitrogen base quite similar to pyridine, the free nitrogen opposite the one bound to the ruthenium metal center should cause this complex to exhibit a pH dependent formal potential, and it may prove interesting in making pyrazine-bridged dimeric ruthenium compounds. The UV-visible spectrum of $PRu^{II}(pyz)W_{11}O_{39}^{5-}$ exhibits a single peak at 452 nm in the region from 300 to 800 nm (Figure 2.6). The kinetics of the ligand exchange were followed at 452 nm since this is the λ_{max} for the pyrazine complex and there is very little absorbance due to the aqua complex at this wavelength. Again, plotting $\ln(A_\infty - A_t)$ versus time yielded a straight line over 4-7 half-lives with a slope of $-k_{obs}$. At 60 °C in pH = 3.0 sulfate solution, the plot of k_{obs} vs. [pyz] when pyrazine is present in a 100-400 molar excess is linear (Figure 2.7); the slope of the line yielding $k = 9.6 \times 10^{-3}\ M^{-1}\ s^{-1}$. This rate constant doesn't change significantly from pH = 3 to pH = 6. Above pH = 6, the tungsten-oxo cage of **1** is not sufficiently stabile with regards to base-catalyzed decomposition to permit reliable measurement of the rate constant. Below pH = 3, a significant percentage of the pyrazine-substituted Ru^{II}-HPA exists with the second nitrogen of pyz protonated. Since

Figure 2.5 Peak potential of the $PRu^{II/III}(py)W_{11}O_{39}^{4-/5-}$ couple vs. solution pH. The line is merely included to show the trend of the electrochemistry and does not reflect a mathematical fit of the data.

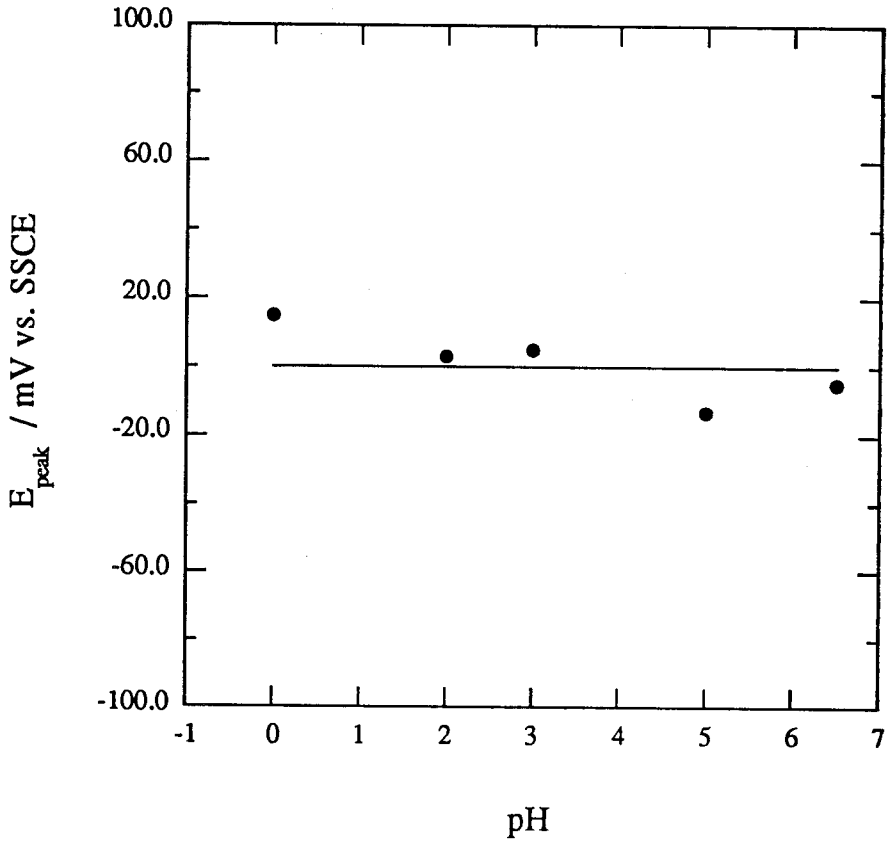

Figure 2.6 UV-visible spectra (at various times) for the ligand exchange reaction of $PRu^{II}(OH_2)W_{11}O_{39}^{5-}$ with pyrazine in a pH = 3.0, Na_2SO_4 solution (μ = 0.3 M) at T = 70 °C.

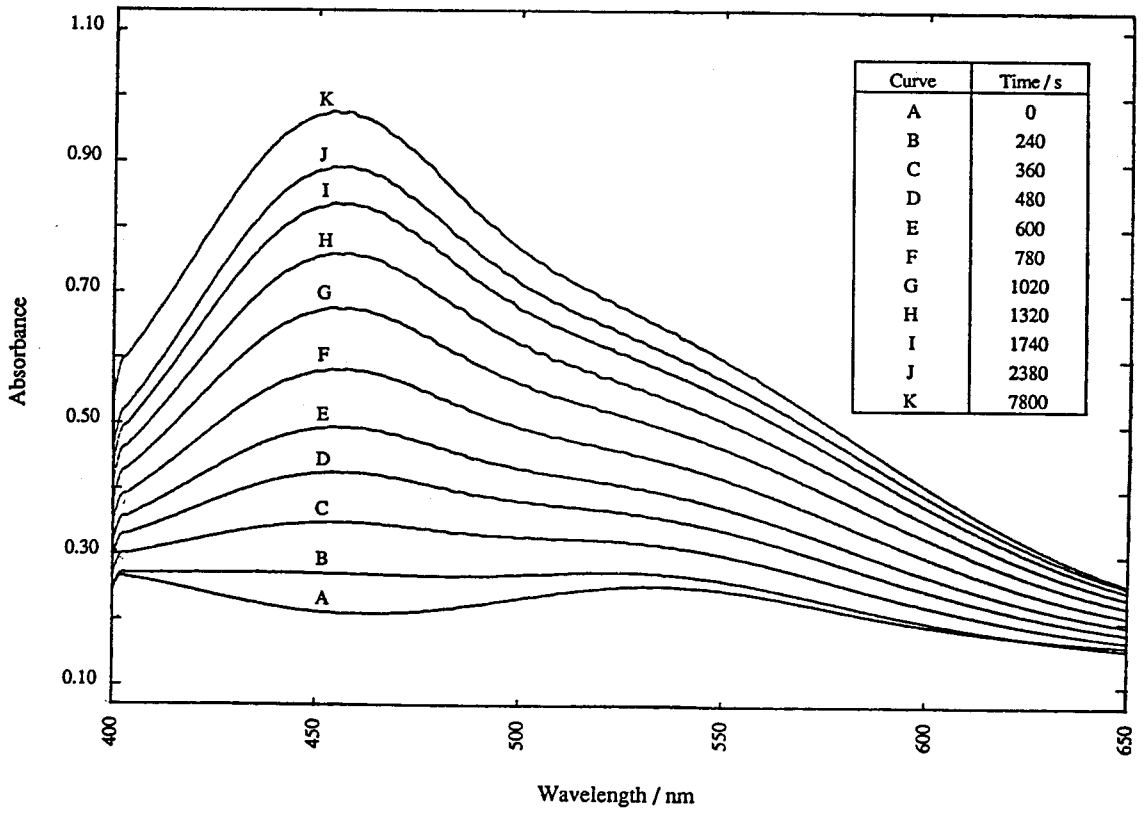

Figure 2.7 k_{obs} vs. the concentration of pyrazine used in the ligand exchange experiments. All experiments were performed in pH = 3.0, Na_2SO_4 solution (μ = 0.3 M) at T = 60 °C.

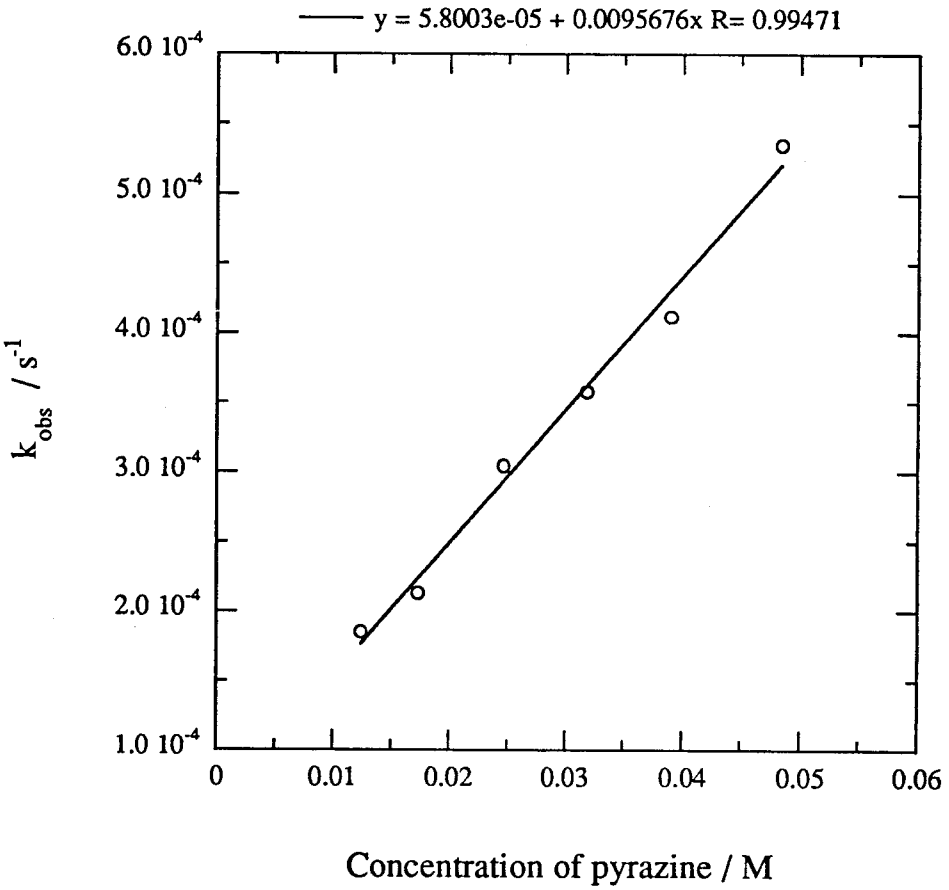

this compound has a λ_{max} at lower energy than the unprotonated form (see below), the kinetics of the reaction cannot be easily calculated. An Arrhenius plot of the ligand exchange data for L = pyz at pH = 3.0 is shown in Figure 2.8. The calculated activation energy is 101 kJ mol^{-1}.

Two separate experiments were performed to measure the pK_a of the unbound nitrogen of pyrazine in $PRu(pyz)W_{11}O_{39}^{5-}$. The first was to monitor the peak potential of the $Ru^{III/II}$(pyz) couple as the solution pH was changed. As seen in Figure 2.9, at pH $\leq$ 2, the peak potential varies approximately 58 mV $decade^{-1}$. The peak potential becomes independent of pH above pH = 3. The intersection of the two lines in Figure 2.9 yields a pK_a value of about 2.5 for the $PRu(pyz)W_{11}O_{39}^{5-}$ anion. The pK_a for this same reaction was also estimated by a spectroscopic technique. A solution of $PRu(pyz)W_{11}O_{39}^{5-}$ in 0.1 M NH_4PF_6 was prepared by reducing an isolated sample of $PRu(pyz)W_{11}O_{39}^{4-}$ by one electron via controlled potential electrolysis. The pH and the UV-visible spectrum of the resulting solution were monitored as an argon-saturated standard solution of H_2SO_4 was added to the reduced ruthenium heteropolyanion solution. The resulting spectral changes are shown in Figure 2.10: the peak shifts from 452 nm to 578 nm upon protonation of the unbound nitrogen of the pyrazine ligand. The pK_a occurs at the pH where ($A_{578}\cdot\varepsilon_{578}$/ $A_{452}\cdot\varepsilon_{452}$) is equal to one. Figure 2.11 shows a plot of ($A_{578}\cdot\varepsilon_{578}$ / $A_{452}\cdot\varepsilon_{452}$) vs. log [$H^+$] which gives a pK_a of 2.8. The molar absorptivity, ε, of the protonated species was calculated by titrating a sample of $PRu(pyz)W_{11}O_{39}^{5-}$ with argon-saturated acid until there was no more increase in the absorbance at 578 nm.

The electrochemistry of the heteropolyanion after pyrazine has displaced the original aqua molecule is quite different from that of the parent compound. The most notable difference is that there is no evidence of oxidation states higher than Ru^{III} which are electrochemically accessible (Figure 2.12). Since the $PRu(pyz)W_{11}O_{39}^{5-}$ has a pK_a of about 2.6 and the aquo complex has a pK_a of 5.1, there is only a small range of pH in

Figure 2.8 Arrhenius plot for the ligand exchange reaction of $PRu^{II}(OH_2)W_{11}O_{39}^{5-}$ with pyrazine in pH = 3.0, Na_2SO_4 solution (μ = 0.3 M).

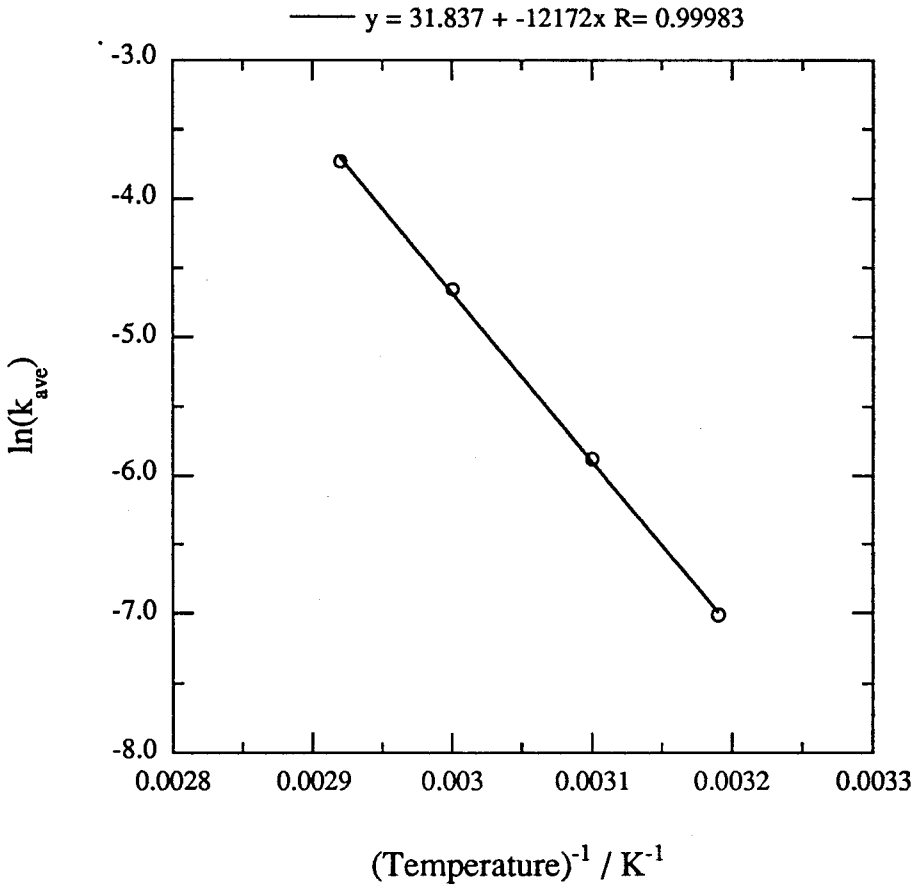

Figure 2.9 Peak potential of the $PRu^{II/III}(pyz)W_{11}O_{39}^{4-/5-}$ couple vs. solution pH. Lines are only meant to emphasize the trends in the electrochemistry and are not intended to represent actual mathematical fits of the data.

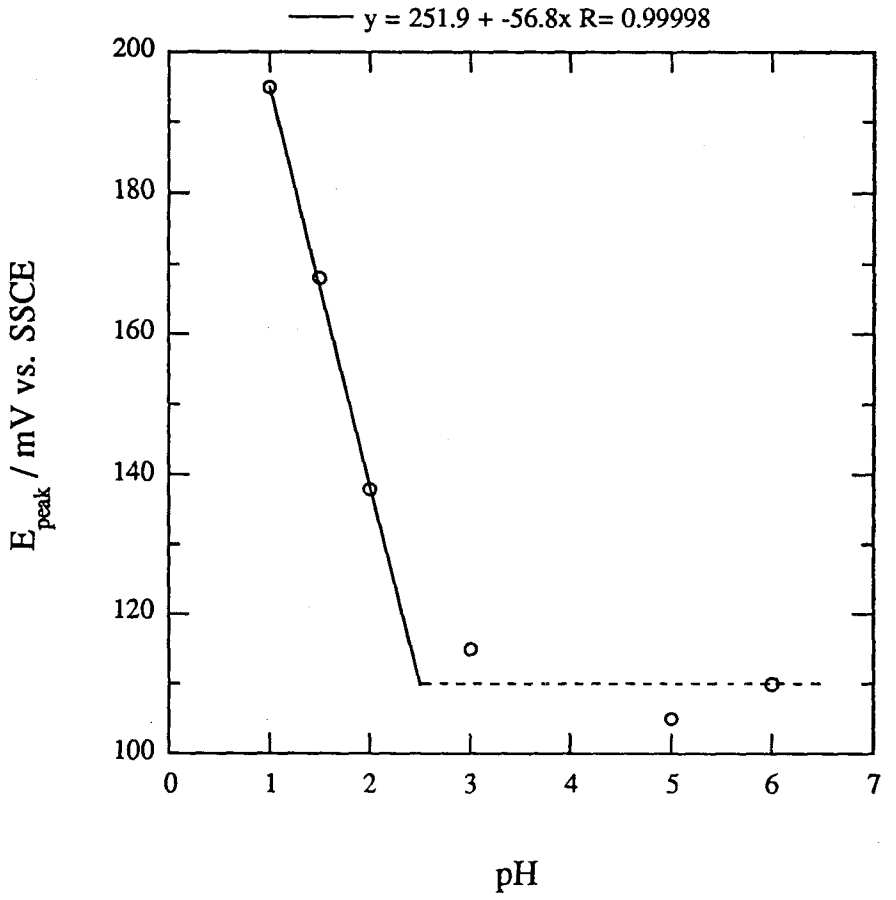

Figure 2.10 UV-visible spectra for the titration of $PRu^{II}(pyz)W_{11}O_{39}^{5-}$ in 0.1 M NH_4PF_6 with 1 M H_2SO_4 to produce $PRu^{II}(pyzH)W_{11}O_{39}^{4-}$.

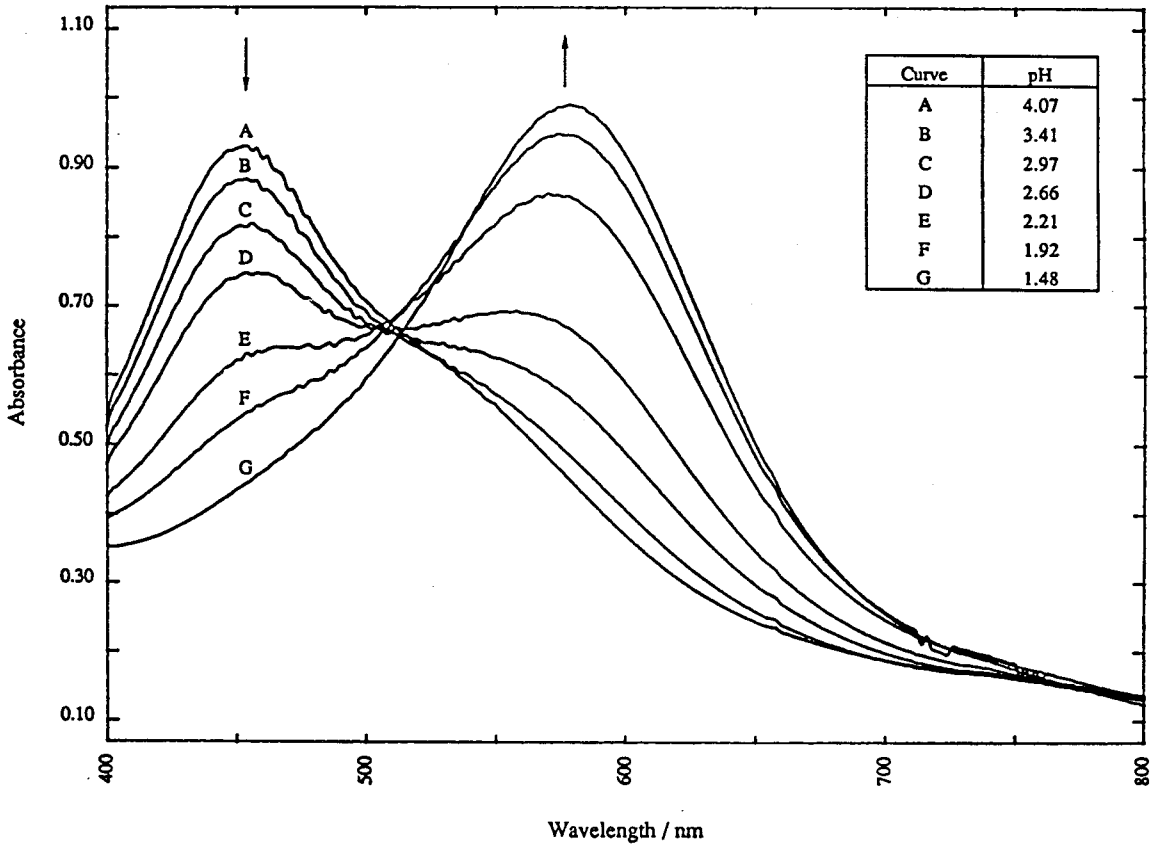

Figure 2.11 Concentration of (protonated / unprotonated) Ru-HPA vs. solution pH. When this ratio is one, pH = pK_a of the uncoordinated nitrogen of the bound pyrazine.

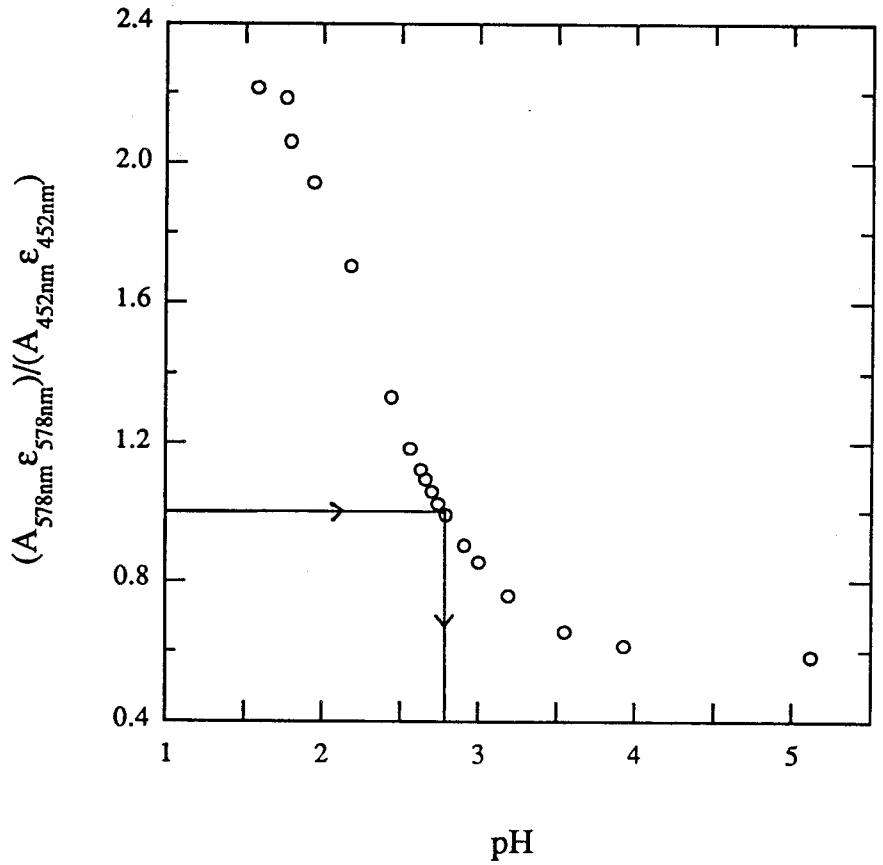

Figure 2.12 Cyclic voltammogram of 0.50 mM $PRu(pyz)W_{11}O_{39}^{4-}$ in a pH = 4.0 lithium acetate buffer (μ = 0.2 M) scanned at 50 mV s^{-1} using an EPG electrode.

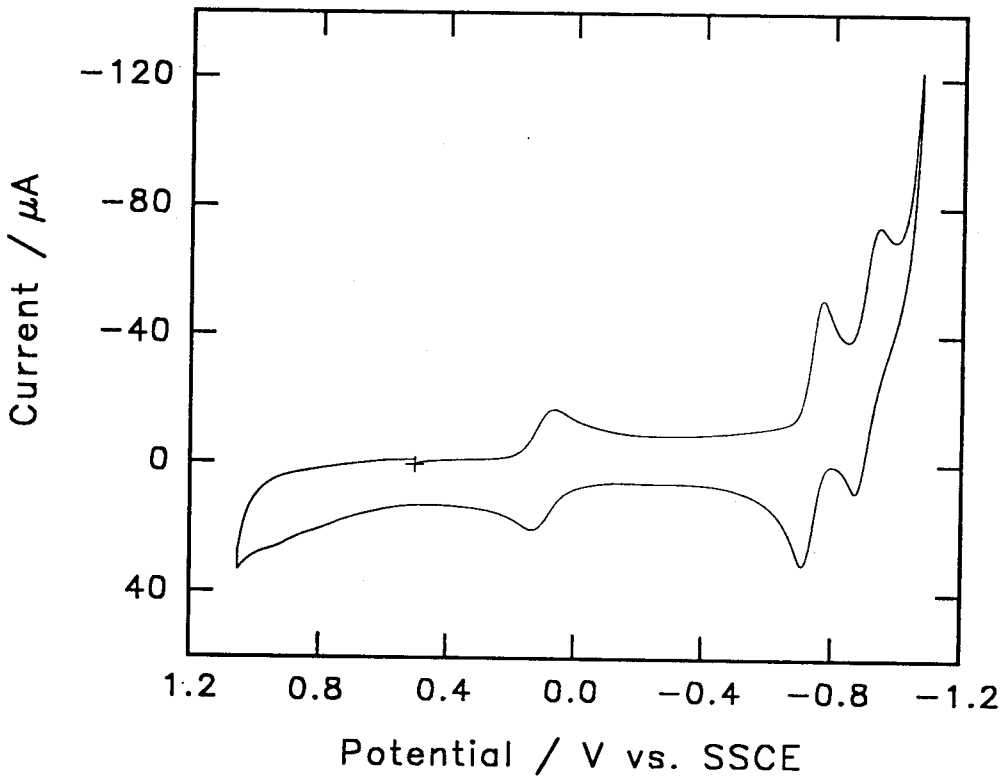

which neither of the complexes' electrochemistry is pH dependent, making comparison of the peak potentials difficult. In general, the $Ru^{III/II}$ wave shifts about 160-170 mV to more positive potentials when pyrazine replaces the aquo ligand on the ruthenium center. As expected, the tungsten-oxo cage waves are much less sensitive to the nature of the sixth ligand on ruthenium, shifting only up to +20 mV upon ligand exchange.

2.3.3 Ligand Exchange with *N*-Methylpyrazinium Iodide

It was of interest to compare the behavior of the protonated pyrazine complex with that of the similar *N*-methylpyrazinium (Mepyz) complex. The UV-visible spectrum of $PRu^{II}(Mepyz)W_{11}O_{39}^{4-}$ has a single peak at 592 nm in the region from 300 to 800 nm (Figure 2.13). Although this peak is near the 530 nm band for the aqua complex, the difference in extinction coefficients is so great (2200 vs. *ca.* 16000 $M^{-1}\,cm^{-1}$) that the kinetics of formation of the *N*-methylpyrazinium complex were straightforward to monitor. As usual, plotting $\ln(A_\infty - A_t)$ versus time yielded a straight line over 4-7 half-lives with a slope of $-k_{obs}$. At 60 °C in a pH = 3.0 buffer, the plot of k_{obs} vs. [Mepyz] (Figure 2.14) is linear when pseudo-first order conditions are used. From these data, a second order rate constant of $6.3 \times 10^{-2}\ M^{-1}\ s^{-1}$ is calculated. This is nearly a factor of seven larger than the corresponding rate constant for pyridine or pyrazine.

The electrochemical behavior of the *N*-methylpyrazinium-substituted ruthenium polyoxotungstate is quite similar to the pyrazine analogue, except that there is no dependence of the peak potential of the $Ru^{III/II}$ wave on pH since there is no free nitrogen site to be protonated. The two waves for the reduction of the tungsten-oxo cage occur at the same potential (within experimental error) regardless of whether the ligand, L = pyz or $Mepyz^+$. Since the $Ru^{III/II}$ peak potential of the protonated pyrazine complex varies depending on the degree of protonation, a direct comparison to the *N*-methylpyrazinium complex is not relevant. But like pyrazine, the $Mepyz^+$ binding does have a significant influence on the $Ru^{III/II}$ potential, shifting it 360 mV positive of the aquoruthenium

Figure 2.13 UV-visible spectra (at various times) for the ligand exchange reaction of $PRu^{II}(OH_2)W_{11}O_{39}^{5-}$ with *N*-methylpyrazinium iodide in pH = 3.0, Na_2SO_4 solution (μ = 0.3 M) at T = 50 °C.

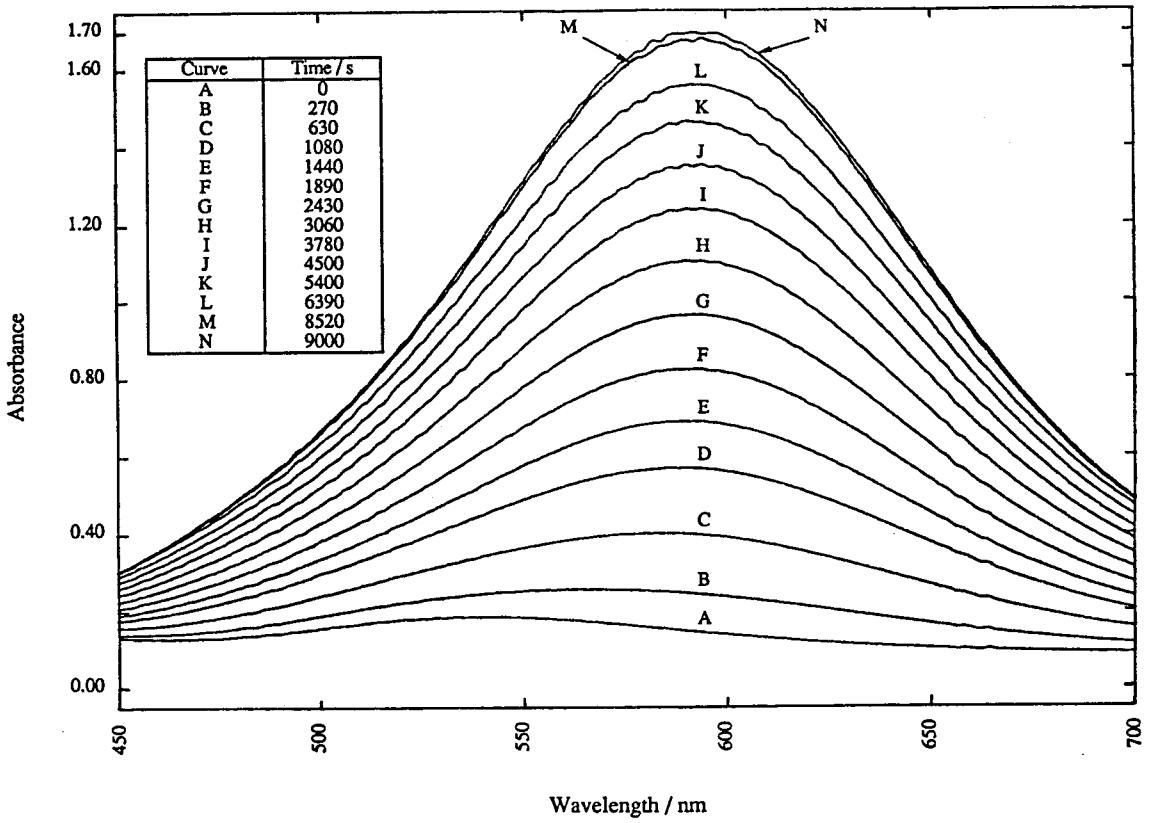

Figure 2.14 k_{obs} vs. the concentration of *N*-methylpyrazinium iodide used in the ligand exchange experiments. All data collected in pH = 3.0 Na_2SO_4 solutions (μ = 0.3 M) at T = 60 °C.

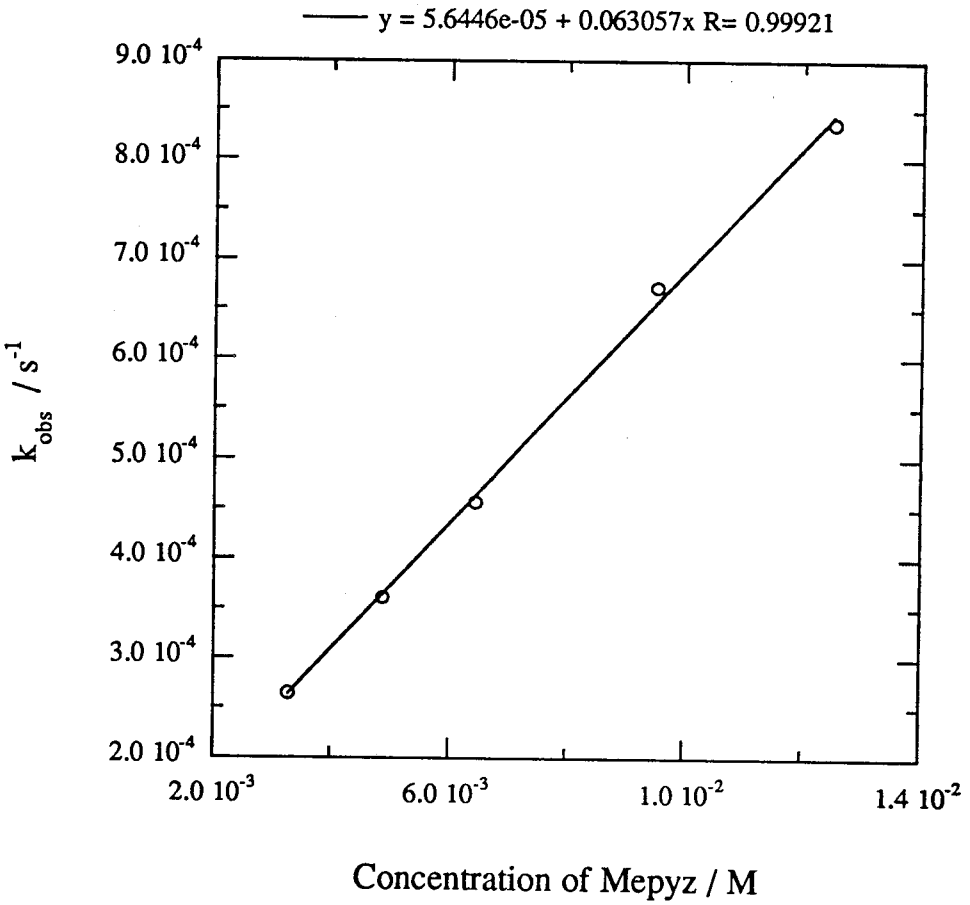

(III/II) couple. As with the other aromatic N-heterocycles, the $Ru^{IV/III}$ and $Ru^{V/IV}$ couples are electrochemically inaccessible in aqueous solvents.

2.4 *Discussion*

2.4.1 Comparison to Model System Electrochemistry

In order to understand the behavior of the ruthenium center when it is coordinated inside the phosphotungstate cage, it is useful to compare its properties with two well-studied complexes: $Ru(NH_3)_5(H_2O)^{2+}$ and $Ru(Hedta)(H_2O)^-$. The former was chosen as a model because it is one of the most completely studied ruthenium complexes in the literature. The latter was included in the study because the anionic edta ligand more closely resembles the tungstate cage than do five ammines. Table 2.1 shows a comparison of the electrochemistry of these three complexes when the sixth coordination site on ruthenium is water, pyridine, pyrazine, pyrazinium, or the *N*-methylpyrazinium cation. Substitution of a nitrogen base for the aqua ligand in these three compounds caused a shift in the ruthenium-based peaks to more positive potentials due to the π-backbonding that occurs when the Ru^{II} center (a good source of π-electrons) binds an aromatic N-heterocycle. The stronger the π-accepting nature of the ligand, the more the peak potential shifts upon ligand exchange. This agrees with previous data by Rong,[2] who studied activated alkenes bound to $PRu(L)W_{11}O_{39}^{n-}$. It is this π-backbonding to the ligand which draws electron density away from the metal that shifts the potential for the electrochemical oxidation of Ru^{II} to more positive values. The backbonding is clearly evident in the case of $Ru(NH_3)_5(Mepyz)^{3+}$, where the $Ru^{III/II}$ peak potential lies nearly one volt more positive than the $Ru^{III/II}A_5(H_2O)$ couple (A = NH_3). It is not surprising that a ruthenium bound to five neutral ammine nitrogens is not equivalent to a ruthenium which is attached to five negatively-charged oxides. Thus $Ru(Hedta)(H_2O)^-$, with its two

neutral nitrogens and three negatively charged carboxylates, was used as a better model system. The replacement of the three ammines by three carboxylates causes a shift in the peak potential to a more negative value, but not to the extent that the five oxides in the polyoxotungstate cage do. This is due to the fact that the HPA is known[2] to be a π-electron accepting ligand itself, and thus competes with the N-heterocyclic ligand for the π-electron density from the metal center. Therefore, replacing the aquo ligand by a nitrogen base in the case of Ru-HPA causes a smaller shift in the peak potential because the tungsten-oxo cage has already shifted the peak potential to more positive potentials when the ligand was water.

2.4.2 Spectroscopy

The spectroscopic data for all of the model compounds and the polyoxotungstate are shown in Table 2.2. In the case of the heteropolyanion, all of the nitrogen bases produce a moderate to strong absorbance in the visible region of the spectrum. This is most likely due to a metal-to-ligand charge transfer band, just as it is for the pentaammine[4c] and the edta[5a] complexes. When L = H_2O, the peaks for the polyoxotungstate are significantly lower in energy than either of the model complexes. The peak at 530 nm has been assigned[2] to a d-d transition and has a much larger extinction coefficient than the corresponding peaks for pentaammine- or edta-bound Ru^{II} (2200 vs. 32 and 260 M^{-1} cm^{-1} respectively) because of a broad, underlying band which extends into the near-IR. Rong assigned this broad absorption to a metal-to-"ligand" charge transfer, where the "ligand" could be any of the four W^{VI} atoms connected to the ruthenium center through a bridging oxide. The charge transfer band at 385 nm has a similar extinction coefficient to $Ru(Hedta)(H_2O)^-$, but the absorption has a λ_{max} 100 nm further to the red, just as in the case of the visible bands. This red-shift occurs because the polyoxotungstate cage is a decent π-acceptor,[2] unlike any of the ligands of the model

compounds (NH_3, H_2O, and edta).

When the spectroscopic data for $PRu(L)W_{11}O_{39}^{n-}$ (Table 2.2) are compared, a simple trend is observed. As the π-acceptor capability of the ligand, L, increases, the energy of the MLCT band goes down. This trend has been previously discussed for the pentaammineruthenium system[11] and the pentacyanoferrate system,[12] and is explained as follows: if the energy of the ruthenium 4d orbitals is held constant by assuming that the extent of the σ-interaction between ruthenium and the various ligands is nearly equal, then the difference in the charge transfer band energies will be due to the relative energy of the π-antibonding orbitals of the ligand. Thus a plot of the reduction potential of the unbound ligands versus the charge transfer energy of the Ru-L complex should show a general linear trend, and it does.[11] While at first glance it appears that the ruthenium heteropolyanion breaks this trend because of the peak for L = pyridine at 520 nm is at lower energy than the pyrazine peak at 452 nm, this is not the case. The band at 520 nm is not a Ru $\longrightarrow$ py(π^*) charge transfer band, rather a Ru $\longrightarrow$ HPA(π^*) CT band. The evidence for this is the fact that this peak is nearly identical to the visible peak for $PRu(OH_2)W_{11}O_{39}^{5-}$ in both wavelength and extinction coefficient, while the peak in the UV undergoes an increase in its extinction coefficient of 140% upon replacing the aqua ligand with pyridine. Thus there is a large $ML_{py}CT$ band at 381 nm which is masking the smaller $ML_{HPA}CT$ band. For L = pyridine, the edta complex is a better model of the heteropolyanion, while the pentaammine compound is less so. The difference in energy of the MLCT bands for $RuA_5(py)^{2+}$ and Ru(py)-HPA has already been cited as evidence that the heteropolyanion is a better π-acceptor ligand than the ammine groups.[2] A similar set of data exists for L = pyrazine. The edta and polyoxotungstate complexes have similar λ_{max} and extinction coefficients, while the pentaammine compound has its absorption at a slightly lower energy. On the other hand, when L = $Hpyz^+$ or $Mepyz^+$, the model complexes have their characteristic MLCT bands at higher energies than the

corresponding heteropolyanion. This reversal of the relative energy of the MLCT bands is due to a known phenomenon of Ru-ammine and Ru(edta) complexes where the ligand occupying the sixth coordination site is a cation such as *N*-methylpyrazinium, namely a very strong resonance interaction.[5a] For example, the compound $Fe(CN)_5(L)^{3-}$ is expected to have a high energy metal-to-ligand charge transfer band because it is relatively difficult to oxidize the ferrous center (e.g., E^o for L = H_2O is +0.39 V) compared to the ruthenium compounds, but the $Fe(CN)_5(Mepyz)^{2-}$ MLCT band is over 100 nm further into the *red* (662 nm)[12b] than either the pentaammine or the edta complex. Since the MLCT band for $PRu(Mepyz)W_{11}O_{39}^{4-}$ occurs at 592 nm, it follows that there is probably a resonance interaction occurring in this case too, but not to the extent to which it occurs in the model systems. The trend set by these four compounds is that the more π-acceptor nature in the five coordinate ligand(s), the less resonance interactions affect the MLCT band.

2.4.3 Kinetics of Ligand Exchange

A compilation of all the ligand exchange data at T = 25 °C and T = 60 °C is shown in Table 2.3. The rate of the ligand exchange reactions when the ruthenium is coordinated to the heteropolyanion were generally very slow and thus were measured at elevated temperatures. The literature data for ligand exchange for the model compounds were obtained at 25 °C so, in order to make comparisons with the polyoxotungstate complexes, extrapolations were necessary. The kinetic data for the heteropolyanion at the lower temperature were estimated from the Arrhenius plots for the appropriate ligand. When the data were available, the same procedure was used to estimate rate constants for the model systems at 60 °C.

In general, ligand exchange reactions at hexacoordinate Ru^{II} are dissociative in nature,[13] with loss of the aqua ligand from the metal center being the slow step in the ligand exchange reaction. As a result, the rate constants for different incoming ligands

show little variation. This is true of both $Ru^{II}A_5(OH_2)$[4e] and of $Ru^{II}(edta)(OH_2)$.[5a] It should be noted that all comparisons to the edta system will be for ruthenium in the dipositive state, since Ru^{III}(edta) ligand exchange reactions proceed by an *associative* mechanism[5a] and are, in general, quite unusual compared to most hexacoordinate Ru^{III} systems. Although the three ligands studied here are not nearly enough on which to base wide-sweeping conclusions on, it seems fairly clear that the ruthenium heteropolyanion follows the same dissociative mechanism that the two model systems do. The two neutral ligands studied herein have essentially identical rate constants, as does dimethyl sulfoxide which was studied by Rong,[2] and the third ligand, the *N*-methylpyrazinium cation, is higher by less than an order of magnitude. This increase in the rate is most likely due to a simple cause: the anionic ruthenium complex attracts the cationic ligand, perhaps causing an increase in the local concentration of the ligand around the metal complex. The same rationale has been used before to explain why the thiocyanate ligand added to $Ru^{II}(edta)(OH_2)^{2-}$ more slowly (by a factor of 5-10) than neutral ligands.[5a]

When the ligand replacing the bound water molecule is pyridine, the order of reactivity is edta complex > pentaammine complex > heteropolyanion. If the rate of substitution for the pentaammine compound is taken as the norm, then neither of the other two complexes come within about two orders of magnitude of that rate. For the edta compounds, this relatively large enhancement of the rate has been attributed to the uncoordinated carboxylate assisting the dissociation of the bound water and because the negatively-charged edta ligand weakens the σ-donation from the outgoing water molecule to the metal center.[5a] It has been noted that for neutral ligands such as isonicatinamide, the rate of substitution onto $Ru^{II}(edta)(OH_2)$ is about two orders of magnitude greater than $Ru^{II}A_5(OH_2)$, which in turn is about two orders of magnitude faster than $Ru^{II}(OH_2)_6$.[5a] Indeed, Taube[4f] has noted that the σ-interactions with the metal center of the isoelectronic series of ligands goes as $NH_3 > H_2O > HF > Ne$. He concludes that the

stronger the polarizability of the ligand, the better it satiates the electron density needs of the transition metal, thus weakening the bond to the sixth (aquo) ligand. It follows that each oxo group of the heteropolyanion is a weaker σ-donor than an ammine because the rate of ligand exchange is about two orders of magnitude slower in the case of the heteropolyanion compared to the ruthenium pentaammine, and a slower substitution rate is indicative of a stronger ruthenium-aquo bond. We believe that the reason the tungsten-oxo cage acts as a poor σ-donor is two-fold. First, the charge density on the cage is smaller than in the case of the edta ligand (due its much larger size), thus the metal center doesn't get as much electron density as might be expected. Second, the ruthenium center has to compete with the W^{VI} atoms for the electron density on the oxo groups, causing them to seem more like "soft" aqua ligands than "hard" oxide ligands.

When L = pyz, the situation is almost identical to that of pyridine. The rate constants are nearly equal, lending credence to the claim that the heteropolyanion follows a dissociative mechanism during ligand exchange. Likewise, both pyridine and pyrazine exchange for the aqua ligand on $PRu(OH_2)W_{11}O_{39}^{5-}$ at a rate about 200 times slower than when $RuA_5(OH_2)^{2+}$ is the ruthenium substrate. This is all consistent with the lower σ-donating abilities of the polyoxotungstate described above. It is interesting to note that all three complexes have nearly the same pK_a value for protonating the uncoordinated nitrogen of the pyrazine bound to the metal center. Both $Ru^{II}A_5(pyz)$[4a] and $Ru^{II}(edta)(pyz)$[14] have a pK_a of 2.5, while the pyrazine bound to the ruthenium heteropolyanion has a pK_a value of about 2.6. Since the pK_a of complexed pyrazine is nearly two orders of magnitude more basic than that of the free ligand ($pK_a = 0.6$),[15] each of the ruthenium metal centers must participate in a significant amount of π-backbonding to pyrazine. Unfortunately, it appears that since each of the three ruthenium compounds donates a sizable amount of electron density to the heterocycle, the pK_a value is not a sensitive measure of the relative amount of π-electron back donation. As demonstrated

above, the MLCT band and the electrochemical peak potential are much more sensitive to the extent of π-backbonding that occurs in these systems.

The kinetics of ligand exchange when the incoming N-heterocycle is the *N*-methylpyrazinium cation vary from the above cases in a fairly predictable manner. For the cationic aquopentaammineruthenium complex, the rate of ligand exchange slows by over an order of magnitude versus neutral ligands. On the other hand, the anionic ruthenium heteropolytungstate and ruthenium edta compounds exchange their aquo ligand for $Mepyz^+$ about 5 to 100 times faster than comparable neutral ligands. Unfortunately, the rate of ligand exchange for the reaction of $Ru(edta)(OH_2)^{2-}$ with $Mepyz^+$ is not known precisely, but the value of 5.6×10^3 M^{-1} s^{-1} reported by Araki *et al.*[5d] is at least an upper limit for this rate constant. One problem with the data for the *N*-methylpyrazinium cation ligand exchange reaction is that the enhancement of the rate for Ru-HPA (compared with neutral ligands) appears to be smaller than it should be. If the rate increases by a factor of 100 (versus neutral ligands) when the 2- charged $Ru(edta)(OH_2)$ complex reacts with $Mepyz^+$, then the 5- charge on Ru-HPA should cause it to have an even larger rate increase, but it does not; the change in the rate compared to neutral ligands increases only by a factor of about six. Fortunately, this apparent anomaly can be explained by considering the charge density of the compounds. By using the Stokes equation[16] (1) and the Stokes-Einstein equation[16] (2), the effective

$$f = 6\pi a\eta \qquad (1)$$

$$f = kT/D \qquad (2)$$

hydrodynamic radius, a, of an ion can be calculated if its diffusion coefficient is known. In these equations, η is the solution viscosity, k is Boltzmann's constant, T is the temperature in Kelvin, and f is the friction coefficient. Using a, we can calculate the surface area of the ion from (3) and the charge density from (4). For Ru-HPA, the

$$A = 4\pi a^2 \qquad (3)$$

$$C.D. = |charge\ of\ ion|/A \quad (4)$$

hydrodynamic radius is about 8 Å, which leads to a charge density of 5.0×10^{-3} Å^{-2}. For comparison, potassium ferrocyanide (also a 4- charged anion) has a diffusion coefficient[17] of 6.3×10^{-6} cm^2 s^{-1} which leads to a = 3.5 Å and a charge density of 2.7×10^{-2} Å^{-2}. This is nearly a factor of six bigger than the Ru-HPA. Indeed, even ruthenium hexaammine has a charge density, 1.9×10^{-2} Å^{-2} ($D = 7.6 \times 10^{-6}$ cm^2 s^{-1} and a = 2.9 Å)[18], that is four times larger despite the fact that it has only half of the charge that the heteropolyanion does. Thus it seems that the lower than expected reactivity of Ru-HPA is due to the fact that its large formal charge is distributed over a quite large surface area.

2.5 *Conclusions*

The most important feature of ruthenium heteropolytungstates which was discovered when comparing them to the $Ru(NH_3)_5(L)^{2+}$ and $Ru(edta)(L)^{2-}$ systems was that the polyoxotungstate is a weaker sigma-donor to ruthenium than either of the model compounds, but it is a better π-acceptor. In general, the heteropolyanion behaves fairly predictably once its donor / acceptor properties are considered. The electrochemistry is rather unremarkable: the more the sixth ligand can accept π-backbonding from the metal center, the more positive the formal potential shifts from the aquo wave. But because the tungsten-oxo cage is a competitor in π-backbonding with the metal center, the magnitude of this shift is smaller than for the pentaammine or edta complexes.

The spectroscopy also follows these trends. The more easily the ligand can accept π-electrons from the ruthenium center, the further the MLCT band shifts to the red. Since the heteropolyanion can act as a π-acceptor too, it competes with the nitrogen-base ligands for the π-electron density surrounding the metal center. As a consequence, the MLCT band occurs at a higher energy than it did for either of the model compounds.

Cationic ligands like protonated pyrazine or *N*-methylpyrazinium present a different situation altogether. These ligands have MLCT bands which are lower in energy for the ruthenium heteropolytungstate than ruthenium pentaammine or ruthenium(edta). This observation is taken as evidence that resonance interactions, which were cited as causing the pentaammine and edta MLCT bands to be much higher in energy than expected, are weaker for the polyoxotungstate.

The replacement of the aqua ligand by N-heterocyclic ligands appears to follow a dissociative pathway just like most hexacoordinate Ru^{II} systems. For the ruthenium heteropolyanion, these ligand exchange reactions are quite slow, about two orders of magnitude slower than $Ru^{II}A_5(OH_2)$, evidence that the heteropolyanion is a weaker σ-donor than the pentaammine. The weaker the interaction between the ruthenium and the polyoxotungstate, the stronger the aqua ligand is attracted to the metal center, and thus the dissociation of the water-ruthenium bond takes longer. The kinetics of exchange when L = $Mepyz^+$ are not as different from the pentaammine as the neutral ligands because of electrostatic effects. Repulsion between the cationic $RuA_5(OH_2)^{2+}$ and $Mepyz^+$ slows this reaction by about an order of magnitude compared to neutral ligands. Likewise, electrostatic attraction between $Ru(edta)(OH_2)^{2-}$ and $Mepyz^+$ increases the rate of ligand exchange by up to two orders of magnitude. Following the trends set by these two compounds, the rate of ligand exchange between Ru-HPA and $Mepyz^+$ should be two to three orders of magnitude faster than when the ligands are neutral, due to the fact that the *N*-methylpyrazinium ion should be strongly attracted to the 5- charge on the polyoxotungstate cage. Since the rate only increases by a factor of about six, it appears that the heteropolyanion's effective charge is much less than its formal charge. This is not surprising since the 5- charge of the Ru^{II}-HPA is spread out over a very large surface area. In addition, as the ligand nears the cage, it approaches toward the ruthenium center, and thus experiences a localized positive charge, even though the overall charge of the

cage is negative. It is not unlikely that this effect should partially cancel the electrostatic attraction between the reactants. This behavior of the heteropolyanion to appear less charged than formally assigned is going to be a reoccurring trend throughout this work.

References

1. Neumann, R.; Abu-Gnim, C. *J. Am. Chem. Soc.* **1990,** *112,* 6025.

2. Rong, C.; Pope, M. T. *Ibid.* **1992,** *114,* 2932.

3. Steckhan, E.; Kandiza, C. *Synlett.* **1992,** 139.

4. a) Ford, P.; Rudd, DeF. P.; Gaunder, R.; Taube, H. *J. Am. Chem. Soc.* **1968,** *90,* 1187.
   b) Armor, J. N.; Scheidegger, H. A.; Taube, H. *Ibid.* **1968,** *90,* 5928.
   c) Zwickel, A. M.; Creutz, C. *Inorg. Chem,* **1971,** *10,* 2395.
   d) Toma, H. E., Malin, J. M. *J. Am. Chem. Soc.* **1972,** *94,* 4039.
   e) Shepherd, R. E.; Taube, H. *Inorg. Chem.* **1973,** *12,* 1392.
   f) Taube, H. In *Survey of Progress in Chemistry*; Scott, A. E., Ed.; Academic Press: New York, 1973; Vol. 6, chapter 1.
   g) Taube, H. *Pure Appl. Chem.* **1979,** *51,* 901.

5. a) Matsubara, T.; Creutz, C. *Inorg. Chem.* **1979,** *18,* 1956.
   b) Diamantis, A. A.; Dubrawski, J. V. *Ibid.* **1981,** *20,* 1142.
   c) Toma, H. E.; Santos, V. S.; Mattioli, M. V. D.; Oliveira, L. H. A. *Polyhedron* **1987,** *6,* 603.
   d) Araki, K.; Shu, C.-F.; Anson, F. C. *Inorg. Chem.* **1991,** *30,* 3043.

6. Tézé, A.; Hervé, G. *J. Inorg. Nucl. Chem.* **1977,** *39,* 999.

7. Bernhard, P.; Biner, M.; Ludi, A. *Polyhedron* **1990,** *9,* 1095.

8. Vogt, L. H., Jr.; Katz, J. L.; Wiberley, S. E. *Inorg. Chem.* **1965,** *4,* 1157.

9. Mukaida, M.; Okuno, H.; Ishimori, T. *Nippon Kagaku Zasski* **1965,** *86,* 589.

10. Bahner, C. T.; Norton, L. L. *J. Am. Chem. Soc.* **1950,** *72,* 2881.

11. Lavallee, D. K.; Fleischer, E. B. *J. Am. Chem. Soc.* **1972,** *94,* 2583.

12. a) Toma, H. E.; Malin, J.M. *Inorg. Chem.* **1973,** *12,* 1039.
    b) Toma, H. E.; Creutz, C. *Ibid.* **1977,** *16,* 545.

13. Basolo, F.; Pearson, R. G. *Mechanisms of Inorganic Reactions,* 2nd ed.; John Wiley & Sons: New York, 1967.

14. Ram, M. S.; Haim, A. *Inorg. Chem.* **1991,** *30,* 1319.

15. Acheson, R. M. *An Introduction to the Chemistry of Heterocyclic Compounds;* Interscience Publishers: New York, 1960; p 299.

16. Atkins, P. W. *Physical Chemistry*, 3rd ed.; W. H. Freeman and Co.: New York, 1986; p 612.

17. McCreery, R. L. *Electroanalytical Chemistry*; Bard, A. J., Ed.; Marcel Dekker: New York, 1991; Vol. 17, p 289.

18. Okajima, T.; Ohsaka, T.; Hatosaki, O.; Oyama, N. *Electrochim. Acta* **1991,** *37,* 1865.

19. Lim, H. S.; Barclay, D. J.; Anson, F. C. *Inorg. Chem.* **1972,** *11,* 1460.

20. Endicott, J. F.; Taube, H. *J. Am. Chem. Soc.* **1962,** *84,* 4984.

Table 2.1 Shift of cyclic voltammetric peak potential when the aqua ligand on the ruthenium complex is replaced by another ligand.

Incoming ligand	$Ru^{II}(NH_3)_5(L)$	$PRu^{II}(L)W_{11}O_{39}$	$Ru^{II}(edta)(L)$
pyridine	+239 mV[a]	+45 mV[b]	+110 mV[c]
pyrazine	+480 mV[b]	+163 mV[b]	+250 mV[c]
pyrazinium	+525 mV[d]	+170 mV[e]	(unknown)
N-methylpyrazinium	+860 mV[d]	+360 mV[f]	+550 mV[g]

a. 0.1 M CF_3COOH / 0.1 M CF_3COONa. Ref. 19.

b. pH = 5.0 sodium acetate buffer (μ = 0.2 M).

c. pH = 5.5 sodium acetate buffer (μ = 0.2 M). Ref. 5a.

d. 0.1 M CF_3COOH / 0.1 M CF_3COONa.

e. pH = 2.0 sodium sulfate buffer (μ = 0.9 M).

f. pH = 3.0 sodium sulfate buffer (μ = 0.3 M).

g. pH = 4.5 sodium acetate buffer (μ = 0.2 M). Ref. 5d.

Table 2.2 Spectroscopic data for various ligands bound to the three ruthenium complexes studied.

	λ, nm (ε, M^{-1} cm^{-1})		
Ligand	$Ru^{II}(NH_3)_5(L)$	$PRu^{II}(L)W_{11}O_{39}$	$Ru^{II}(edta)(L)$
water	420 (100)[a] 328 (260)	530 (2200)[b] 385 (2500)	427 (260)[c] 282 (2900)
pyridine	408 (7770)[d]	520 (2500)[b] 381 (6000)	382 (6760)[c]
pyrazine pyrazinium cation	472 (10700)[d] 529 (12000)[e]	452 (11300) 578 (*ca.* 12000)	463 (11600)[c] 545 (n. r.)[f]
N-methylpyrazinium	540 (16000)[g]	592 (16027)	558 (19400)[c]

a. Ref. 20.

b. Ref. 2.

c. Ref. 5a.

d. Ref. 4e.

e. Ref. 4a.

f. Ref. 14. ε value was not reported.

g. Ref. 4d.

Table 2.3 Ligand exchange kinetic data for various ligands replacing the aqua ligand on the three ruthenium complexes studied.

	k, $M^{-1} s^{-1}$			
Ligand	Temperature	$Ru^{II}A_5(L)^{2+}$	$PRu^{II}(L)$-HPA	$Ru^{II}(edta)(L)^{2-}$
py	25 °C	9.3×10^{-2} [a]	1.2×10^{-4} [b]	20 [c]
py	60 °C	2.3 [d]	1.1×10^{-2}	n. a.[e]
pyz	25 °C	5.6×10^{-2} [a]	1.1×10^{-4} [b]	n. a. [f]
pyz	60 °C	2.2 [d]	9.6×10^{-3}	n. a.[f]
Mepyz	25 °C	6.9×10^{-3} [g]	n. a.[e]	$\leq 5.6 \times 10^{3}$ [h]
Mepyz	60 °C	n. a.[e]	6.3×10^{-2}	n. a.[e]

a. Ref. 4e.

b. estimated from Arrhenius plot.

c. estimated from data in Ref. 5a.

d. estimated from data in Ref. 4e.

e. not available.

f. not available. See text in Ref. 5a.

g. estimated from data in Ref. 4d.

h. Ref. 5d.

Chapter Three

Electron Transfer Kinetics

3.1 *Introduction*

One of the many properties a compound needs to possess in order to be an efficient electrochemical catalyst is a facile electron transfer (et) with the substrate it is reacting with. Since the ruthenium-substituted heteropolytungstate anion (Ru-HPA) under investigation is a relatively new species,[1] its electron transfer properties have not been studied to any great extent. The only information available on electron transfer with the ruthenium center inside the polyoxotungstate cage is the self-exchange rate constant, reported by Rong[1] to be 1.2×10^6 M^{-1} s^{-1}. Since this number is orders of magnitude larger than common ruthenium species, it was proposed that the electron is not confined to the orbitals of the ruthenium center, but is delocalized over the entire cage. It would be interesting to see if a detailed electron transfer study could provide any experimental evidence to support this proposal.

Fortunately for us, ruthenium complexes are among the most frequently studied reactants of all transition metal electron transfer reactions. These reactions range from those involving simple compounds such as ruthenium ammines and polypyridyl complexes[2-6] to those involving more complex organometallic[7] and porphyrinic[8] species. Ruthenium compounds have even been used to measure electron transfer rate constants in biochemical systems.[9,10] This wealth of electron transfer information concerning ruthenium should be useful in characterizing the properties of the Ru-HPA. In addition, over the past 30 years the theoretical basis of electron transfer between various types of oxidants and reductants has been studied extensively.[11-14] This work has progressed to the point where simple (and even many complex) electron transfer reaction rates can be predicted with increasing accuracy. The Marcus equation for simple outer sphere et will provide another tool with which to understand the electron transfer properties of ruthenium-substituted heteropolytungstate anions. For example, will the delocalization of

the electron in the reduced complex yield a pathway by which abnormally fast electron transfer can occur, or will the π-electron backbonding from the ruthenium center to the cage disperse the electron density away from the metal and make it less reactive than a common Ru^{II} reductant?

3.2 *Experimental*

3.2.1 Syntheses

Potassium 11-tungstophosphate ($K_7PW_{11}O_{39}\cdot xH_2O$) was synthesized based on the method of Tézé and Hervé[15] (for the silicon lacunary ion) with the substitution of Na_2HPO_4 for Na_2SiO_3. Hexaaquoruthenium (II) *p*-toluenesulfonate $Ru(OH_2)_6(C_7H_7SO_3)_2$ was prepared by the literature method.[16] Cesium undecatungstophospho(aqua)ruthenium (III), $Cs_4PRu(OH_2)W_{11}O_{39}\cdot 5H_2O$, was made using the procedure of Rong and Pope (with the modification mentioned in Chapter 1).[1] Chloropentaammineruthenium (III) chloride, $Ru(NH_3)_5(Cl)Cl_2$, was synthesized following literature methods.[17] Potassium undecatungstophospho(aqua)iron (III), $K_4PFe(OH_2)W_{11}O_{39}$, was prepared *in situ* by the addition of a ferric salt, usually ferric nitrate, to a solution containing an equimolar amount of the unsubstituted lacunary ion $K_7PW_{11}O_{39}$.[18] 12-Phosphotungstic acid, $H_3PW_{12}O_{40}$, was purchased from Johnson-Matthey and used as received. Ruthenium (III) hexaammine chloride was bought from Strem and used without further purification. The water used in all the experiments was house deionized water that had been further purified by passage through either a Barnstead NANOpure or a Millipore Milli-Q_{plus} water purification system, and was tested to have a resistance of at least 18.2 MΩ cm.

Potassium Trioxalatocobaltate(III)

A modified version of the standard literature procedure[19] was used to synthesize this compound. 2.52 g (20.0 mmol) oxalic acid, 7.36 g (40.0 mmol) potassium oxalate, and then 2.40 g (20.2 mmol) cobaltous carbonate were dissolved in 50 mL of boiling water. The cobalt salt must be added slowly as much CO_2 is evolved. The purple-red solution was well stirred and then cooled to 40 °C. The flask was put into a water bath thermostatted at 31 ± 1 °C, 6 g of lead dioxide were added, and the solution was stirred well. 5 mL of glacial acetic acid/water (50/50 by volume) was then added over the course of 30 minutes. Stirring was continued an additional 30 minutes after addition of the acid was completed, then the solution was suction filtered to remove the unreacted lead dioxide. While stirring the filtrate well, 60 mL of 95% ethanol was added and the solution was cooled in the refrigerator for 30 minutes. The fine green needles which precipitated were collected by suction filtration. The product was dissolved in 35 mL water and then reprecipitated with 35 mL ethanol. The chilling and filtration steps were repeated, the crystals washed with ethanol, and then dried overnight in a darkened hood. 6.1 g (60% yield) of fine dark green crystals were collected. *BEWARE*: solutions of cobalt oxalate (and to a lesser extent, the salt itself) are photosensitive and should be kept in foil-wrapped flasks at all times.

Ruthenium (II) Hexaammine Solution

24.6 mg (79 μmol) ruthenium (III) hexaammine chloride was dissolved in 10 mL of the desired buffer solution, and then argon was bubbled through the solution for at least 30 minutes. About 2 g of freshly-made zinc amalgam was introduced and then the flask was covered with aluminum foil. The Zn[Hg] is allowed to react for about half an hour while sparging of the solution with argon continued. The color of the solution changed from colorless to pale yellow, indicating that the reaction was complete. When stored in the dark under argon and a piece of Zn[Hg], the Ru^{II} solution is stable for several hours.

Ruthenium (II) Aquopentaammine Solution

This was prepared in a manner similar to ruthenium (II) hexaammine, except that the starting material was chloropentaammineruthenium (III) chloride and the solvent was always pure water. Several buffers (especially those containing sulfate or acetate anions) were found to either precipitate the Ru^{II} salt or significantly accelerate the decomposition of the complex. This complex is even more light sensitive than hexaammine, so it is important to keep the solution in a foil-covered flask. The color of the solution changes from colorless to bright yellow upon reduction of the ruthenium center. If the solution begins to turn orange or green, the ruthenium complex is decomposing and should be disposed of. Under proper care, the Ru^{II} salt is generally stable for a couple of hours.

3.2.2 Physical Measurements

The rotating disk electrode experiments were performed using one of two set-ups. The first included a motor and controller from Oxford Electrodes, while the potential was controlled by a Princeton Applied Research Corp. (PARC) Model 173 Potentiostat/ Galvanostat equipped with a PARC Model 176 current-to-voltage converter and a PARC Model 175 Universal Programmer. The data were collected on a Houston Instruments 2000-5-5 X-Y recorder. The second RDE set-up used included a Pine AFRDE5 bipotentiostat, a Pine ASR2 rotator/controller, and a Kipp & Zonen BD91 XYY't recorder. The working electrode was a home-built edge-plane graphite (EPG) electrode (Union Carbide) unless otherwise mentioned. The auxiliary electrode was a piece of platinum wire and the reference electrode was either a saturated sodium calomel electrode (SSCE) or a Ag/AgCl reference electrode (in 3M NaCl) from Bioanalytical Systems. The perfluorinated ion-exchange polymer Nafion used in measuring the heterogeneous electron transfer rate constant of Ru-HPA was purchased as a 5% solution (Aldrich) and further diluted with 2-propanol. Kinetic experiments which were performed on air-saturated solutions were done without any special pretreatment and the cell was left

exposed to the atmosphere while experiments were in progress. The concentration of dioxygen in air-saturated solutions at ambient laboratory temperature was taken to be 0.28 mM. When the electron transfer rate was measured using oxygen-saturated solutions, the solution was sparged with dioxygen for at least 15 minutes and was sealed from the atmosphere. While the experiments were underway, a stream of dioxygen was passed over the solvent in order to minimize variation in the dioxygen concentration (assumed to be 1.4 mM). During the blank experiments, the solution was saturated with argon (minimum of 15 minute sparge) and the cells were again kept sealed from the atmosphere. Controlled potential electrolyses were done using a Bioanalytical Systems BAS100 or BAS100B electrochemical analyzer. The working electrode for these experiments was a piece of carbon cloth (Union Carbide, VCK grade), while the auxiliary and reference electrodes were the same as for the RDE experiments. A standard two-compartment cell was used to keep the working and auxiliary electrodes separated. The argon in these experiments was passed through two bubbling towers containing aqueous solutions of vanadium (II) to scavenge for any residual dioxygen in the gas, and then through a bubbling tower of water before reaching the electrochemical cell. The electron transfer rate constants were also measured spectroscopically using either a Hewlett-Packard HP8450A UV-visible spectrometer equipped with an HP89100A temperature controller and a Compaq DeskPro personal computer or an HP8452A spectrometer equipped with an HP89090A Peltier temperature controller and an HP Vectra 486/66 computer. All experiments were performed at ambient laboratory temperatures (22 ± 2 ^{o}C) except the kinetic experiments measured photometrically: these were thermostatted at 25 ^{o}C. The current-time curves from the kinetic experiments measured via RDE were digitized using a Logitech ScanMan Model 32 handheld scanner, a Gateway 2000 386SX/16 computer and Un-Scan-It (Silk Scientific Corp.). The digitized data were manipulated and graphed using Sigmaplot (version 5.0, Jandel Scientific).

3.3 *Results*

3.3.1 Homogeneous Electron Transfer Studies with Cobalt Oxalate

The search for suitable oxidants with which to study the electron transfer kinetics of the oxidation of $PRu^{II}(OH_2)W_{11}O_{39}^{5-}$ is detailed in the Discussion Section of this chapter. In the presence of an excess quantity of cobalt oxalate (minimum Co / Ru ratio of 5:1), the electron transfer between Co^{III} and Ru^{II} followed simple pseudo-first order kinetics. The rate of electron transfer was measured by following the decrease in absorbance of the Ru^{II}-HPA peak at 530 nm. This absorbance decays exponentially with time (Figure 3.1), allowing the calculation of the pseudo-first order rate constant from the slope of the $\ln(A_t - A_\infty)$ vs. time plot (Figure 3.2), where A_t is the absorbance at time = t after the reactants were mixed and A_∞ is the absorbance at "infinite" time. Table 3.1 contains data for the $Co^{III}(ox)_3$ / Ru^{II}-HPA et reaction at constant pH. Although the rate of reaction increases over the range of ionic strength investigated as expected, the magnitude of the rate enhancement (by a factor of about four) going from 0.05 to 1.0 M salt concentration seems to be rather small. While this result may seem to indicate serious problems with the data, this development is not as problematic as it initially seems and will be explained in the Discussion Section of this chapter. Table 3.2 contains a compilation of electron transfer rate data between cobalt oxalate and the reduced ruthenium heteropolyanion for experiments performed in solutions of varied pH. The range of pH investigated is approximately centered around the pK_a (5.1)[1] of the aquo group attached to the ruthenium center. Unfortunately, this survey could not be expanded, as experiments performed under more acidic conditions gave non-linear $\ln(A_t - A_\infty)$ vs. time plots, and more basic solutions were prone to have a significant amount of decomposition of the tungsten-oxo cage framework. Within the span of solution pH investigated, the et rate constant does not vary significantly.

Figure 3.1 Absorbance versus time curve for the reaction of 3.0 mM cobalt oxalate with 0.37 mM $PRu^{II}(OH_2)W_{11}O_{39}^{5-}$ in pH = 5.0 lithium acetate buffer (μ = 0.2 M) at 25 °C.

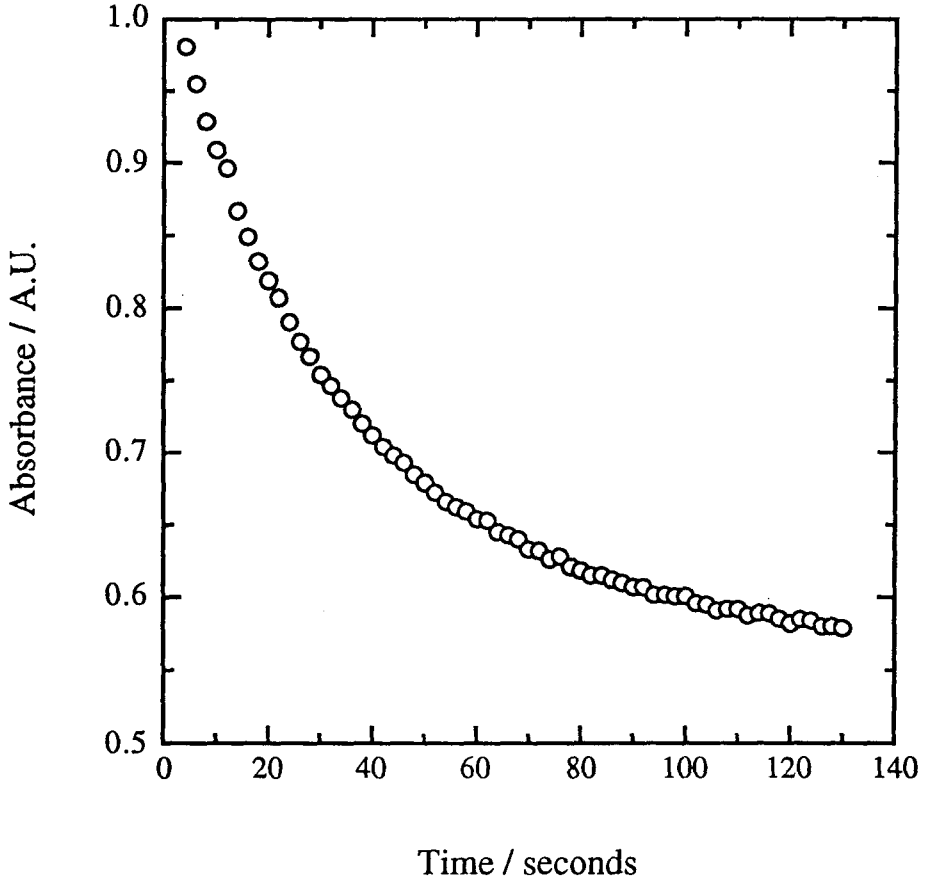

Figure 3.2 A log plot of the absorbance vs. time data from Figure 3.1 showing the pseudo-first order behavior of the cobalt oxalate / Ru-HPA system. These data span approximately 5.4 half-lives.

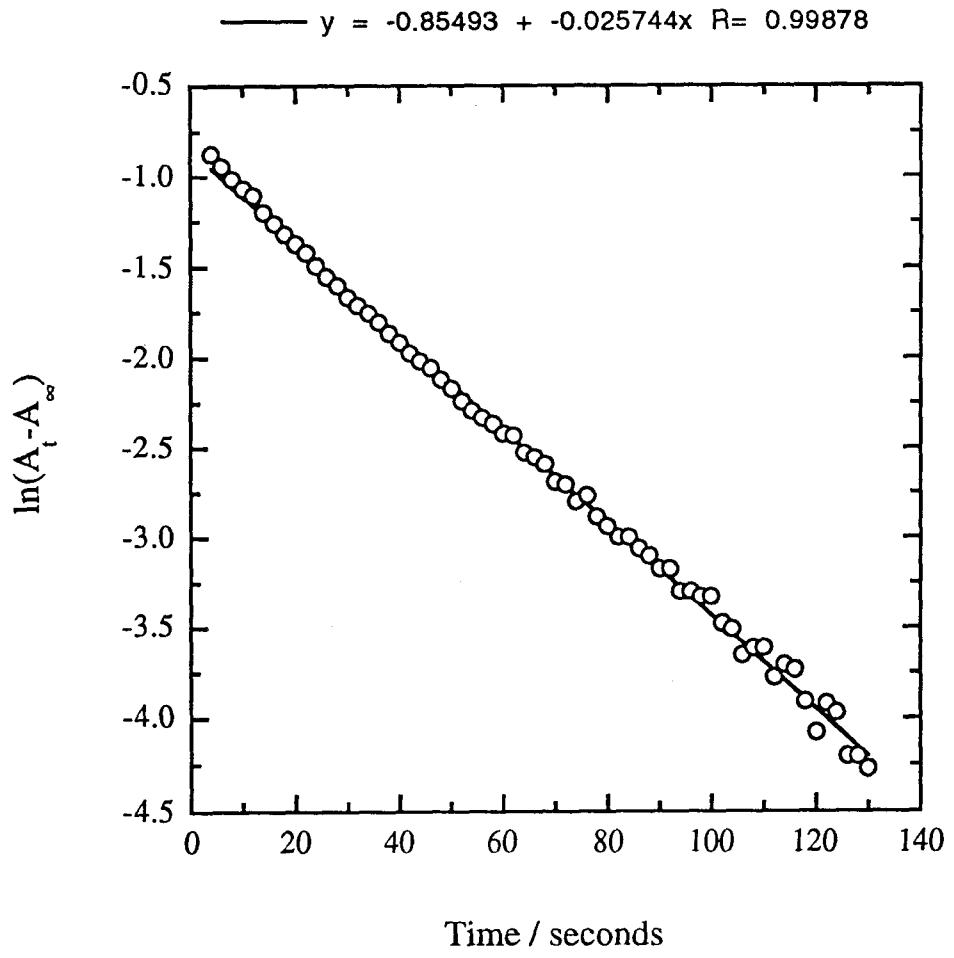

In order to be able to understand more clearly how the Ru-HPA's et characteristics relate to other ruthenium complexes, a comparison to a simple ruthenium "standard system" was performed. The choice of ruthenium hexaammine as the model ruthenium compound was based on the availability of electron transfer data for the oxidant used here and because of its well-studied et properties in general. The reaction between ruthenium hexaammine and cobalt oxalate is very fast, proceeding at 2.2 x 10^5 M^{-1} s^{-1}.[3] This rate constant is almost identical to that (1.5 x 10^5 M^{-1} s^{-1}) predicted by Marcus theory[14] (equation 1) if the self-exchange rate constants (k_{11} and k_{22}) for ruthenium hexaammine

$$k_x = (k_{11}k_{22}K_{eq}f)^{1/2} \qquad (1)$$

and cobalt oxalate are adjusted to the experimental ionic strength (μ = 55 mM) via the Debye-Hückel relationship[20] (equation 2), where k is the rate constant at ionic strength μ,

$$\log(k) = \log(k_o) + (2z_Az_BA\mu^{1/2})/(1 + \mu^{1/2}) \qquad (2)$$

k_o is the theoretical rate at ionic strength equal to zero, z_X is the charge on compound X, and A is a solvent-based factor which is equal to 0.509 for water at 298 K. The Marcus theory prediction for the reaction of Ru^{II}-HPA with $Co^{III}(ox)_3$ is dependent on the solution ionic strength and varies from 2 M^{-1} s^{-1} (at μ = 0.05 M) to 2 x 10^5 M^{-1} s^{-1} (at μ = 1.0 M).

3.3.2 Homogeneous Electron Transfer Studies with Dioxygen

Dioxygen was chosen as the second oxidant to study for several reasons. It is neutral and therefore calculating Marcus fits should be greatly simplified because of the lack of ionic strength-dependent rate constants. Also, it would be interesting to test whether the Ru^{II}-HPA could reduce dioxygen completely to water. Though not an initial goal of this project, an efficient dioxygen reduction catalyst is always worthy of further study. But, as expected, the ruthenated heteropolytungstate is just another catalyst which converts dioxygen to hydrogen peroxide. To measure whether Ru-HPA produces water or hydrogen peroxide during the electron transfer reaction with dioxygen, the following

experiment was done. An argon-flushed UV-visible cuvette was filled with 2 mL of a 0.41 mM Ru^{II}-HPA solution and sealed with a rubber septum. Upon addition of 150 μL of dioxygen-saturated solution, the decay in the absorbance (A) at 530 nm was monitored and found to decrease from 0.987 to 0.701. If dioxygen is reduced to water by the four-electron pathway, all of the ruthenium should now be in the tripositive state, but after bubbling dioxygen through the cuvette for several minutes, the absorbance was found to have decreased further to 0.420. The ratio of ΔA (partially oxidized Ru center) to ΔA (fully oxidized Ru center) is 50.4%. After taking into account the amount of dioxygen which leaked through the septum (by running a blank experiment where the injected solution was argon-saturated instead of O_2-saturated), this ratio was found to be 47.1%. If dioxygen was acting as a two-electron oxidant (thus producing only hydrogen peroxide), a ratio of 48.7% is predicted.

The electron transfer experiments were performed either by monitoring the decrease in absorbance of the Ru^{II} peak at 530 nm, or by rotating disk electrode voltammetry. Because of the low solubility of dioxygen in aqueous solvents, the concentration of Ru^{II}-HPA was in the range of 40-250 μM; thus producing small absorbances and even smaller ΔA during the electron transfer reactions, so an electrochemical method of rate measurement was favored. This type of experiment utilizes an RDE to monitor continuously the extent of reaction between dioxygen and Ru^{II}-HPA. By poising the RDE at a potential several hundred millivolts positive of the $Ru^{III/II}$ formal potential, a steady-state current is measured which decays as dioxygen oxidizes the ruthenium complex. Unlike spectroscopy, where the change in absorbance is fixed by the difference in extinction coefficient of the Ru^{II} and Ru^{III} forms of the complex, the change in current in the voltammetry experiment is determined by the rotation rate of the RDE: the faster the electrode is rotated, the larger the current. By rotating at 2500 rpm, changes of several microamps were observed for even the lowest

concentrations of Ru-HPA. The current vs. time plots (see Figure 3.3) were characterized by exponential decays just like the absorbance vs. time plots (Figure 3.4) when pseudo-first order conditions were used. As expected, both the spectroscopic and voltammetric data give linear log plots (Figures 3.5 and 3.6). Generally, dioxygen was the reactant in excess, but a few experiments were also done with the heteropolyanion in excess to verify that the reaction was first order in each reactant. Tables 3.3 and 3.4 contain data for the dioxygen/Ru^{II}-HPA electron transfer reaction at various solution pH and ionic strengths. At μ = 1.0 M, the et rate constant is 2.3 $\pm$ 1.3 M^{-1} s^{-1} over the entire pH range. As was the case when the oxidant was cobalt oxalate, there does not appear to be an appreciable change in the et rate when the solution pH is greater than the pK_a of the aquo ligand occupying the sixth coordination site on the ruthenium metal center. The kinetic data for the reduction of dioxygen by other ruthenium model compounds and related polyoxotungstates are found in Table 3.5. There seems to be a consistent problem in these data that the second order rate constant measured for air-saturated solutions is larger than the corresponding rate for dioxygen-saturated solutions. This will be analyzed in the Discussion Section, but for now I will assume that the slower rates are more accurate, since the ruthenium hexaammine/dioxygen rate more closely agrees with the literature value[4] when the solutions are O_2-saturated. Qualitatively, the magnitudes of the et rate constants for Ru^{II}-HPA and the model complexes are reasonable, since the driving forces for the electron transfer reactions are in the following order:

$$Ru^{II}(NH_3)_6 > Ru^{II}(NH_3)_5(OH_2) >> Ru^{II}\text{-HPA} \sim Fe^{II}\text{-HPA} \sim PW_{12}O_{40}^{4-}$$

As expected, the rate of electron transfer calculated from Marcus theory for Ru^{II}-HPA is much closer to the experimentally measured value now that ionic strength effects are not a factor. The calculated value of 10 M^{-1} s^{-1} is quite close to the average experimental value of 2.5 M^{-1} s^{-1}. Likewise, the Marcus prediction for ruthenium hexaammine (22 M^{-1} s^{-1}) is close to the experimentally measured rate of 73 M^{-1} s^{-1}. The only "failure"

Figure 3.3 Current versus time curve for the reaction of dioxygen (1.3 mM) with 0.091 mM $PRu^{II}(OH_2)W_{11}O_{39}^{5-}$ in pH = 5.4 lithium acetate buffer (μ = 1.0 M) at 22 °C. The EPG electrode was poised at +200 mV vs. Ag/AgCl and rotated at 2500 rpm.

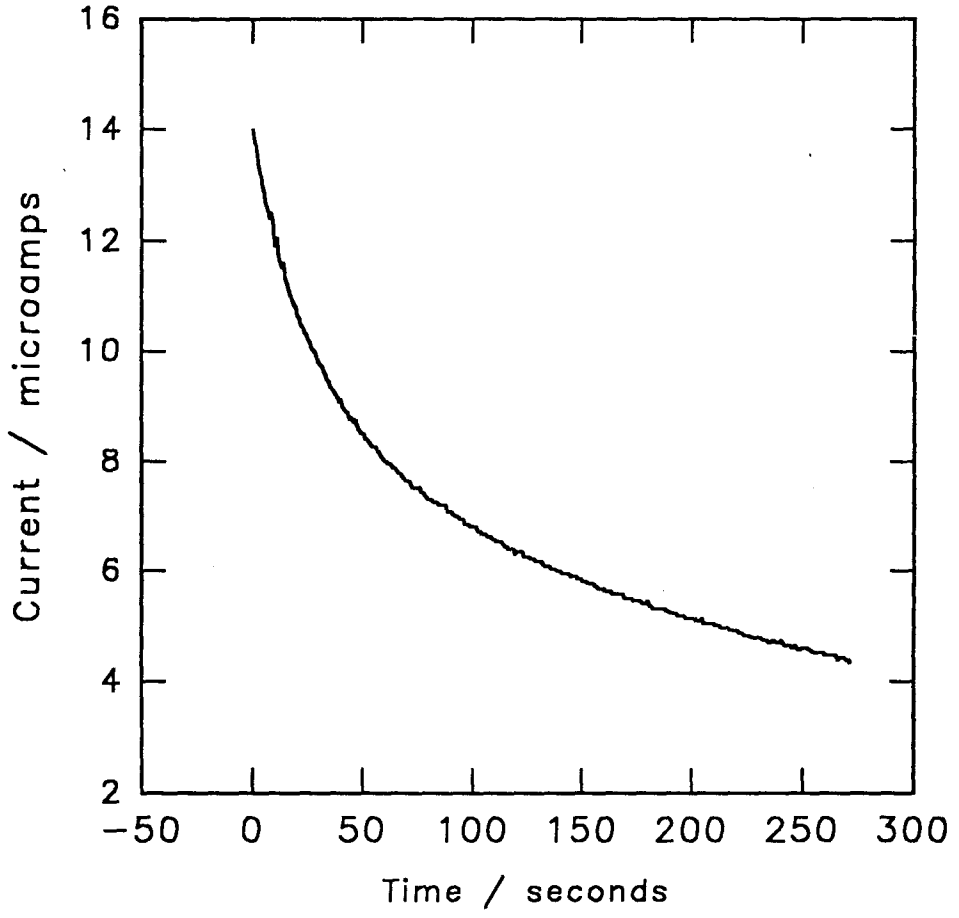

Figure 3.4 Absorbance versus time curve for the reaction of 1.0 mM dioxygen with 0.13 mM $PRu^{II}(OH_2)W_{11}O_{39}^{5-}$ in pH = 5.4 lithium acetate buffer (μ = 1.0 M) at 25 °C.

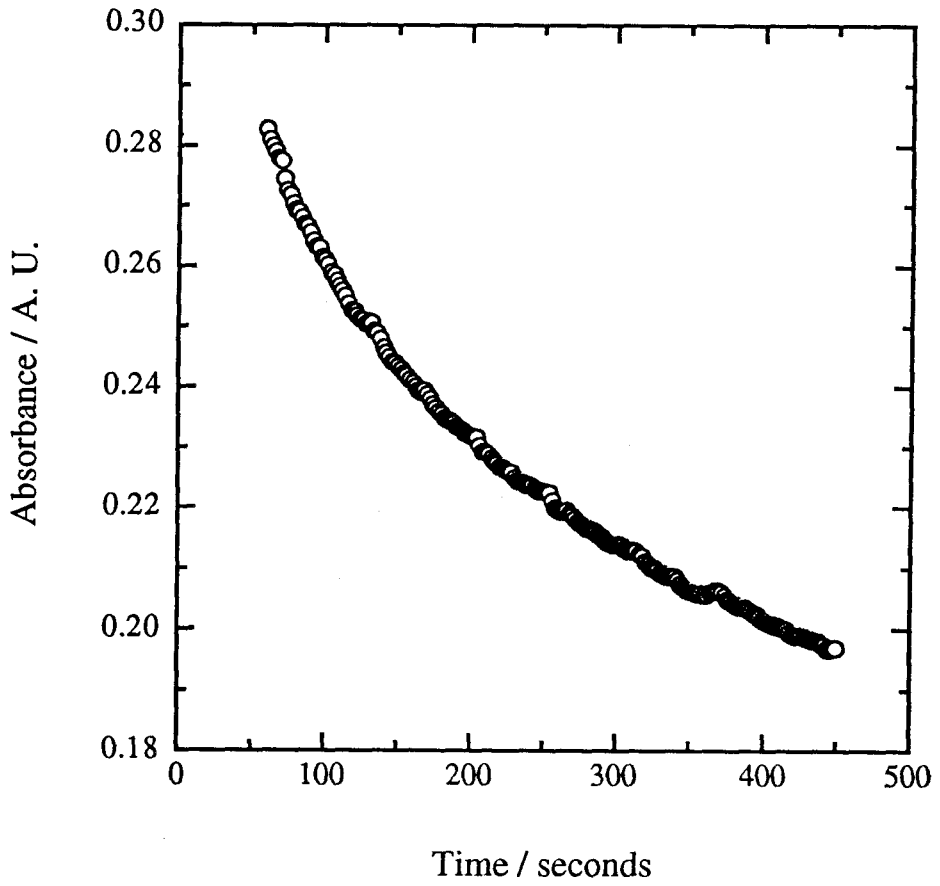

Figure 3.5 A log plot of the current vs. time data shown in Figure 3.3 showing the pseudo-first order behavior of the dioxygen / Ru-HPA system when monitored by RDE. These data span approximately 6.1 half-lives.

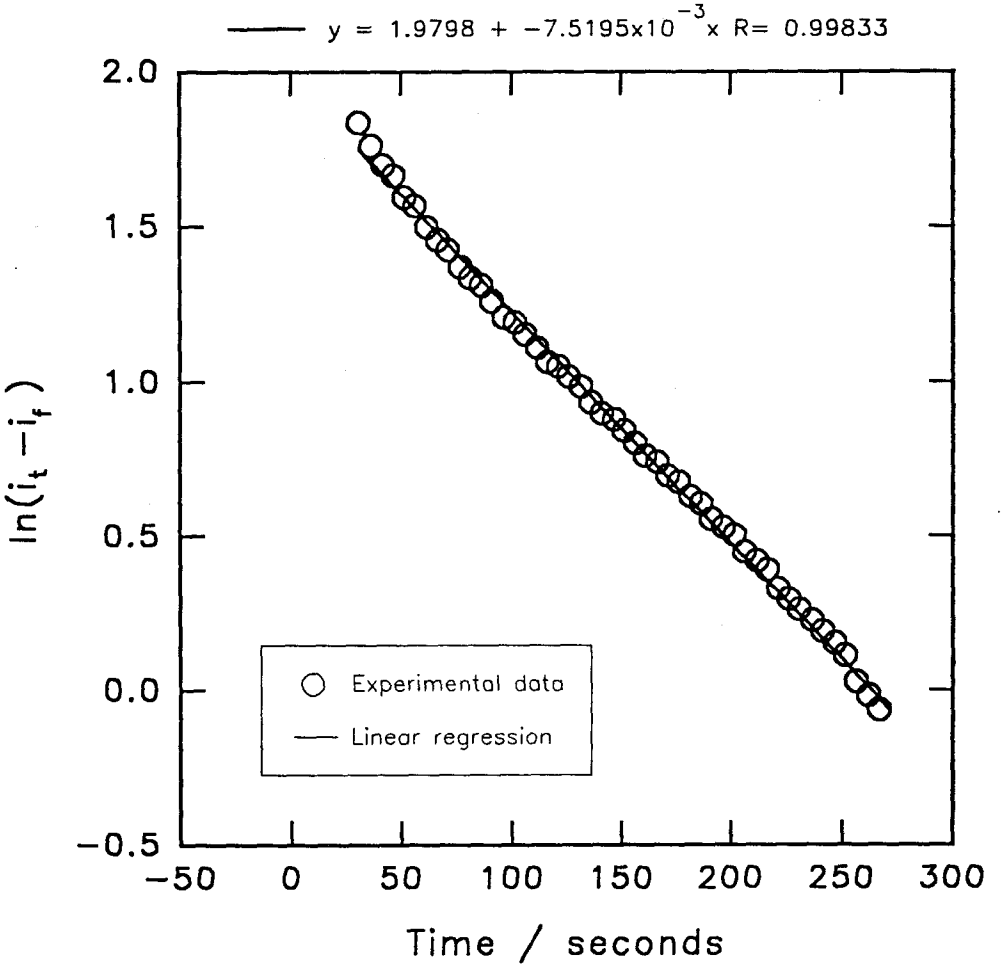

Figure 3.6 A log plot of the absorbance vs. time data shown in Figure 3.4 showing the pseudo-first order behavior of the dioxygen/Ru-HPA system when monitored by spectroscopy. These data span approximately 6.2 half-lives.

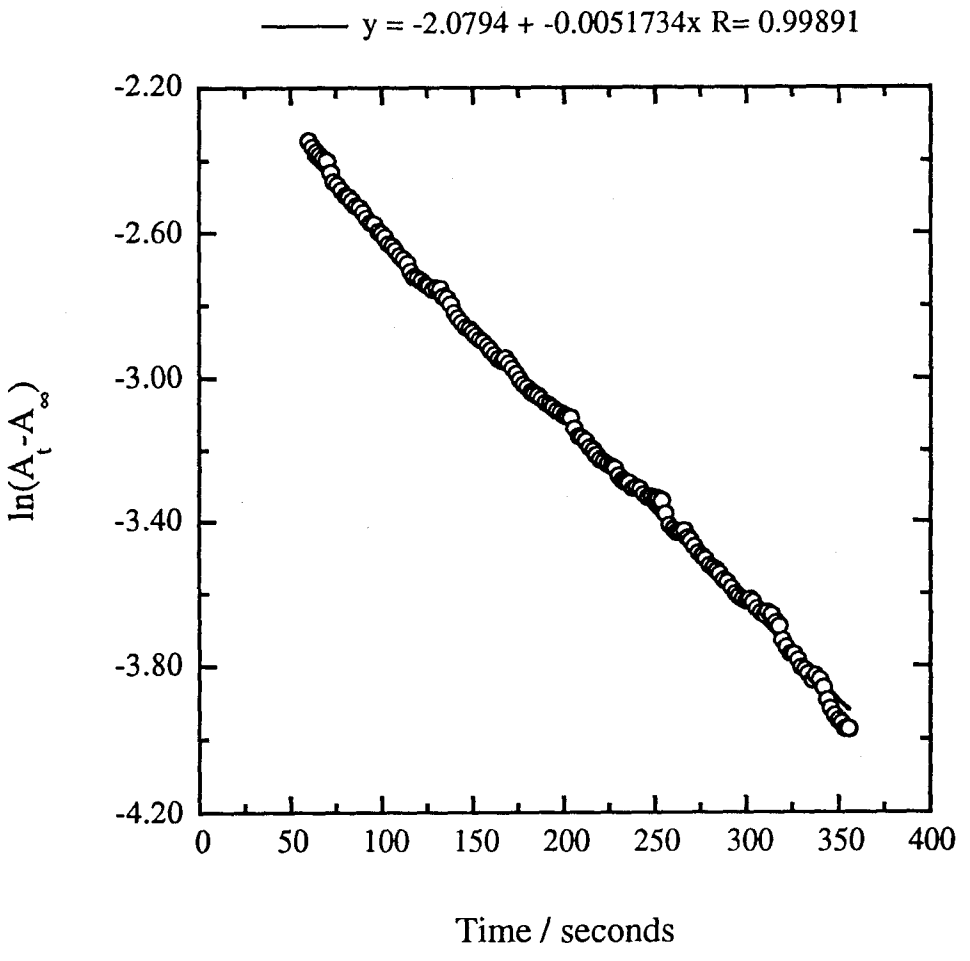

of Marcus theory occurs when trying to predict the rate of oxidation of reduced phosphotungstic acid by dioxygen. As shown in Table 3.5, the measured rate is 2.1 M^{-1} s^{-1}, but the calculated value is 82 M^{-1} s^{-1}.

3.3.3 Heterogeneous Electron Transfer Studies

In order to complete the comparison of the electron transfer properties of the ruthenium-substituted heteropolytungstate anion with ruthenium hexaammine, the heterogeneous et rate constant for Ru-HPA was studied. Using the method developed by Nicholson,[21] the heterogeneous et rate constant, k^o, can be extracted from cyclic voltammetric data via equation 3. The value of Ψ is directed related to the separation,

$$\Psi = [k^o(D_o/D_r)^{\alpha/2}]/[D_o\pi v(nF/RT)]^{1/2} \qquad (3)$$

ΔE_p, between the cathodic and anodic peaks of the CV. The relationship between ΔE_p and Ψ varies depending on how far beyond the peak potential the sweep goes before the scan is reversed. For the experiment described here, the potential scan was reversed at approximately 150 mV beyond the peak potential, and thus the ΔE_p / Ψ data used were those tabulated by Heinze.[22] Table 3.6 shows the data collected for both $Ru^{III}(NH_3)_6$ and Ru^{III}-HPA in a pH = 2.0 sodium sulfate buffer. Ruthenium hexaammine has a heterogeneous electron transfer rate constant[23] of about 1.2 cm s^{-1} and will be assumed to exhibit completely reversible behavior over the range of scan rates presented in Table 3.6. Thus any deviation from the theoretical value of ΔE_p = 60 mV will be attributed to uncompensated cell resistance. This value is then subtracted from the ΔE_p for Ru^{III}-HPA in order to get the peak separation "corrected" for IR drop, ΔE_p^*. Only the voltammograms which showed significant deviations from Nernstian behavior (i.e., ΔE_p^* > 75 mV) were used to calculate k^o. The average heterogeneous electron transfer rate constant for Ru^{III}-HPA measured by this technique is 3 x 10^{-2} cm s^{-1}. Because this value of k^o was determined from only three data points and because the cyclic voltammetric ΔE_p data did not smoothly increase with scan rate, this number is suspect and a second

method for determining k^o was also used. A rotating disk electrode was employed to record voltammograms for the reduction of Ru^{III}-HPA to Ru^{II}-HPA in a pH = 2.0 sodium sulfate buffer at several different rotation rates. For each curve, the background-subtracted current at several potentials on the rising portion of the wave is measured (Table 3.7). Using these data, a Koutecky-Levich plot[24] is constructed for each of the different potentials. These plots should be linear (equation 4)[25] and have y-intercepts

$$i^{-1} = (i_{kin})^{-1} + (i_{lim})^{-1} = (i_{kin})^{-1} + (0.201nFAC_o{}^*D_o{}^{2/3}\upsilon^{-1/6}\omega^{1/2})^{-1} \qquad (4)$$

equal to the kinetic component of the current to the minus one power. An example of a Koutecky-Levich plot using data in Table 3.7 is shown in Figure 3.7. By plotting $\log(i_{kin})$ vs. E, a Tafel plot[26] is obtained. By simply using this Tafel plot to find the value of i_{kin} at the formal potential of the ruthenium complex, k^o can be easily calculated from equation 5,[27] as the exponential term drops out and the bulk concentration of the

$$i_{kin} = (nFAC_o{}^*k^o)\exp[-\alpha nf(E - E^o)] \qquad (5)$$

ruthenium complex in solution and the area of the electrode used in the experiment are known. By this method, the heterogeneous electron transfer rate constant for Ru-HPA is about 7×10^{-3} cm s^{-1} for the data in Table 3.7, but this value varies by nearly two orders of magnitude depending on the experimental conditions (see Table 3.8).

An estimate of k^o can also be made via the Marcus theory for heterogeneous electron transfer.[13] By knowing the self-exchange rate constant, k_{11}, an estimate of k^o can be made from equation 6, where Z_{el} is the collision frequency at the electrode and

$$k^o = Z_{el}(k_{11}/Z_{soln})^{1/2} \quad \text{or} \quad k^o \sim (k_{11}/10^3)^{1/2} \qquad (6)$$

Z_{soln} is the collision frequency in the solution. Using a value[28] of 4×10^3 M^{-1} s^{-1} for the self-exchange rate constant for ruthenium hexaammine, a k^o of 2 cm s^{-1} is calculated, in good agreement with the experimentally measured value. Likewise, using Rong's value[1] of 1.2×10^6 M^{-1} s^{-1} for the k_{11} for Ru-HPA, a k^o of 35 cm s^{-1} is predicted by equation 6. Since this theoretical rate is several orders of magnitude larger than the values obtained

Figure 3.7 A Koutecky-Levich plot of 0.30 mM $Cs_4PRu(OH_2)W_{11}O_{39}$ in pH = 2.0 sodium sulfate buffer (μ = 0.9 M). The current was measured at E = -60 mV vs. SSCE for each rotation rate.

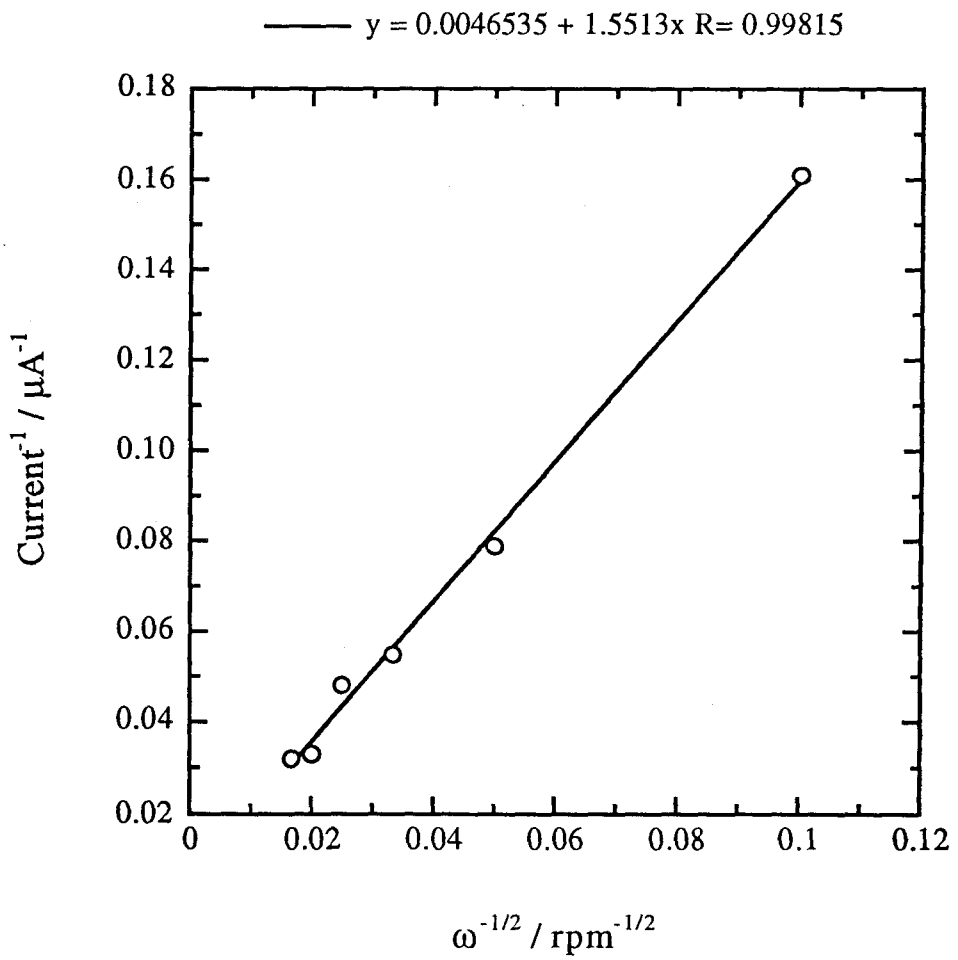

experimentally, the reported value of the self-exchange electron transfer rate constant (measured by ^{31}P NMR line broadening)[1] was initially called into question.

In order to calculate the self-exchange rate constant for Ru-HPA by an alternative method, the following experiment was performed. A glassy carbon electrode was spin-coated with a thin (approximately 100 nm) film of the persulfonated polymer Nafion, and then the sodium ions in this film were exchanged for ruthenium hexaammine. By using rotating disk voltammetry, the rate constant for the electron transfer reaction between $Ru^{II}A_6$ (A = NH_3) in the film (the electrode is held at a potential several hundred millivolts more negative than the $Ru^{III/II}A_6$ couple) and Ru^{III}-HPA in solution can be measured. In all these experiments, a small amount of RuA_6Cl_3 was added to the solution containing the heteropolytungstate, as it has been shown[29] that small quantities (2-10 μM) of the hexaammine salt in solution are quite effective at minimizing the leeching of the ruthenium salt out of the film without affecting the outcome of the experiment. Using the data in Table 3.9, the kinetic component of the RDE current can be obtained from the y-intercept of the Koutecky-Levich plot. Before continuing, a check of the system should be performed. If the current measured at the RDE is limited by the rate of electron transfer through the film, rather than by the rate of electron transfer between the two ruthenium complexes, then this experiment cannot provide the desired information. The current limited by the rate of electron "diffusion" through the Nafion film is called i_E,[30] and is easily obtained from chronocoulometric experiments performed

$$i_E = (\pi S^2)/(4FA\Gamma) \qquad (7)$$

in a pure supporting electrolyte solution, where S is the slope of the Anson plot,[31] F is Faraday's constant, A is the area of the electrode, and Γ is the amount of $Ru^{II}A_6$ in the film. In all of these experiments, i_E ranged from 350-400 μA, while the measured kinetic current was usually around 25-35 μA, so the current is definitely limited by the rate of et

between the two ruthenium species. The cross reaction rate constant, k_x, can then be calculated using equation 8,[32] where C_{HPA} is the concentration of Ru^{III}-HPA in solution

$$k_x = i_{kin}(FC_{HPA}\Gamma_m)^{-1} \quad (8)$$

and Γ_m is the amount of $Ru^{II}A_6$ close enough to the surface of the film to directly participate in the et reaction with the heteropolytungstate. This quantity has been reported to be 6.3×10^{-11} mol cm^{-2} for a Nafion film saturated with $Ru^{III}A_6$ as was the one used in this study.[33] From this experiment, k_x values in the range of $2\text{-}4 \times 10^7$ M^{-1} s^{-1} were obtained. The self-exchange rate constant for Ru-HPA can be calculated using Marcus theory[14] (equation 1) if some assumptions are made. First, the self-exchange rate constant for RuA_6 in the Nafion is assumed to be the same as it is in solution, and second, the f factor in the Marcus equation is set equal to unity. An average value of 2.4×10^6 M^{-1} s^{-1} is calculated for the heterogeneous rate constant for Ru-HPA, in fine agreement with the 1.2×10^6 M^{-1} s^{-1} value reported by Rong.[1]

A final attempt to accurately measure k^o for Ru-HPA was made by trying to fit the entire RDE curves measured using an EPG electrode with computer simulated data. Unfortunately, this tactic never produced unambiguous data, as the RDE curves were nearly Nernstian. This was demonstrated by the fact that (a) computer simulated data using the Nernst equation[34] (9) were nearly as good a fit to the experimental curves as

$$E = E_{1/2} + (RT/nF)\ln[(i_{lim} - i)/i] \quad (9)$$

were the data generated by the quasi-reversible version of the Levich equation[35] (10) using the optimized values of k^o and α (see Figure 3.8), and (b) Tomes plots[34] (see

$$i^{-1} = (nFC_o^*Ak_f)^{-1}[1 + (D_o^{-2/3}k_f + D_R^{-2/3}k_b)/(0.201\upsilon^{1/6}\omega^{1/2})] \quad (10)$$

Figure 3.9) for RDE curves measured under various solution pH conditions had an average slope of 58.3 mV (the purely Nernstian value is theoretically 59.1 mV). No other attempts were made to measure the heterogeneous electron transfer rate constant of the ruthenium-substituted heteropolytungstate anion.

Figure 3.8 (A). Comparison of experimental RDE data (solid line) and the fit (open circles) calculated from the quasi-reversible Levich equation. Best fit occurred when $\alpha = 0.75$, $k^o = 2.3 \times 10^{-3}$ cm s^{-1}, and $\omega = 1600$ rpm.
(B). Comparison of the two calculated fits to the experimental RDE data: quasi-reversible Levich equation (open cicles) and the Nernst equation (open squares). The Levich fit was calculated using the same parameters as in (A).

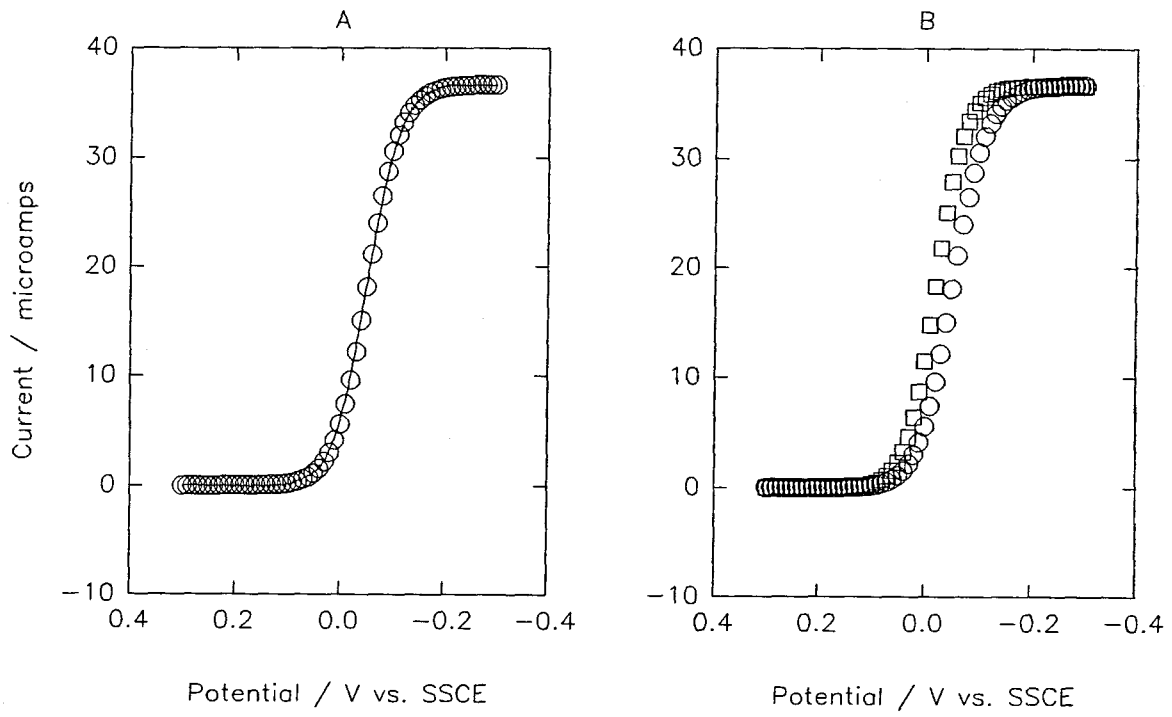

Figure 3.9 Tomes plot for 0.30 mM $Cs_4PRu(OH_2)W_{11}O_{39}$ in pH = 2.0 sodium sulfate buffer (μ = 0.9 M) at 900 rpm.

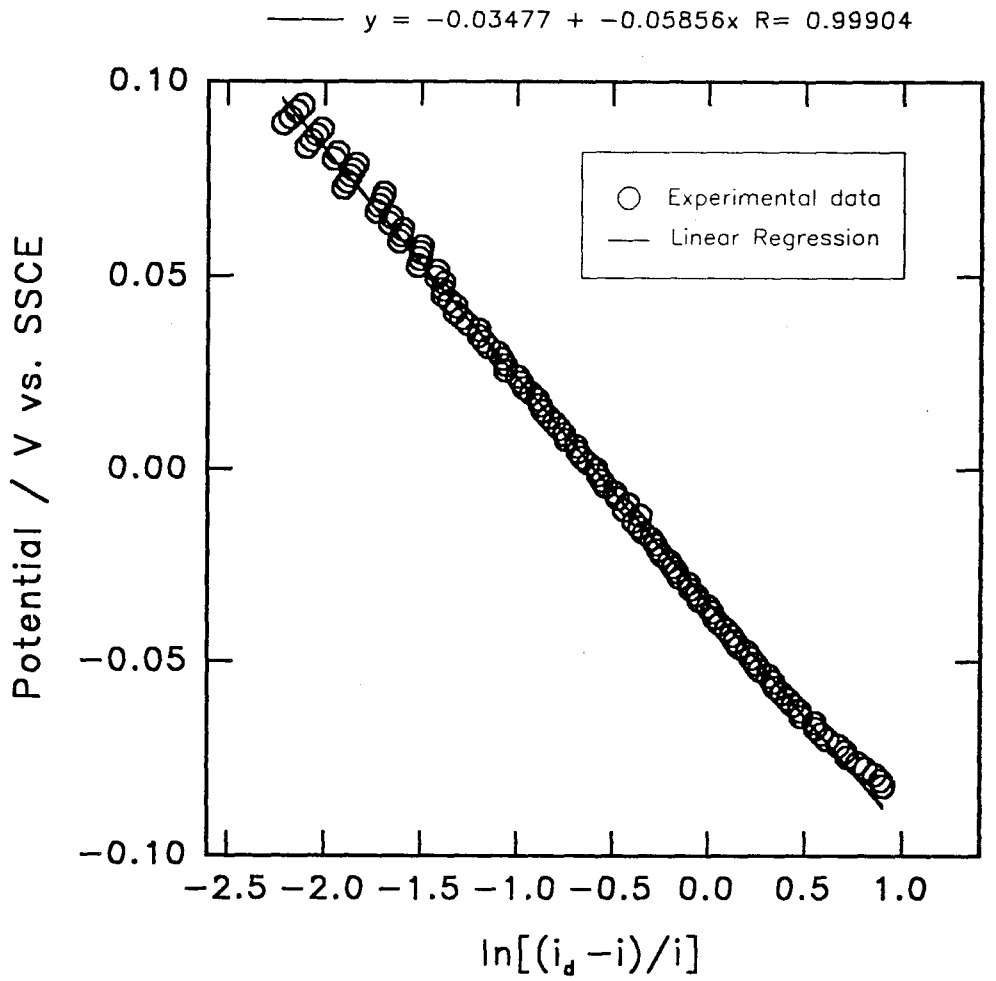

3.4 *Discussion*

In the beginning of the electron transfer work with Ru^{II}-HPA, the goal was to pick a couple of oxidants which have been studied with common ruthenium (II) complexes and then contrast and compare the homogeneous electron transfer rate for Ru^{II}-HPA with these model ruthenium compounds. Unfortunately, the first choice for an oxidant, cobalt hexaammine, was a poor one. Mixing $Co^{III}A_6$ (or any multiply-charged cationic oxidant) with the anionic Ru^{II}-HPA merely causes the precipitation of the ruthenium complex with no electron transfer detected. Choosing a neutral oxidant was easy enough (since dioxygen was used to oxidize Ru^{II}-HPA in the synthesis of Ru^{III}-HPA), but finding an anionic oxidant which had a reasonable driving force (the $Fe^{III}(CN)_6$ / Ru^{II}-HPA reaction, for example, is much too fast to measure without a stopped flow apparatus), no spectroscopic interferences with Ru^{II}-HPA (Co^{III}(edta) has a MLCT band at the exact same wavelength as Ru^{II}-HPA), and well-documented et data with Ru^{II} model complexes was not easy. Fortunately, cobalt oxalate satisfies all of these criteria and was chosen as the anionic oxidant for this study.

3.4.1 Electron Transfer to Cobalt Oxalate

The first oxidant studied was cobalt oxalate and right from the beginning it was obvious that this electron transfer reaction was unusual. As shown in Table 3.1, there is almost no change in the et rate when the solution ionic strength is varied by nearly two orders of magnitude. Assuming a simple correlation between μ and et rate constant, such as in the Debye-Hückel equation (2), a change in ionic strength from 50 mM to 1.0 M should produce an increase in rate of about five orders of magnitude. The experimental variation of a factor of four is almost within experimental error, implying that $PRu(OH_2)W_{11}O_{39}^{5-}$ acts as if it is nearly uncharged. This discrepancy leads to the lack of any correlation between the rate calculated by Marcus theory and the experimental

rate. However, I believe this deviation from the expected rates is not a case of the failure of Marcus theory as much as an example of poor assumptions leading to poor results. The Debye-Hückel equation approximates the reactants as point charges, and while this may be a fair assumption for species such as protons or chloride ions, it most certainly is not the case with heteropolyanions. The calculated hydrodynamic radius for Ru-HPA is on the order of 8 Å, so the 5- charge on the complex is spread over a large surface area. This is the same behavior that was observed when studying the ligand exchange kinetics between $PRu^{II}(OH_2)W_{11}O_{39}^{5-}$ and *N*-methylpyrazinium; namely, the Ru-HPA acts as if it has a much lower effective charge than the 5- formally assigned to it (see Section 2.4.3). Overall, it is not difficult to imagine that the $Co^{III}(ox)_3$ oxidant experiences only a small fraction of the 5- charge attributed to the Ru-HPA, and thus little change occurs in the electron transfer rate when the ionic strength is varied.

The electron transfer reaction between Ru^{II}-HPA and $Co^{III}(ox)_3$ was also studied at constant ionic strength to see if changing the solution pH had any effect on the rate constant. Assuming a simple outer sphere electron transfer mechanism, no change in the rate is expected when the pH is less than the pK_a of the aquo ligand on Ru^{II}-HPA (5.1), but a slowing of the rate at solution pH greater than 5.1 would not be surprising, as the aquo ligand in the sixth coordination site of the ruthenium (II) center would have to lose a proton as well as an electron. On the other hand, increasing the solution pH > pK_a will cause the formal potential of the $Ru^{III/II}$ couple to shift to more negative values, increasing the driving force of the reaction and thus a faster rate should be observed. Unfortunately, experimental difficulties limit the range of pH that can be surveyed. Above pH = 6.0, the cage is unstable and begins to decompose to WO_4^{2-}. Although the electron transfer rate should be measurable down to at least pH = 0, below pH = 4.0 the plots of $\ln(A_t - A_\infty)$ vs. time are non-linear. This deviation from pseudo-first order behavior most likely indicates the presence of an impurity, such as copper, which could

catalyze the reaction, similar to the problems that Taube[36] and Shepherd[37] had with iron catalyzing the reaction of $Ru^{II}A_6$ with dioxygen. Fortunately, measuring precise electron transfer rate data over a large pH range was not the primary goal of this work, so measurements were restricted to pH values that yielded linear $\ln(A_t - A_\infty)$ vs. time plots. Considering the fairly small pH range which has been investigated, it appears that there is little change in the et rate with pH.

3.4.2 Electron Transfer to Dioxygen

The electron transfer studies using dioxygen as the oxidant were simplified by the fact that as a neutral species, no ionic strength dependence of the rate should exist. Kinetic data for the reaction between Ru^{II}-HPA and dioxygen show little variation (see Tables 3.3 and 3.4) in the rate when either the ionic strength or pH of the medium is changed. Finding a consistent value of 2.5 M^{-1} s^{-1} for this rate constant was encouraging, so the theoretical rate constant was calculated via the Marcus theory (10 M^{-1} s^{-1}) and was found to be close to the experimentally determined value. Two ruthenium compounds were chosen as model systems to compare the heteropolytungstate data with: $Ru^{II}A_6$ and $Ru^{II}A_5(OH_2)$. Ruthenium hexaammine was chosen again because its well-characterized behavior, simple outer-sphere electron transfer mechanism, and known self-exchange rate constant make it an ideal model compound. Aquopentaammine ruthenium (II) was also investigated since the presence of the aquo group makes it more closely resemble the ruthenium center in the polyoxotungstate cage than does ruthenium hexaammine. In addition, the rate of its reaction with dioxygen was slow enough to be measured without requiring a stopped-flow apparatus (unlike the $Co^{III}(ox)_3/Ru^{II}A_5(OH_2)$ system, which was too fast to measure). Initially, there was some discrepancy between the experimentally measured value of the rate constant for the reaction of $Ru^{II}A_6$ with O_2 (this work) and the literature value published by Taube.[4] Fortunately, review of later papers[36] by the same author indicated that the value reported in this initial paper (126 M^{-}

^{1} s^{-1}) was in error; the authors most likely forgot to take into account that dioxygen is a two electron oxidant, and thus all of their rate constants were off by a factor of two. Another problem encountered was that the rate constant for electron transfer measured in O_2-saturated solutions was always smaller than when the solutions were saturated with air (see Table 3.5). This problem occurred for both $RuA_5(OH_2)$ and RuA_6 (these were the only reductants that reacted fast enough to measure accurately the rate of et with air-saturated solutions). This result is not surprising as several authors[36,37] have noted that dioxygen et reactions with ruthenium ammine complexes are often complicated by adventitious Fe^{II} impurities which catalyze the reduction of the hydrogen peroxide produced by the Ru^{II}/O_2 reaction. Shepherd[37] was successful in measuring H_2O_2-ruthenium ammine et rates by avoiding acetate buffers (thought to contain iron) in favor of phosphate buffers which render iron impurities inocuous. As shown in Table 3.5, this switch in media seems to be beneficial for $RuA_5(OH_2)$ but not RuA_6. The trouble could be more basic than a problem with the buffer salt; perhaps there is a metal impurity in the acid or contamination of the glassware which leads to this discrepancy. The largest rate increase observed (38%, for $RuA_5(OH_2)$ at pH = 5.4) is well within the 100% increase in rate observed by Stanbury.[36] This problem was not pursued any further since the data for O_2-saturated solutions seemed to be fairly accurate. That was the only system studied when the rate was measured using the three heteropolyanions. The value of about 65 M^{-1} s^{-1} for RuA_6 correlates nicely with the value reported here (Table 3.5). Again, Marcus theory is able to predict accurately the kinetics of this reaction, yielding an expected rate constant of 22 M^{-1} s^{-1}. Since the self-exchange rate constant for $Ru^{II}A_5(OH_2)$ is not known, it was not possible to calculate a rate based on Marcus theory for its oxidation by dioxygen. The experimental rates for these three ruthenium compounds seem to be controlled simply be the driving force of the reaction. While the two model complexes have similar formal potentials ($Ru^{III/II}A_6$ is slightly more negative),[38] the $Ru^{III/II}$ couple

for Ru-HPA appears nearly 200 mV more positive. The electron transfer rates follow the same trend, with ruthenium hexaammine having a slightly larger rate constant than its pentaammineaquo counterpart, and both of these reacting more than an order of magnitude faster than the heteropolytungstate.

Since the dioxygen system appears to be uncomplicated, Ru^{II}-HPA was also compared to two heteropolytungstate model complexes to see what effect (if any) the ruthenium metal center has on the electron transfer. The $Fe^{III/II}$ formal potential of $Cs_4PFe(OH_2)W_{11}O_{39}$ is generally within 30 mV of the $PRu^{III/II}(OH_2)W_{11}O_{39}$ couple (more positive than the Ru peak when they are not equal). As expected, since the driving force of the electron transfer reaction is nearly equal to that of Ru-HPA, Fe^{II}-HPA reacts with dioxygen at approximately the same rate (1 M^{-1} s^{-1}) as Ru^{II}-HPA. Likewise, the first one electron reduction wave for phosphotungstic acid in molar acid is also within 5 mV of the $Ru^{III/II}$ peak, and as expected, the rate (2 M^{-1} s^{-1}) is nearly equal to that for Ru-HPA. The calculated rate for $PW_{12}O_{40}^{4-}$ is the only case for the dioxygen et reactions where the experimental value (2 M^{-1} s^{-1}) differs significantly from the theoretical number (82 M^{-1} s^{-1}). This appears to be due to a slight controversy concerning the true value of the self-exchange rate constant for the first electron reduction of $PW_{12}O_{40}^{3-}$. The value used in the above calculation (8.2 x 10^7 M^{-1} s^{-1}) was measured via ^{31}P NMR line-broadening,[39] but another value (1.5 x 10^6 M^{-1} s^{-1}) was reported using ^{17}O NMR at a slightly different ionic strength.[40] If this smaller self-exchange rate constant is used in the Marcus theory calculation, the predicted rate is only 12 M^{-1} s^{-1}, much closer to the experimental value than the number reported above.

3.4.3 Heterogeneous Electron Transfer

All attempts at directly measuring the heterogeneous electron transfer rate constant for the ruthenium-substituted heteropolytungstate anion were unsuccessful. Using the changes in the $Ru^{III/II}$ peak separation in the cyclic voltammetric experiments

to measure k^o is the least accurate method because experimental factors such as the cell resistance also play a part in this phenomenon. Separating the contributions of these various factors to the peak separation is difficult. Comparisons to the $Ru^{III/II}$ couple of ruthenium hexaammine were unsuccessful, probably due to inaccuracies in the ΔE_p data for Ru-HPA. As seen in Table 3.6, the peak separation does not increase smoothly with faster scan rates, but rather abruptly jumps to larger values on at least two different occasions. Realizing the weaknesses of the experiment, another method was investigated. By measuring the kinetic component of the limiting current in an RDE experiment, the heterogeneous electron transfer rate constant can be calculated using equation 5. This method is more accurate because the kinetic component of the RDE current can be easily obtained directly from the experimental data (by making a Koutecky-Levich plot). The only drawback to this method is that as the k^o increases, the quantity that is being measured, i_{kin}^{-1}, approaches zero. This significantly increases the error in measuring i_{kin} and eventually leads to Tafel plots which are non-linear. This seems to be true for the heteropolyanion, as k^o calculated by this method varies over nearly three orders of magnitude. A final attempt to extract the heterogeneous electron transfer rate constant from the RDE data was made by trying to fit the experimental curve using the Levich equation for quasi-reversible couples (equation 11) and optimizing the variables. Unfortunately, k^o was too large to measure by this method because the data fit the Nernstian response theory. This evidence was further supported by the fact that Tomes plots of the RDE data also indicated that the $Ru^{III/II}$ couple was behaving in a Nernstian fashion.

The only experiment which was able to provide any truly useful information was the measurement of the self-exchange rate constant of $Ru^{III/II}$-HPA. This experiment also makes use of RDE, but has the important difference being that the signal measured (limiting current) increases as the rate of reaction increases. The only assumption made

in this case is that the self-exchange rate constant of RuA_6 inside the Nafion film is comparable to that in solution. Results published previously[33] indicate that this is at least a reasonable estimation of the true value. Indeed, the self-exchange rate constant calculated for Ru-HPA by this method (2.4×10^6 M^{-1} s^{-1}) is in excellent agreement with the ^{31}P NMR-derived value in the literature (1.2×10^6 M^{-1} s^{-1}).[1] Using Marcus theory for heterogeneous electron transfer (see equation 6), an estimate of k^o can be made from the self-exchange rate constant. Using the data for Ru-HPA, a value of 35-50 cm s^{-1} is obtained. This number is about two orders of magnitude larger than the heterogeneous electron transfer rate constant of RuA_6 (1.2 cm s^{-1}),[23] so even if the Marcus equation overestimates k^o by a factor of 10, it is clear that measuring k^o for Ru-HPA will be impossible using conventional electrochemical methods.

3.5 *Conclusions*

In general, the electron transfer studies provided evidence that the ruthenium-substituted heteropolytungstate anion is a fairly straightforward electron transfer system. With the exception of the previously noted tendency to act as if it is much less charged than formally dictated, the Ru-HPA et reaction is quite comparable to both the ruthenium and the heteropolyanion model systems. When the oxidant is $Co^{III}(ox)_3$, the non-ideal behavior of the HPA precludes using Marcus theory to make an accurate prediction of the electron transfer rate. A qualitative comparison to the model species $Ru^{II}A_6$ indicates that the rate measured for Ru^{II}-HPA is not unrealistic. True, the rate for $Ru^{II}A_6$ is four orders of magnitude larger than the heteropolytungstate, but then it also has an extra 200 mV driving force and attractive electrostatic interactions in its favor.

When dioxygen is the oxidant, the rate of electron for Ru^{II}-HPA is reasonable in both a qualitative and quantitative sense. All of the reductants studied have rates of

electron transfer which correlate nicely with the amount of driving force the reaction with O_2 possesses. When the information needed to calculate a rate constant is available, these numbers are generally in fine agreement with the experimentally measured values.

Although the et data for Ru^{II}-HPA oxidation at various solution pH's is rather limited, especially at pH's greater than the pK_a of $PRu(OH_2)W_{11}O_{39}^{4-}$, the general trend emerging is that the rate of electron transfer above and below the pK_a value are nearly the same. While the rate above the pK_a might be expected to slow since the ligand on the metal center has to rearrange from aquo to hydroxo, this is not the only factor which has to be considered. As the pH increases beyond the pK_a, the $Ru^{III/II}$ potential shifts to more negative values, thus increasing the driving force of the electron transfer reaction. When both of these trends are considered, it is not surprising that there is not much change in the et rate whether the pH is above or below the heteropoly's pK_a value.

Finally, the electron transfer studies were inconclusive in determining whether the electron added to Ru^{III}-HPA is delocalized over the entire cage. The fact that the self-exchange rate constant for Ru-HPA is three orders of magnitude larger than that for RuA_6, five orders of magnitude larger than that for $Ru(OH_2)_6$, and approximately equal to that of phosphotungstic acid, which is known to have its extra electron delocalized over all of its 12 tungsten atoms, is the evidence on which Pope based this hypothesis. On the other hand, the rate data, especially for the reaction with $Co^{III}(ox)_3$, seem to contradict this claim. If $Co^{III}(ox)_3$ could approach the cage from any direction, instead of being forced to approach head-on towards the ruthenium atom, it seems likely statistically that more et reactions would occur at one of the eleven tungsten atoms rather than the single ruthenium center. This being the case, the anion-anion repulsion should be greater for the encounter with the bulk of the cage compared to doing et with the ruthenium center, which should be positively charged. But this would lead to a more significant ionic strength dependence than is observed. Although the evidence is not conclusive, it

seems more likely that the electron is delocalized, and that the dilution of the heteropolytungstate's charge due to its large surface area occurs to such an extent that the traits that we expect to observe (such as a strong dependence of the rate on ionic strength) simply are too weak to be unambiguously detected.

References

1. Rong, C.; Pope, M. T. *J. Am. Chem. Soc.* **1992,** *114,* 2932.

2. Lane, B. C.; Lester, J. E.; Basolo, F. *J. Chem. Soc., Chem. Commun.* **1971,** 1618.

3. Rillema, D. P.; Endicott, J. F.; Patel, R. C. *J. Am. Chem. Soc.* **1972,** *94,* 394.

4. Pladziewicz, J. R.; Meyer, T. J.; Broomhead, J. A.; Taube, H. *Inorg. Chem.* **1973,** *12,* 639.

5. a) Liu, D. K.; Brunschwig, B. S.; Creutz, C.; Sutin, N. *J. Am. Chem. Soc.* **1986,** *108,* 1749.
   b) Melton, J. D.; Espenson, J. H.; Bakac, A. *Inorg. Chem.* **1986,** *25,* 4104.
   c) Xiao, X. M.; Haga, M. A.; Matsumurainoue, T.; Ru, Y.; Addison, A. W.; Kano, K. *J. Chem. Soc., Dalton* **1993,** 2477.

6. Yonemoto, E. H.; Riley, R. L.; Kim, Y. I.; Atherton, S. J.; Schmehl, R. H.; Mallouk, T. E. *J. Am. Chem. Soc.* **1992,** *114,* 8081.

7. Finke, R. F.; Vögeli, R. H.; Langanis, E. D.; Bökelheide, V. *Organometallics* **1983,** *2,* 347.

8. a) Prasad, D. R.; Ferraudi, G. *J. Phys. Chem.* **1982,** *86,* 4037.
   b) Barley, M. H.; Dolphin, D.; James, B. R. *J. Chem. Soc., Chem. Commun.* **1984,** 1499.

9. a) Orellana, G.; Kirschdemesmäker, A.; Barton, J. K. *Photochem. and Photobiol.* **1991,** *54,* 499.
   b) Murphy, C. J.; Arkin, M. R.; Jenkins, Y.; Ghatlia, N. D.; Bossmann, S. H.; Turro, N. J.; Barton, J. K. *Science* **1993,** *262,* 1025.

10. a) Anast, J. M.; Hamburg, A. W.; Margerum, D. C. *Inorg. Chem.* **1983,** *22,* 2139.
    b) Casimiro, D. R.; Richards, J. H.; Winkler, J. R.; Gray, H. B. *J. Phys. Chem.* **1993,** *97,* 13073.
    c) Meier, M.; Vandeldik, R.; Chang, I. J.; Mines, G. A.; Wuttke, D. S.; Winkler, J. R.; Gray, H. B. *J. Am. Chem. Soc.* **1994,** *116,* 1577.

11. a) Marcus, R. A. *J. Phys. Chem.* **1963,** *67,* 853.
    b) Marcus, R. A. *Ibid.* **1968,** *72,* 891.

12. Marcus, R. A. *J. Chem. Phys.* **1965,** *43,* 679.

13. Marcus, R. A. *Electrochim. Acta* **1968,** *13,* 995.

14. Marcus, R. A.; Sutin, N. *Biochim. Biophys. Acta* **1985,** *811,* 265.

15. Tézé, A.; Hervé, G. *J. Inorg. Nucl. Chem.* **1977,** *39,* 999.

16. Bernhard, P.; Biner, M.; Ludi, A. *Polyhedron* **1990,** *9,* 1095.

17. Vogt, L. H., Jr.; Katz, J. L.; Wiberley, S. E. *Inorg. Chem.* **1965,** *4,* 1157.

18. Toth, J. E.; Anson, F. C. *J. Electroanal. Chem.* **1988,** *256,* 361.

19. Palmer, W. G. *Experimental Inorganic Chemistry*; Cambridge Univ. Press: Cambridge, 1954; p 550.

20. Espenson, J. H. *Chemical Kinetics and Reaction Mechanisms*; McGraw-Hill: New York, 1981; p 176.

21. Nicholson, R. S. *Anal. Chem.* **1965,** *37,* 1351.

22. Heinze, V. J. *Angew. Chemie* **1984,** *96,* 823.

23. Hsueh, C. C.; Brajter-Toth, A. *Anal. Chem.* **1993,** *65,* 1570.

24. Levich, V. G. *Physicochemical Hydrodynamics*; Prentice-Hall: Englewood Cliffs, NJ, 1962; pp 345-357.

25. Bard, A. J.; Faulkner, L. R. *Electrochemical Methods*; J. Wiley and Sons: New York, 1980; p 291.

26. Ref. 25, p 106.

27. Ref. 25, p 107.

28. Taube, H. In *Advances in Chemistry*; Raymond, K. N., Ed.; ACS Symposium Series 162: Washington, DC, 1977; p 127.

29. Xie, Y.; Anson, F. C. *J. Electroanal. Chem.* **1993,** *349,* 325.

30. Andrieux, C. P.; Saveant, J.-M. *Ibid.* **1982,** *134,* 163.

31. Anson, F. C. *Anal. Chem.* **1966,** *38,* 54.

32. Oyama, N.; Anson, F. C. *Ibid.* **1980,** *52,* 1192.

33. Sabatani, E.; Anson, F. C. *J. Phys. Chem.* **1993,** *97,* 10158.

34. Ref. 25, p 160.

35. Ref. 25, p 292.

36. Stanbury, D. M.; Haas, O.; Taube, H. *Inorg. Chem.* **1980,** *19,* 518.

37. Kristine, F. J.; Johnson, C. R.; O'Donnell, S.; Shepherd, R. E. *Ibid.* **1980,** *19,* 2280.

38. Lim, H. S.; Barclay, D. J.; Anson, F. C. *Ibid.* **1972,** *11,* 1460.

39. Kozik, M.; Hammer, C. F.; Baker, L. C. W. *J. Am. Chem. Soc.* **1986,** *108,* 2748.

40. Piepgrass, K. W. Ph.D. Thesis, Georgetown University, 1989.

Table 3.1 Electron transfer data for the reaction of cobalt oxalate with Ru-HPA at various solution ionic strengths (pH constant at 5.0 using a lithium acetate buffer) at 25 °C.

μ, M	$[Ru^{II}]$, mM	$[Co^{III}]$, mM	k_{obs}, s^{-1}	k, M^{-1} s^{-1} a
0.05	0.381	2.97	1.7×10^{-2}	5.6 (4)
	0.370	3.46	1.9×10^{-2}	5.4 (3)
	0.364	3.97	2.1×10^{-2}	5.4 (4)
0.2	0.039	0.207	2.3×10^{-3}	11 (2)
	0.038	0.334	3.2×10^{-3}	9.6 (2)
	0.038	0.468	4.7×10^{-3}	10 (1)
	0.383	2.45	2.5×10^{-2}	10 (2)
	0.368	2.97	2.2×10^{-2}	7.5 (3)
	0.367	3.48	3.4×10^{-2}	9.8 (4)
	0.353	3.98	3.2×10^{-2}	8.0 (2)
	0.331	4.61	2.9×10^{-2}	6.3 (1)
1.0	0.030	0.248	4.5×10^{-3}	18 (2)
	0.030	0.369	6.1×10^{-3}	16 (2)
	0.030	0.465	7.7×10^{-3}	17 (2)
	0.369	2.97	5.8×10^{-2}	19 (3)
	0.360	3.47	6.8×10^{-2}	20 (3)
	0.347	4.00	7.2×10^{-2}	18 (1)
	0.358	4.43	9.4×10^{-2}	21 (2)
	0.334	4.61	8.2×10^{-2}	18 (2)

a. Number in parentheses is the number of experiments that the rate was averaged from.

Table 3.2 Electron transfer data for the reaction of cobalt oxalate with Ru-HPA at various solution pH's (ionic strength constant at μ = 0.2 M) using a lithium acetate buffer at 25 °C.

pH	$[Ru^{II}]$, mM	$[Co^{III}]$, mM	k_{obs}, s^{-1}	k, M^{-1} s^{-1} a
5.75	0.387	2.26	1.5×10^{-2}	6.8 (6)
	0.391	2.36	1.5×10^{-2}	6.4 (1)
	0.376	3.47	2.4×10^{-2}	6.9 (12)
	0.366	4.44	3.0×10^{-2}	6.7 (11)
	0.356	5.52	4.1×10^{-2}	7.4 (2)
5.0	0.039	0.207	2.3×10^{-3}	11 (2)
	0.038	0.334	3.2×10^{-3}	9.6 (2)
	0.038	0.468	4.7×10^{-3}	10 (1)
	0.383	2.45	2.5×10^{-2}	10 (2)
	0.368	2.97	2.2×10^{-2}	7.5 (3)
	0.367	3.48	3.4×10^{-2}	9.8 (4)
	0.353	3.98	3.2×10^{-2}	8.0 (2)
	0.331	4.61	2.9×10^{-2}	6.3 (1)
4.0	0.375	2.96	3.2×10^{-2}	11 (3)
	0.370	3.47	3.5×10^{-2}	10 (3)
	0.364	3.96	4.3×10^{-2}	11 (3)

a. Number in parentheses is the number of experiments that the rate was averaged from.

Table 3.3 Electron transfer data for the reaction of dioxygen with Ru-HPA at constant (μ = 1.0 M) solution ionic strength.

pH	$[Ru^{II}]$, mM	$[O_2]$, mM	k_{obs}, s^{-1}	k, M^{-1} s^{-1} c
2.0 a	0.128	1.00	3.9×10^{-3}	1.9 (1)
	0.149	0.93	3.5×10^{-3}	1.9 (1)
	0.224	0.70	2.8×10^{-3}	2.0 (1)
	0.038	1.27	6.5×10^{-3}	2.6 (2)
	0.054	1.22	5.6×10^{-3}	2.3 (3)
3.0 a	0.039	1.27	3.1×10^{-3}	1.2 (3)
	0.056	1.22	2.4×10^{-3}	1.0 (5)
	0.085	1.12	2.5×10^{-3}	1.1 (4)
5.0 b	0.150	0.93	5.2×10^{-3}	2.8 (3)
	0.180	0.84	4.7×10^{-3}	2.8 (4)
	0.224	0.70	3.6×10^{-3}	2.6 (4)
5.4 b	0.048	1.33	9.6×10^{-3}	3.6 (3)
	0.091	1.27	8.8×10^{-3}	3.5 (2)
	0.100	1.12	7.3×10^{-3}	3.3 (3)
	0.129	1.00	5.8×10^{-3}	2.9 (3)
	0.150	0.93	4.1×10^{-3}	2.2 (4)
	0.180	0.84	3.5×10^{-3}	2.1 (3)

a. LiCl/HCl solution.

b. LiAc/HAc buffer.

c. Number in parentheses is the number of experiments that the rate was averaged from.

Table 3.4 Electron transfer data for the reaction of dioxygen with Ru-HPA at constant (μ = 0.2 M) solution ionic strength.

pH	$[Ru^{II}]$, mM	$[O_2]$, mM	k_{obs}, s^{-1}	k, M^{-1} s^{-1} [b]
5.0 [a]	0.128	1.00	1.1×10^{-2}	5.7 (2)
	0.150	0.93	6.5×10^{-3}	3.5 (2)
	0.180	0.84	5.9×10^{-3}	3.5 (2)
	0.225	0.70	3.2×10^{-3}	2.3 (2)
5.75 [a]	0.128	1.00	6.8×10^{-3}	3.4 (2)
	0.150	0.93	5.5×10^{-3}	3.0 (2)
	0.180	0.84	4.4×10^{-3}	2.6 (2)
	0.225	0.70	3.5×10^{-3}	2.5 (1)

a. LiAc/HAc buffer.

b. Number in parentheses is the number of experiments that the rate was averaged from.

Table 3.5 Electron transfer data for the reaction of dioxygen with various reductants at constant (μ = 1.0 M) solution ionic strength.

Reductant	pH	Gas [a]	k, M^{-1} s^{-1}	Experiments
$Ru^{II}A_6$	0.0	O_2	77	4
	0.0	air	85	4
	2.0	O_2	80	2
	2.0	air	88	2
	5.4	O_2	72	3
	5.4	air	79	3
	6.0	O_2	64	2
	6.0	air	75	2
$Ru^{II}A_5(OH_2)$	0.0	O_2	37	4
	0.0	air	43	4
	2.0	O_2	43	4
	2.0	air	47	3
	5.4	O_2	77	4
	5.4	air	106	3
	6.0	O_2	42	4
	6.0	air	50	4
Fe^{II}-HPA	2.0	O_2	0.77	6
	5.4	O_2	0.67	7
	6.0	O_2	1.3	6
$PW_{12}O_{40}^{4-}$	0.0	O_2	2.1	7

a. The gas used to sparge solution. Air ~ 0.28 mM and O_2 ~ 1.4 mM in dioxygen.

Table 3.6 Cyclic voltammetric data for calculating the heterogeneous electron transfer rate constant of Ru-HPA in pH = 2.0 sodium sulfate buffer (μ = 0.9 M).

v, mV s^{-1}	ΔE_p (RuA_6)	ΔE_p (RuHPA)	ΔE_p^* (RuHPA)[a]	k^o_{calc}, cm s^{-1}
50	66 mV	73 mV	67 mV	--- [b]
250	69 mV	72 mV	63 mV	--- [b]
500	78 mV	78 mV	60 mV	--- [b]
1003	81 mV	83 mV	62 mV	--- [b]
2007	85 mV	87 mV	62 mV	--- [b]
3531	98 mV	104 mV	66 mV	--- [b]
5120	111 mV	142 mV	91 mV	2.9×10^{-2}
6606	112 mV	149 mV	97 mV	2.7×10^{-2}
8192	113 mV	146 mV	93 mV	3.4×10^{-2}

a. $\Delta E_p^* = \Delta E_p$ (RuHPA) - [ΔE_p (RuA_6) - 60 mV]. See text for a more details.

b. ΔE_p^* is too close to being completely reversible to accurately calculate k^o.

Table 3.7 Rotating disk electrode data for the reduction of 0.30 mM $Cs_4PRu(OH_2)W_{11}O_{39}$ in pH = 2.0 sodium sulfate buffer (μ = 0.9 M) for use in calculating the heterogeneous electron transfer rate constant of the $Ru^{III/II}$ couple.

	RDE current measured at several potentials				
ω, rpm	E = 20 mV	E = 0 mV	E = -20 mV	E = -40 mV	E = -60 mV
100	0.8 μA	1.6 μA	2.9 μA	4.6 μA	6.2 μA
400	1.3 μA	2.5 μA	4.5 μA	8.8 μA	12.6 μA
900	2.9 μA	5.4 μA	8.6 μA	13.5 μA	18.2 μA
1600	3.2 μA	5.9 μA	10.0 μA	14.0 μA	20.8 μA
2500	3.8 μA	7.3 μA	14.0 μA	21.8 μA	30.7 μA
3600	4.0 μA	8.3 μA	14.5 μA	23.7 μA	31.7 μA

Table 3.8 Calculated values of k^o (RDE method) for the $Ru^{III/II}$-HPA couple at various electrodes and solution pH.

[Ru-HPA], mM	pH	Electrode material	k^o, cm s^{-1}
0.35	2.0	EPG	4.0×10^{-3}
0.30	2.0	EPG	7.3×10^{-3}
0.35	4.0	EPG	7.7×10^{-2}
0.35	5.5	EPG	4.3×10^{-3}
0.33	2.0	Pt	5.5×10^{-3}
0.35	4.0	Pt	9.1×10^{-4}

Table 3.9 RDE data for the cross-reaction between $Ru^{II}A_6$ ($\Gamma = 3 \times 10^{-9}$ mol cm^{-2}) inside a Nafion film and Ru^{III}-HPA (0.20 mM) in pH = 2.0, 0.1 M $LiClO_4$ containing 10 μM RuA_6Cl_3. The electrode was held at E = -0.55 V vs. Ag/AgCl in order to reduce all RuA_6 inside the film.

	Background subtracted limiting current	
$\omega^{1/2}$, $rpm^{1/2}$	Trial #1	Trial #2
10	4.8 μA	4.3 μA
20	7.3 μA	7.1 μA
30	10.0 μA	9.8 μA
40	12.2 μA	12.3 μA
50	14.2 μA	14.4 μA
60	16.4 μA	16.5 μA
70	18.5 μA	18.6 μA

Chapter Four

Catalytic Oxidation (or Reduction) of Organic and Inorganic Substrates

4.1 *Introduction*

When designing a transition metal catalyst to oxidize organic substrates, several features are required for good activity. First, the transition metal should be easily oxidizable to high valence states. Good oxidation catalysts usually have one or more metal-oxo group which participates in the reaction, and oxo groups are generally present only when transition metals are oxidized to the 4+, or higher, oxidation state. Second, the catalyst should be capable of multielectron transfers. This allows faster, more complete oxidations without the problem of radical-derived side reactions. Here again, the highly oxidized transition metal will come into play, as a metal oxidized by two or more electrons above its initial oxidation state is more likely to be a multielectron catalyst than a metal which is only oxidized by a single electron. Finally, the catalyst should have an easily accessible binding site where the substrate can coordinate directly to the catalytically active metal. Obviously, this site (a metal-oxo group, for example) must be renewable and not easily poisoned so that the catalyst can perform many turnovers unhindered.

Since the mid-1960's,[1] various groups have been perfecting the synthesis of analogues of silico- and phosphotungstic acid ($XW_{12}O_{40}^{n-}$, X = Si, P, etc.) where one of the 12 tungsten atoms and its terminally-bound oxo group have been replaced by a different transition metal. The defect (or lacunary)[2] ion, $XW_{11}O_{39}^{m-}$, has been found to accommodate nearly any transition metal desired in its oxo-rich cavity.[3-5] Despite the similarities between a catalytic metal center bound to a multidentate organic ligand, such as a porphyrin, and the same metal bound to the multidentate heteropolytungstate anion (HPA),[6] no catalytic studies using these compounds began until nearly 20 years had past since Baker's first heteropolytungstate paper.[7,8] The iron-substituted HPA was found to be an especially good electrocatalyst, reducing hydrogen peroxide to water[9] and nitrite

salts to ammonia.[10] The latter reaction was most notable because it demonstrated that the catalyst was capable of doing multielectron transfer (a net six electron reduction of nitrite was performed in only two steps). Drawing on the success of this electrocatalyst, the next logical step was to investigate whether a similarly impressive reaction could occur when *oxidizing* the substrate. Since the highest oxidation state electrochemically accessible in Fe-HPA is Fe^{III}, the catalytic center was going to have to be replaced by one which would be more strongly oxidizing. When this study was initially undertaken, only one brief communication[5b] existed in the literature which described high valent transition metal-substituted heteropolytungstate anions being studied as oxidation catalysts. Initial studies[11] showed both the Cr- and Ru-HPA's to be worthy of further investigation, but, as detailed in Section 1.4, the Cr-HPA was found to be poorly behaved and not a promising electrocatalyst. Luckily, the ruthenium-substituted version of this catalyst was a vastly improved species, with ruthenium oxidation states ranging from 2+ to 5+ electrochemically available.

There is a wealth of information in the literature concerning the oxidation of organic substrates by high-valent ruthenium-oxo (Ru=O) species. These catalysts range from fairly simple complexes, such as mono-[12] and dioxo[13] ruthenium bipyridine compounds, to ruthenium-oxo dimers with complex multidentate ligands,[14] and many other variations.[15] Very few of these reports, unfortunately, concern the oxidation of substrates which are feasible for use as fuels in a fuel cell. This is perhaps an eloquent comment on the difficulty of designing oxidation catalysts which will be effective in a fuel cell, and why there are no efficient, low-cost fuel cells on the market yet despite nearly thirty years of research into this area. But as the push for "cleaner" energy continues to grow, we keep learning more about what it takes to efficiently catalyze reactions, and thus move closer to solving this problem.

4.2 *Experimental*

4.2.1 Materials

The unsubstituted lacunary ion, $K_7PW_{11}O_{39}$, was synthesized using the standard literature preparation for making $K_8SiW_{11}O_{39}$,[16] but substituting Na_2HPO_4 for Na_2SiO_3. Slight modifications (detailed in Section 1.4) were also made in the published synthesis[5c] of the ruthenium-substituted heteropolytungstate anion. The source of ruthenium (II) for this reaction was $Ru(OH_2)_6(C_7H_7SO_3)_2$, prepared by the method of Bernhard.[17] All buffer solutions were made using house deionized water that had been further purified by passage through either a Barnstead NANOpure or a Millipore $MilliQ_{plus}$ water purification system, and tested to have a resistance of at least 18.2 MΩ cm. All other reagents employed in this study were of the highest purity available and were used without further purification.

4.2.2 Physical Measurements

Cyclic voltammetric experiments were performed using a Princeton Applied Research Corp. (PARC) Model 173 Potentiostat / Galvanostat equipped with a PARC Model 176 current-to-voltage converter and a PARC Model 175 Universal Programmer. Data were collected on a Houston Instruments 2000-5-5 X-Y recorder. Rotating disk electrode experiments were performed using either a motor and controller from Oxford Electrodes in addition to the above system (used to collect data at medium to very slow rotation rates), or a Pine AFRDE5 bipotentiostat with a Pine ASR2 rotator/controller (employed when medium to very fast rotation rates were needed) was used. The Pine RDE set-up also included a Kipp & Zonen BD91 XYY't recorder. Unless otherwise mentioned, the working electrode was a home-built edge-plane graphite (EPG) electrode (Union Carbide). The auxiliary electrode was a small piece of platinum wire, and the reference electrode was either a saturated sodium calomel electrode (SSCE) or a Ag/AgCl

reference electrode from Bioanalytical Systems. All RDE experiments were performed in a standard two compartment cell, while the cyclic voltammograms were recorded using either a one or two compartment cell. Every electrochemical experiment was preceded by vigorous sparging of the solution with argon gas. This argon was passed through two bubbling towers containing acidic vanadium (II) solutions (to scavenge for any residual dioxygen in the gas) and then through a bubbling tower containing pure water (to remove any trace of acidic vapor from the argon) before reaching the electrochemical cell. This action removes nearly all dioxygen from the cell and allows the electrochemistry of the catalyst and substrate to be viewed without interference.

4.3 *Results*

4.3.1 Catalysis of the Oxidation of Benzyl Alcohol

The first substrate studied was benzyl alcohol. While not particularly useful as a fuel cell feedstock, this molecule is easily oxidizable and thus a good place to begin this survey. Shown in Figure 4.1 is a representative cyclic voltammogram of $Cs_4PRu(OH_2)W_{11}O_{39}$ in a pH = 4.0 buffer in the presence and absence of benzyl alcohol. Oxidation of the alcohol occurs only after the ruthenium center is oxidized to the 5+ state at this pH, even though both the Ru^{IV} and Ru^{V} complexes exist as the Ru oxo species. The increase in the anodic $Ru^{V/IV}$ peak current is due to the oxidation of alcohol by the oxidized Ru-HPA catalyst and not by direct oxidation of the substrate at the EPG electrode, as benzyl alcohol is not oxidized at EPG under these conditions unless the potential is greater than 1.2 V (see Figure 4.2). All studies of the catalytic oxidation benzyl alcohol by Ru-HPA were performed in a pH = 4.0, 0.2 M lithium acetate buffer using an EPG electrode. Under these conditions, the separation between the $Ru^{IV/III}$ and the $Ru^{V/IV}$ couples is large enough that catalysis occurs only after the ruthenium center is

Figure 4.1 A cyclic voltammogram of 0.41 mM $Cs_4PRu(OH_2)W_{11}O_{39}$ in a pH = 4.0, 0.2 M lithium acetate buffer with (- - - -) and without (------) 2.0 mM benzyl alcohol. The scan rate was 50 mV s^{-1}.

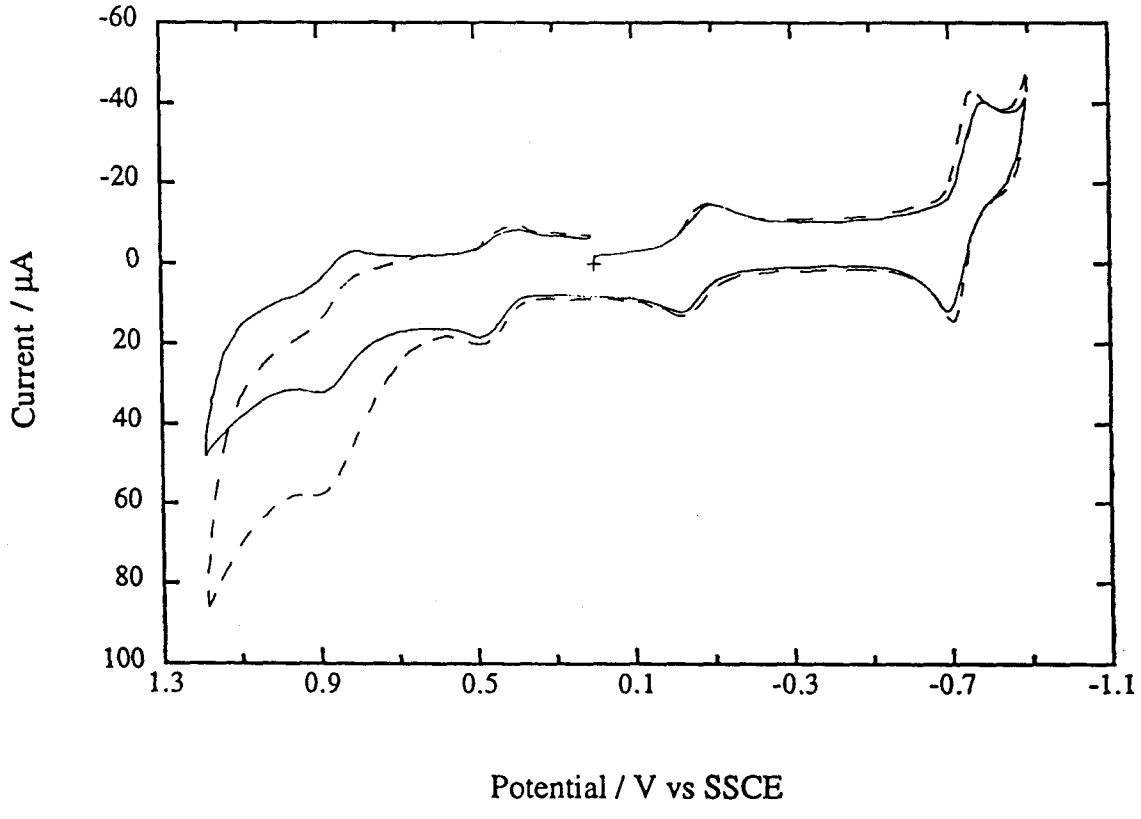

Figure 4.2 A cyclic voltammogram of a pure pH = 4.0, 0.2 M lithium acetate buffer with (- - - -) and without (------) 2.0 mM benzyl alcohol. The scan rate was 50 mV s^{-1}.

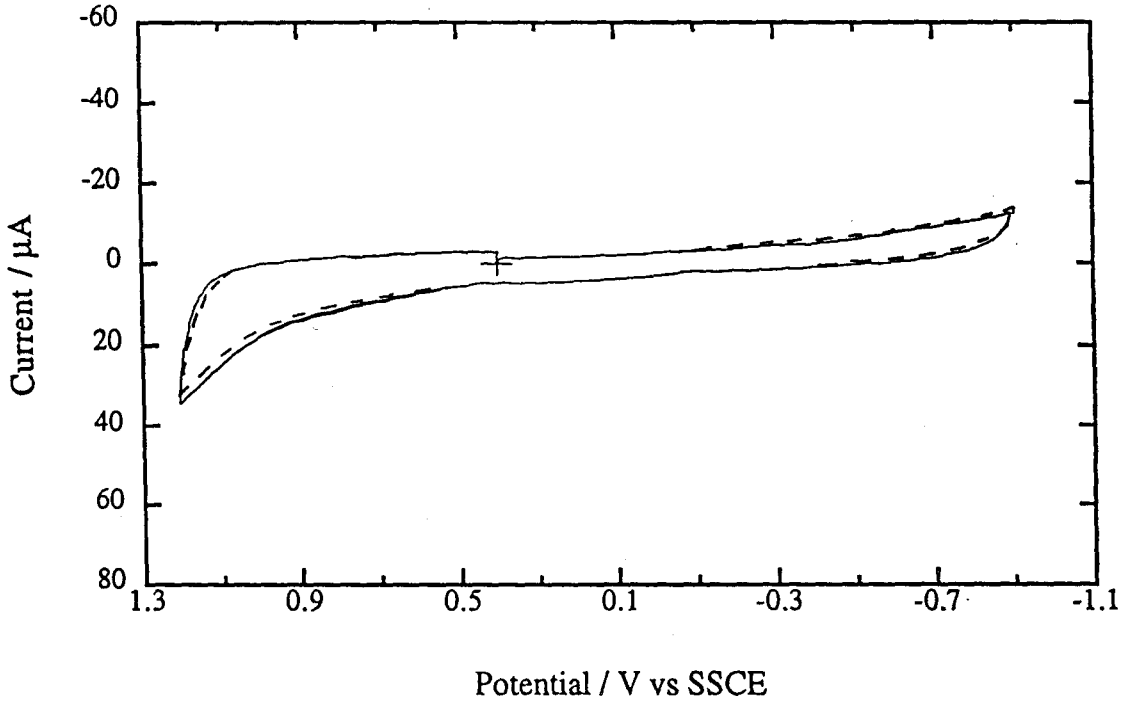

oxidized to the 5+ state. These conditions provide an excellent system to study, as the RDE response of the $Ru^{IV/III}$ wave can be monitored as the "control" where no changes in the plateau current should occur, while the $Ru^{V/IV}$ plateau current can be measured in order to extract the kinetic information concerning the catalysis reaction.

The general scheme for a catalytic reaction where the substrate is being oxidized is as follows:

$$R \rightleftharpoons O + ne^- \quad (1)$$

$$O + Z \xrightarrow{k'} R + Y \quad (2)$$

where R and O are the reduced and oxidized forms of the catalyst, Z is the substrate, and Y is the product of the reaction. In order to determine k', any of nearly a half a dozen electrochemical techniques can be utilized, but rotating disk electrode (RDE) voltammetry is by far the simplest, as, under certain conditions, it allows the direct calculation of the catalytic rate constant without the need for working curves or curve-fitting. To obtain k' from the RDE curves, conditions must be found such that the limiting current of the catalytic wave is independent of the rate of rotation of the EPG electrode. This is accomplished at very low rotation rates,[18] so it is important to have a rotator which operates smoothly even at rotation rates below 100 rpm. Luckily, the Oxford Electrodes rotator used in these experiments was specifically designed for such an experiment. Visual calibration of the rotation rate demonstrated that the Oxford motor was fairly accurate (for example, if the rotator was set to 25 rpm, the motor would perform 25 rotations in 60.0 $\pm$ 0.5 s) down to 16 rpm. Experiments performed using 0.30 mM $Cs_4PRu(OH_2)W_{11}O_{39}$ in a pH = 4.0, 0.2 M lithium acetate buffer to catalyze the oxidation of 2.9 to 18 mM benzyl alcohol (Table 4.1) were all found to display rotation rate-independent plateau currents at very slow rotation rates. In order to save time and to avoid possible problems with ill-defined plateaus, the entire RDE trace was usually not recorded at every rotation rate. Rather, the EPG was held at a potential corresponding to

either the $Ru^{IV/III}$ plateau (+0.60 V vs. SSCE) or the $Ru^{V/IV}$ plateau (+1.0 V vs. SSCE) and the current for each rotation rate is recorded. A slightly troublesome characteristic of transition metal-substituted heteropolytungstate anions is that when measuring the RDE limiting current by this method, constant plateau currents are not initially observed. Instead, the current decays for a period of time after application of the potential before reaching a steady value. It has been found that waiting 60 s between applying the potential and measuring the first datum allows enough time for the current to reach a fairly constant plateau. No time delay, save for that necessary to change the rotation rate, is needed after the initial waiting period. It is also helpful to begin the measurement at the highest rotation rate and proceed to the slowest, as this allows the steady-state currents to be reached quicker, thus improving the reproducibility of the data. Taking these precautions, the measured plateau currents were found to be reasonably precise. As expected, the data in Table 4.1 generally display the characteristics of rotation rate-independent limiting currents at slow rotation rates (Figure 4.3). This plot also demonstrates the fact that the $Ru^{IV/III}$ couple is unaffected by the addition of substrate to the solution, as the Levich plot of these data is linear and has a y-intercept close (0.3 μA) to the expected value of zero.[19] By making Levich plots for all the data in Table 4.1, the value of the rotation rate-independent plateau current can be estimated for each concentration of benzyl alcohol. Then, by using equation (3),[20] the rate of catalytic

$$i_{cat}\ (\text{limiting value}) = nFAD^{1/2}C_o^*(k'C_z^*)^{1/2} \qquad (3)$$

reaction can be calculated for each of these experiments. In this equation, n is the number of electrons transferred, F is Faraday's constant, A is the area of the EPG electrode, D is the diffusion coefficient of the catalyst (calculated from the slope of the Levich plot for the $Ru^{V/IV}$ couple when no substrate is present), C_o^* is the bulk concentration of the catalyst, and C_z^* is the bulk concentration of the substrate. The calculated value of k' for the oxidation of benzyl alcohol by Ru-HPA is $28 \pm 7\ M^{-1}\ s^{-1}$. Likewise, data taken when

Figure 4.3 Levich plot of $Ru^{IV/III}$ and $Ru^{V/IV}$ RDE plateau currents for the oxidation of 0.30 mM $Cs_4PRu(OH_2)W_{11}O_{39}$ in a pH = 4.0, 0.2 M lithium acetate buffer containing 8.7 mM benzyl alcohol.

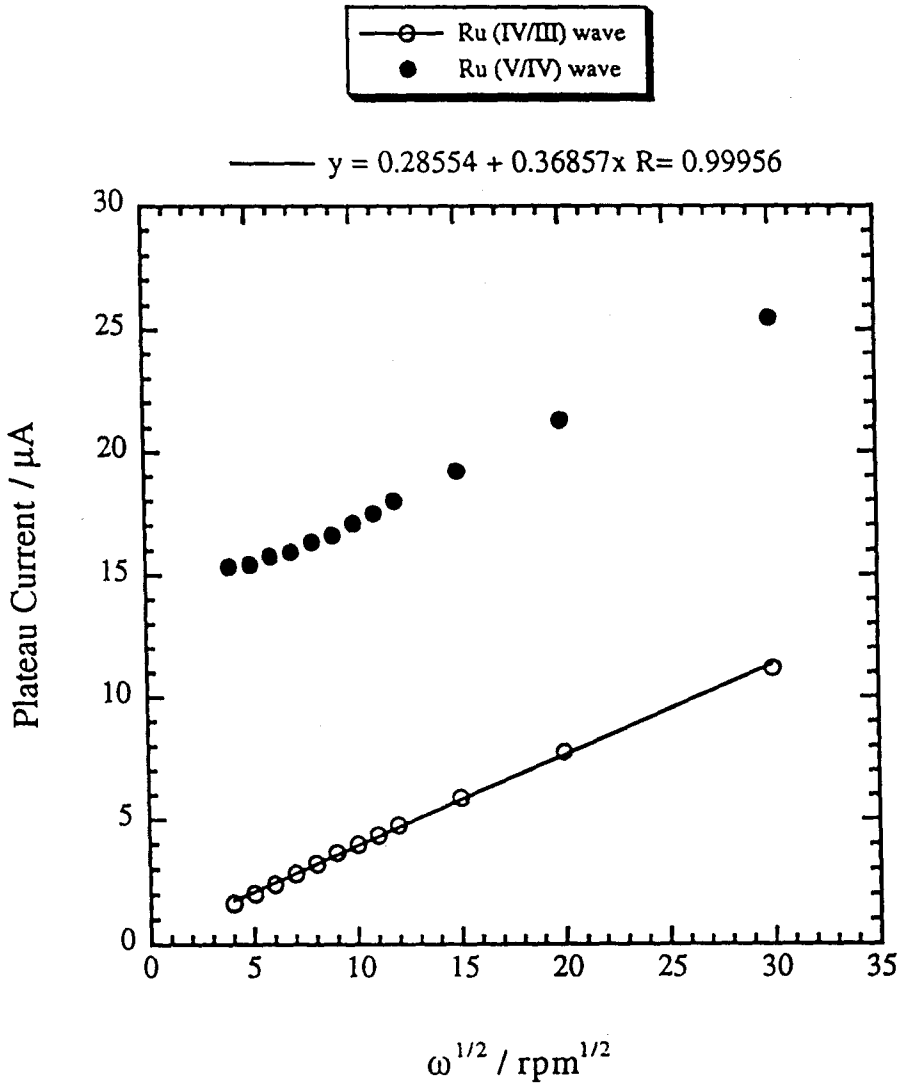

the entire RDE curve was measured yielded a rate of 34 ± 10 M^{-1} s^{-1} when analyzed via (3). Another way to analyze the RDE data which does not rely on estimating the rotation rate-independent plateau current from Levich plots is to divide (3) by the Levich equation to get (4).[21] Here, the slope of the i_{cat}/i_{Lev} vs. $\omega^{-1/2}$ plot (Figure 4.4) is used to calculate

$$i_{cat}/i_{Lev} = 1.61\omega^{-1/2}D^{-1/6}\nu^{1/6}(k'C_z^*)^{1/2} \qquad (4)$$

the rate constant instead of the less reliable current extrapolation method. Agreement between the rates calculated by (3) and those derived from (4) is excellent, with k' = 30 ± 10 M^{-1} s^{-1} for the latter method.

Unfortunately, there is a limit to the amount of benzyl alcohol which can be present in the solution before problems arise. As seen in Figure 4.5, the Levich plot of the catalytic current when the concentration of benzyl alcohol is 30 mM is much different than the earlier ones. Instead of having the current deviate from linearity by reaching a minimum and plateauing, the current at slow rotation rates is actually smaller than expected if no catalysis was occurring. This response is indicative of some sort of passivation, either a deactivation of the catalyst which prevents, or at least slows, the binding of the substrate, or some problem with the EPG electrode itself which significantly decreases the rate at which the reduced catalyst is reoxidized at the surface of the electrode. This phenomenon occurs at rather irregular intervals, sometimes requiring more or less benzyl alcohol before passivation sets in, but it eventually happens in every experiment.

The product of the oxidation of benzyl alcohol by Ru-HPA is most likely benzaldehyde. Although the catalyst is able to oxidize the aldehyde, the reaction occurs at a much slower rate than oxidation of the alcohol (compare Figure 4.1 with Figure 4.6). Even though the concentration of benzaldehyde is 20 times that of benzyl alcohol in these two cyclic voltammograms, it still gives a catalytic peak current which is about three times smaller than that of benzyl alcohol. In addition to having the advantage in

Figure 4.4 Plot of i_{cat}/i_{Lev} vs. $\omega^{-1/2}$ for 0.30 mM $Cs_4PRu(OH_2)W_{11}O_{39}$ in pH = 4.0, 0.2 M lithium acetate containing 18 mM benzyl alcohol.

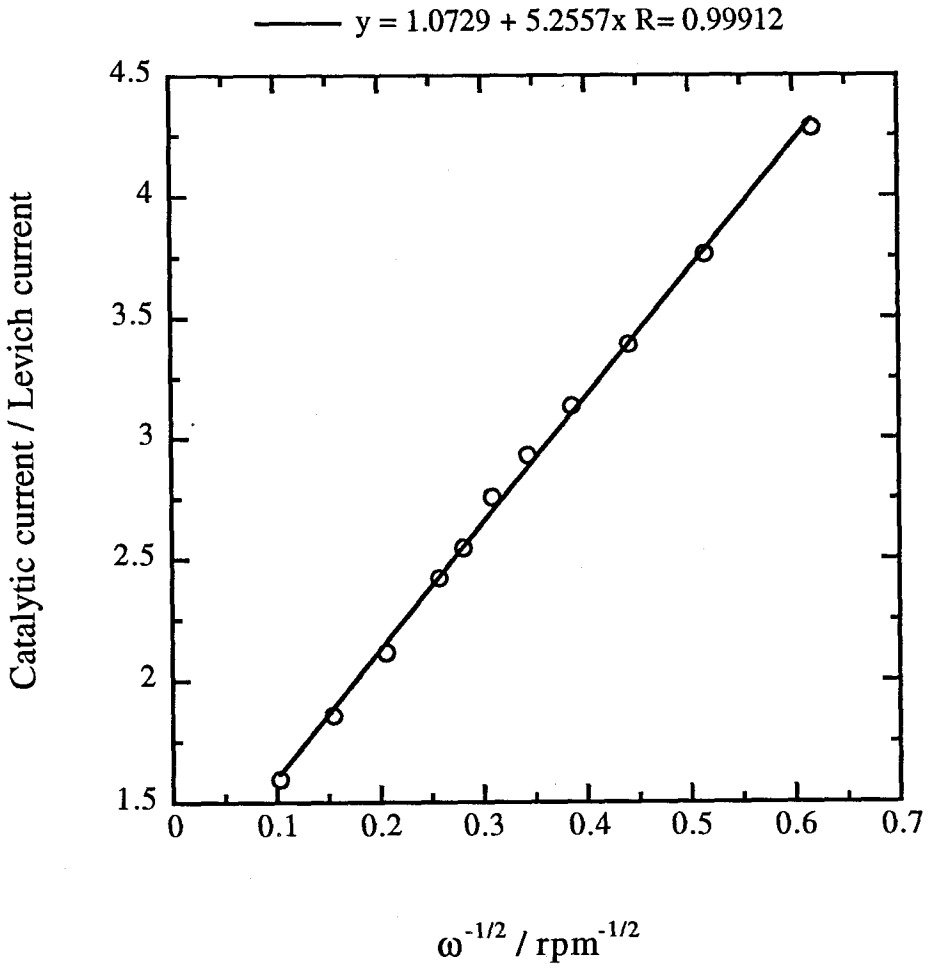

Figure 4.5 Levich plot of $Ru^{IV/III}$ and $Ru^{V/IV}$ RDE plateau currents for the oxidation of 0.35 mM $Cs_4PRu(OH_2)W_{11}O_{39}$ in a pH = 4.0, 0.2 M lithium acetate buffer containing 30 mM benzyl alcohol.

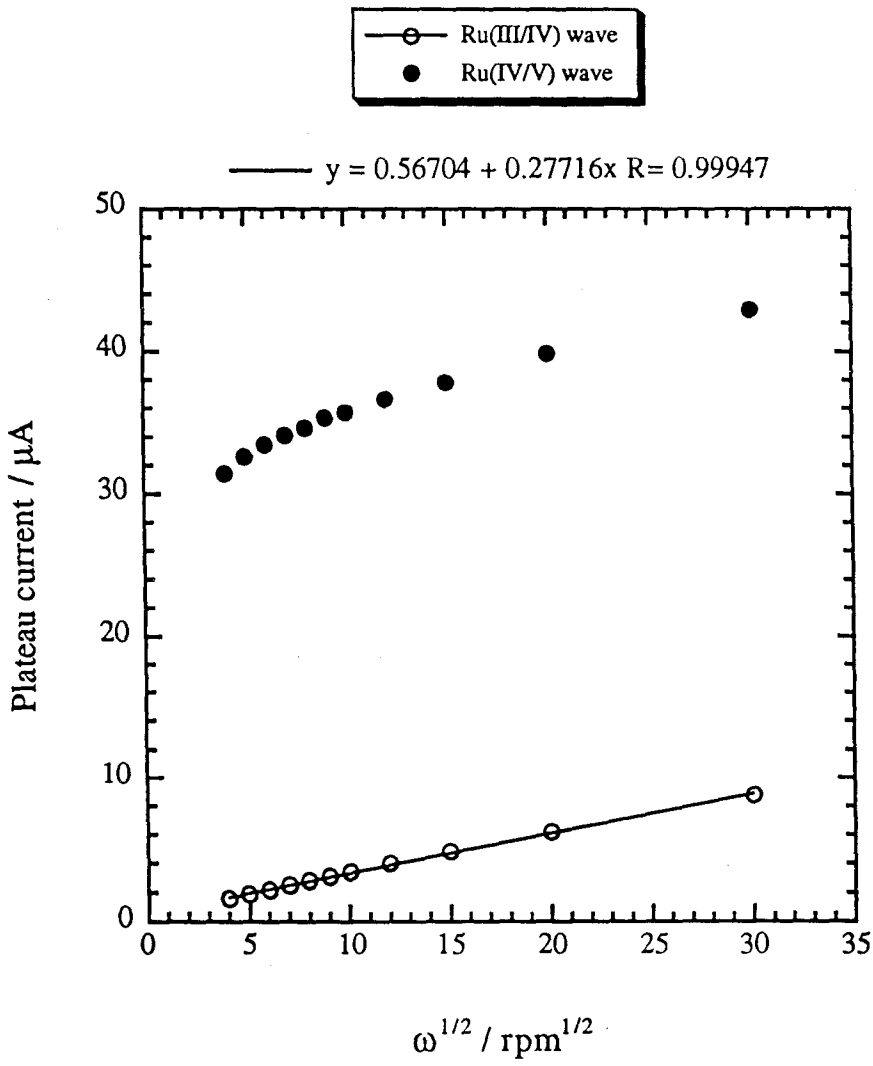

Figure 4.6 A cyclic voltammogram of 0.37 mM $Cs_4PRu(OH_2)W_{11}O_{39}$ in a pH = 4.0, 0.2 M lithium acetate buffer with (- - - -) and without (——) 40 mM benzaldehyde. The scan rate was 50 mV s^{-1}.

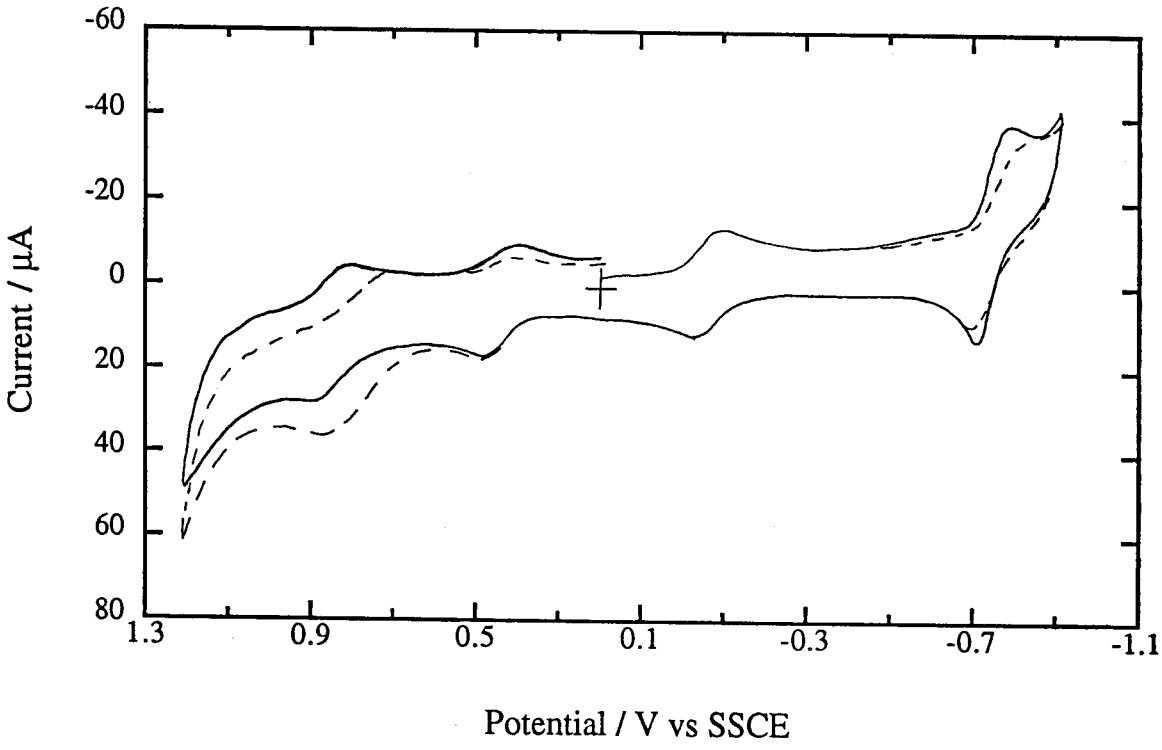

reaction rate, benzyl alcohol is also present in a much larger concentration than benzaldehyde, which also favors stopping the reaction at the aldehyde. Finally, during an RDE experiment, the solution at the electrode surface is constantly being replaced by fresh bulk solution, so any benzaldehyde produced will be swept away from the electrode before it has the chance to react with more oxidized catalyst.

4.3.2 Catalysis of the Oxidation of Methanol

Although the catalysis of benzyl alcohol was successful, it represents only the beginning of the investigation into the activity of Ru-HPA as an oxidation catalyst. Much more important is its activity when the test substrate is more realistic (i.e., a species expected to be used as a fuel in a "real world" cell). With this in mind, the second substrate tested was methanol. Methanol is essentially benzyl alcohol with the phenyl group replaced by a proton. Unfortunately, this simplification has a large effect on the reactivity of the substrate, as the general reactivity trend of alcohols towards oxidation is methyl < primary < secondary < benzylic.[12b,22] It is not surprising then that the cyclic voltammogram of Ru-HPA in the presence of a 100-fold molar excess of methanol shows only a very small increase in the $Ru^{V/IV}$ anodic peak current (Figure 4.7). While this is fairly clear evidence that the catalysis of methanol by Ru-HPA is a very slow reaction, quantitation of the rate by the RDE methods described above was attempted. Much larger substrate-to-catalyst ratios were used (Table 4.2) than the previous study, and still no deviation from linear Levich plots was observed for either the $Ru^{IV/III}$ or $Ru^{V/IV}$ waves. At last, when the substrate-to-catalyst ratio was 660:1, the reaction displayed rotation rate-independent plateau currents and the catalytic rate constant could be extracted. Using equation (3), a rough estimate of the rate constant can be made. The value obtained from this calculation (on the order of 10^{-1} M^{-1} s^{-1}) is more than two orders of magnitude lower than the rate constant for catalysis of the oxidation of benzyl alcohol by Ru^{V}-HPA, as expected. Unfortunately, because of its low value, the rate constant

Figure 4.7 A cyclic voltammogram of 0.40 mM $Cs_4PRu(OH_2)W_{11}O_{39}$ in a pH = 4.0, 0.2 M lithium acetate buffer with (- - - -) and without (——) 42 mM methanol. The scan rate was 50 mV s^{-1}.

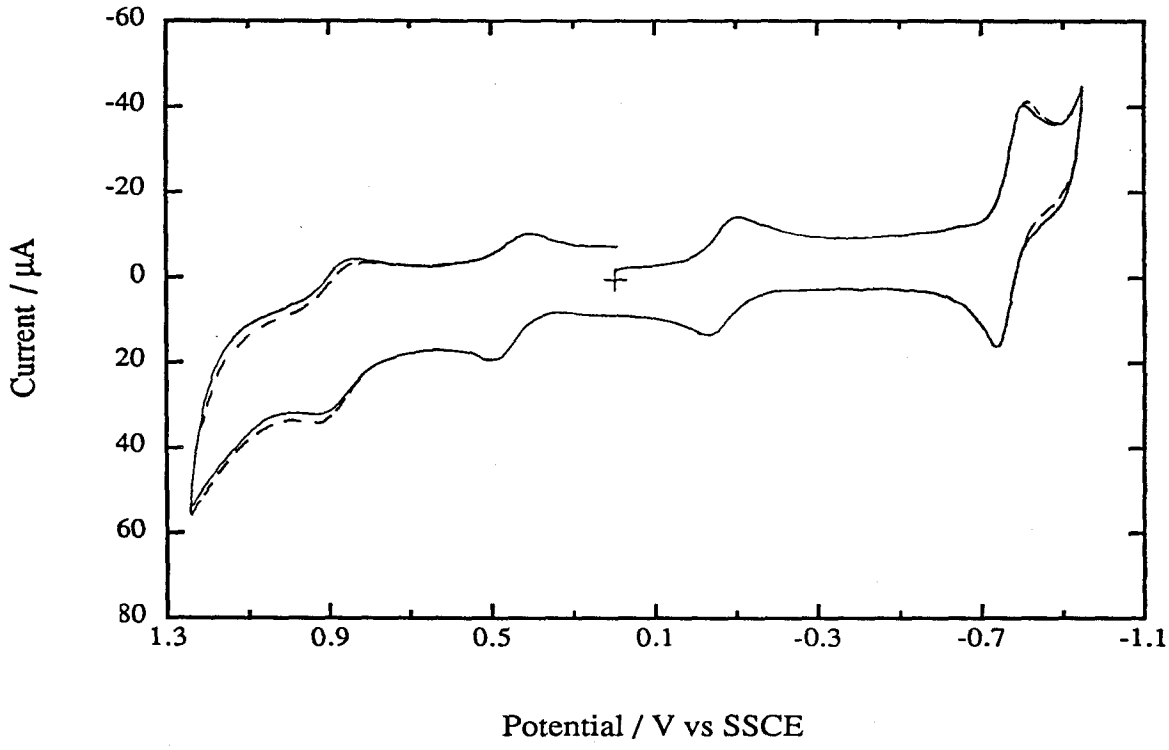

evaluated for methanol oxidation was only approximate. The uncertainty could be as large as an order of magnitude. Since this rate appears to be much too low to be useful in a fuel cell, no further investigations using methanol as the substrate, such as attempting a more precise rate constant measurement or an analysis of the products of the reaction, were undertaken.

4.3.3 Catalysis of the Oxidation of Other Alcohols

According to the alcohol reactivity trend mentioned above, secondary alcohols should be nearly as reactive as benzylic alcohols, so another oxidative catalysis reaction was attempted using 2-propanol as the substrate. 2-propanol is a cheap, commonly used alcohol which could possibly be used as the fuel in a fuel cell. The cyclic voltammogram of Ru-HPA catalyzing the oxidation of 2-propanol in a pH = 2.0 sulfate buffer (not shown) indicated that 2-propanol was probably going to fall in between methanol and benzyl alcohol in reactivity, just as predicted. Cursory attempts at calculating the rate constant yielded a value on the order of 5-10 M^{-1} s^{-1}. The catalysis of 2-propanol by Ru-HPA was not pursued beyond this point.

Previous studies[12c,d] reported that phenol was a substrate easily oxidized by Ru^{IV}=O compounds. While not particularly useful in a fuel cell, phenol would be an interesting substrate to perform kinetic studies on, especially if it reacted with Ru-HPA to give quinone, since this would provide evidence for C-H bond activation. Cyclic voltammetric experiments performed at pH = 2 appear to indicate that phenol is oxidized by Ru-HPA in the 4+ state (Figure 4.8), but the potential where this reaction occurs is very close to that of direct phenol oxidation at the bare EPG electrode. No rate constants for the catalysis of phenol by Ru-HPA were measured under these conditions, as the rate constant calculated would almost surely be a combination of the rates of phenol oxidation by the catalyst and directly at the electrode surface. Since the $Ru^{IV/III}$ peak potential is pH dependent, the cyclic voltammogram of phenol oxidation at pH = 4.0 (not shown) was

Figure 4.8 A cyclic voltammogram of 0.35 mM $Cs_4PRu(OH_2)W_{11}O_{39}$ in a pH = 2.0, 0.3 M sodium sulfate buffer with (- - - -) and without (——) 5.1 mM phenol. The scan rate was 50 mV s^{-1}.

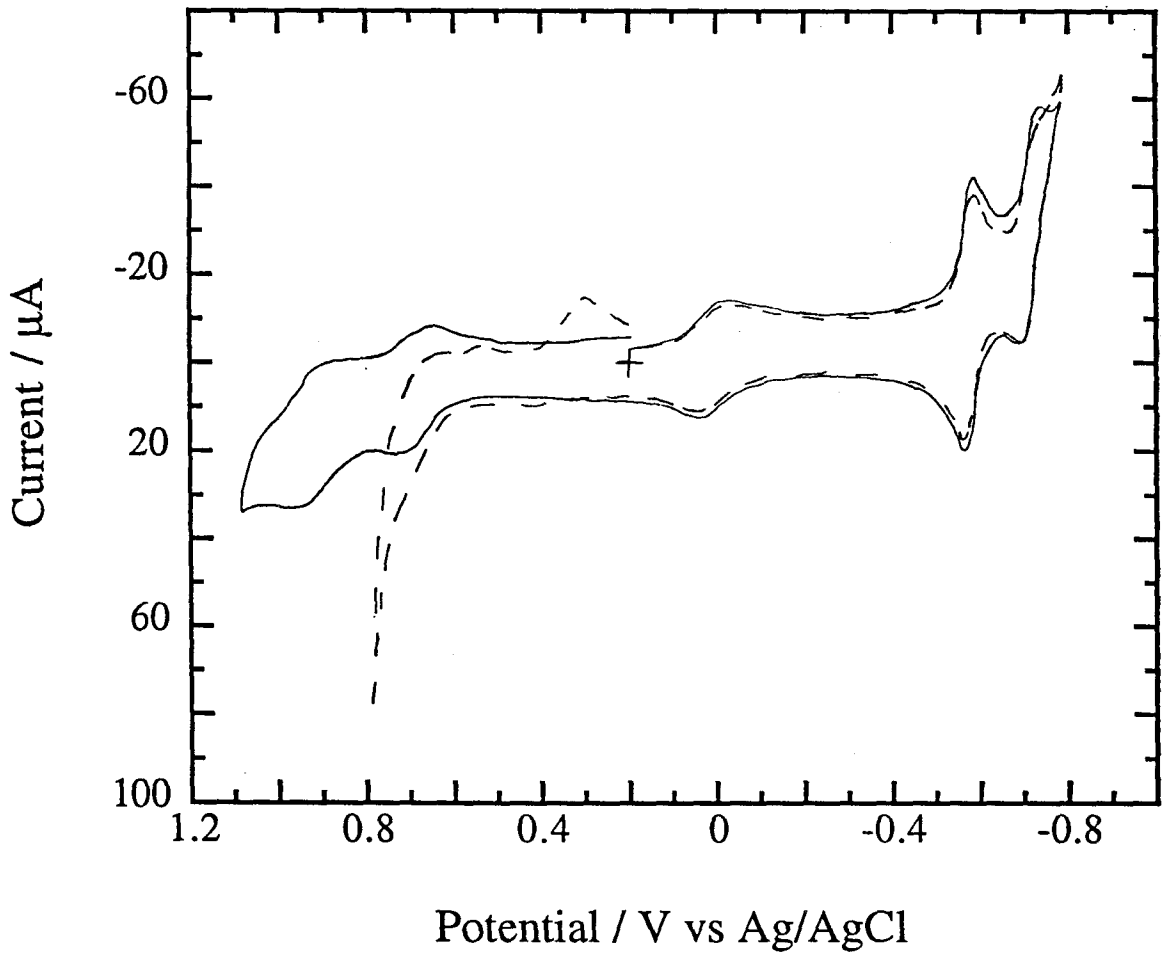

also measured in hopes that the catalytic reaction would occur at a potential far enough negative of the direct oxidation that kinetic information could be obtained. Unfortunately, no catalytic current was seen at the $Ru^{IV/III}$ anodic wave under these conditions. Because of this inability to sufficiently separate the catalytic and non-catalytic oxidation of phenol, no kinetic studies were attempted.

4.3.4 Catalysis of the Oxidation of Other Organic Substrates

Although methanol is generally one of the most common substrates tested for use in the anodic compartment of a fuel cell, it is by no means the only one. Other C_1 compounds such as formaldehyde or sodium formate/formic acid are also considered to be possibilities. With this in mind, both of these compounds were tested (by cyclic voltammetry) to see if they could be catalytically oxidized by Ru-HPA. Formaldehyde is oxidized by Ru-HPA in a pH = 2.0 sulfate buffer (not shown), but like benzaldehyde, evidence of catalysis occurs only after a huge excess (100:1 or more) of substrate is present. Even under conditions where catalysis occurs, the amount of catalytic current is quite small compared to the uncatalyzed peak current, so the rate of oxidation is surely too slow to be useful. Sodium formate is an even poorer substrate for oxidation by Ru-HPA. The CV of Ru-HPA at pH = 4.0 in the presence of a 25-fold molar excess of sodium formate (not shown) displayed no evidence of formate oxidation at any potential up to and including +1.2 V vs. SSCE. Although the ruthenium center in the heteropolytungstate cage can exist in the highly oxidized Ru^{V}=O state, it appears that this particular form of ruthenium is not as reactive as was hoped at the beginning of this project. No further catalytic studies were performed using organic substrates.

4.3.5 Catalysis of the Oxidation and Reduction of Inorganic Substrates

Although the majority of the substrates in the following study are not generally considered to be candidates for use in fuel cells, all are useful in other areas and finding a better catalyst for their oxidation or reduction could be important. Sodium oxalate was

the first inorganic substrate to be studied. At low (~5 mM) concentrations, the addition of sodium oxalate to a solution of Ru-HPA at pH = 2.0 has almost no effect except to shift the peak potential of some of the Ru-HPA couples a few millivolts more negative (as the solution pH changes slightly) and to shift the anodic potential limit to values about 150 mV less positive (as oxalate is oxidized directly at the electrode at a potential more negative than the solvent). At higher concentrations of substrate (50 mM), what looked like the start of catalysis at the Ru^{V} wave at lower oxalate concentrations is overrun by the direct oxidation of oxalate at the electrode surface (see Figure 4.9). The larger amount of oxalate also shifts the pH of the solution to a higher value, thus causing the negative potential shift in the pH-dependent Ru-HPA waves. Although the problems which occurred under these conditions might be lessened at a different pH, or perhaps by using an electrode which is poorer at directly oxidizing oxalate, the data presented above indicate that the catalytic rate of oxalate oxidation is probably fairly slow. Therefore, oxalate was not pursued any further as a candidate for catalytic studies.

Hydrazine sulfate was selected as the second inorganic substrate to be tested. Unfortunately, it appears to behave in a manner similar to sodium oxalate. At low substrate concentrations (~10:1 substrate-to-catalyst ratio), there appears to be a small enhancement in the peak current of the $Ru^{IV/III}$ anodic wave, but this new development is partially obscured by direct oxidation of substrate at the electrode at a potential only a 100 mV more positive (see Figure 4.10). Additional substrate only makes this condition worse, to the point where the ruthenium catalytic current is totally engulfed in the larger electrode-based oxidation current. Evidently, the catalyst provides little improvement over the bare EPG electrode when it comes to oxidizing hydrazine sulfate under these conditions.

Despite the fact that the main goal of this project was to study the ruthenium-substituted heteropolytungstate for catalytic activity in performing oxidations, it could

Figure 4.9 A cyclic voltammogram of 0.35 mM $Cs_4PRu(OH_2)W_{11}O_{39}$ in a pH = 2.0, 0.3 M sodium sulfate buffer in the absence (——) and presence (· · · · · = 4.9 mM) and (– – – = 50 mM) of sodium oxalate. The scan rate was 50 mV s^{-1}.

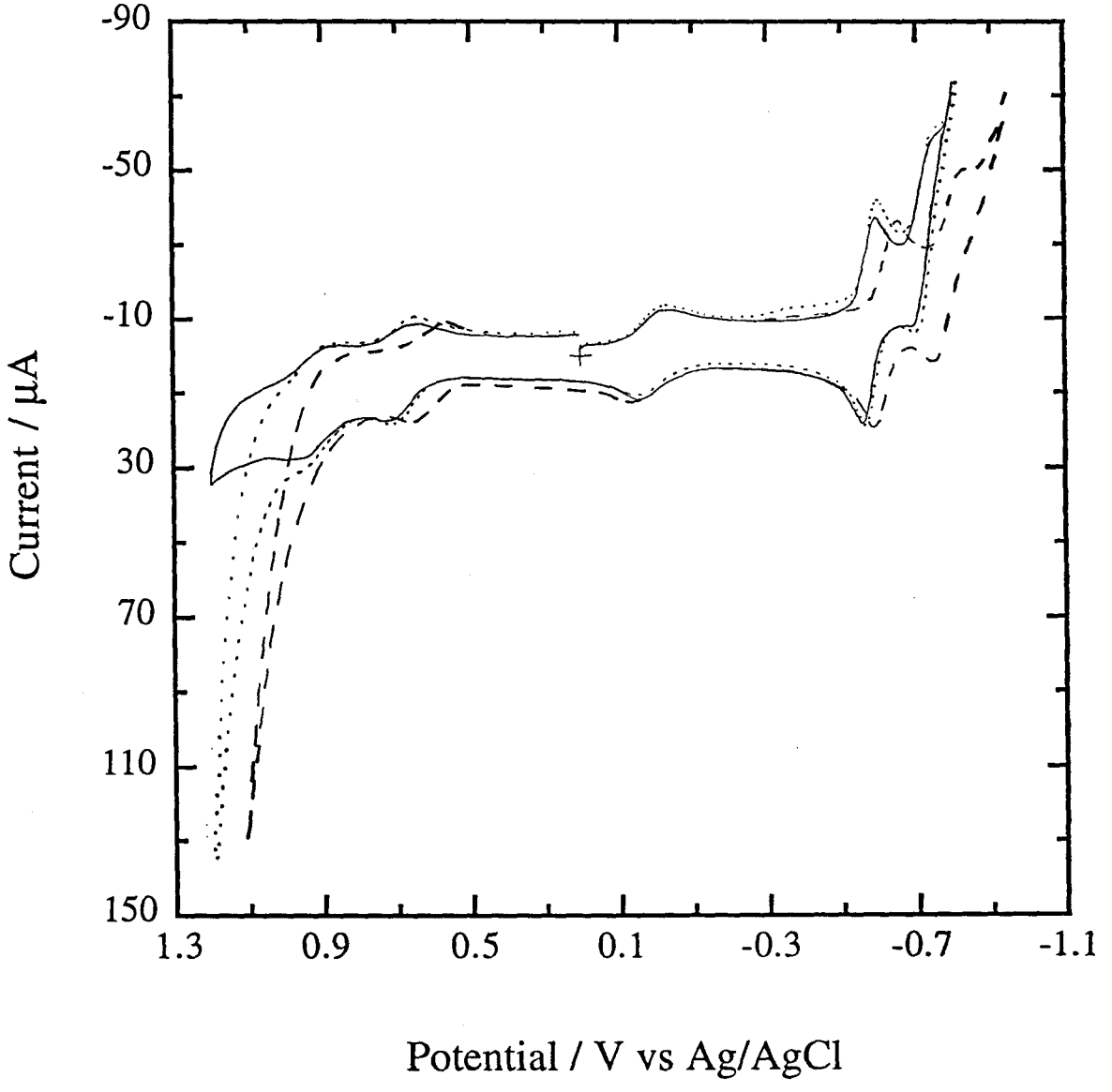

Figure 4.10 A cyclic voltammogram of 0.30 mM $Cs_4PRu(OH_2)W_{11}O_{39}$ in a pH = 2.0, 0.3 M sodium sulfate buffer in the absence (——) and presence (· · · · · = 3.2 mM) and (– – – = 16 mM) of hydrazine sulfate. The scan rate was 50 mV s^{-1}.

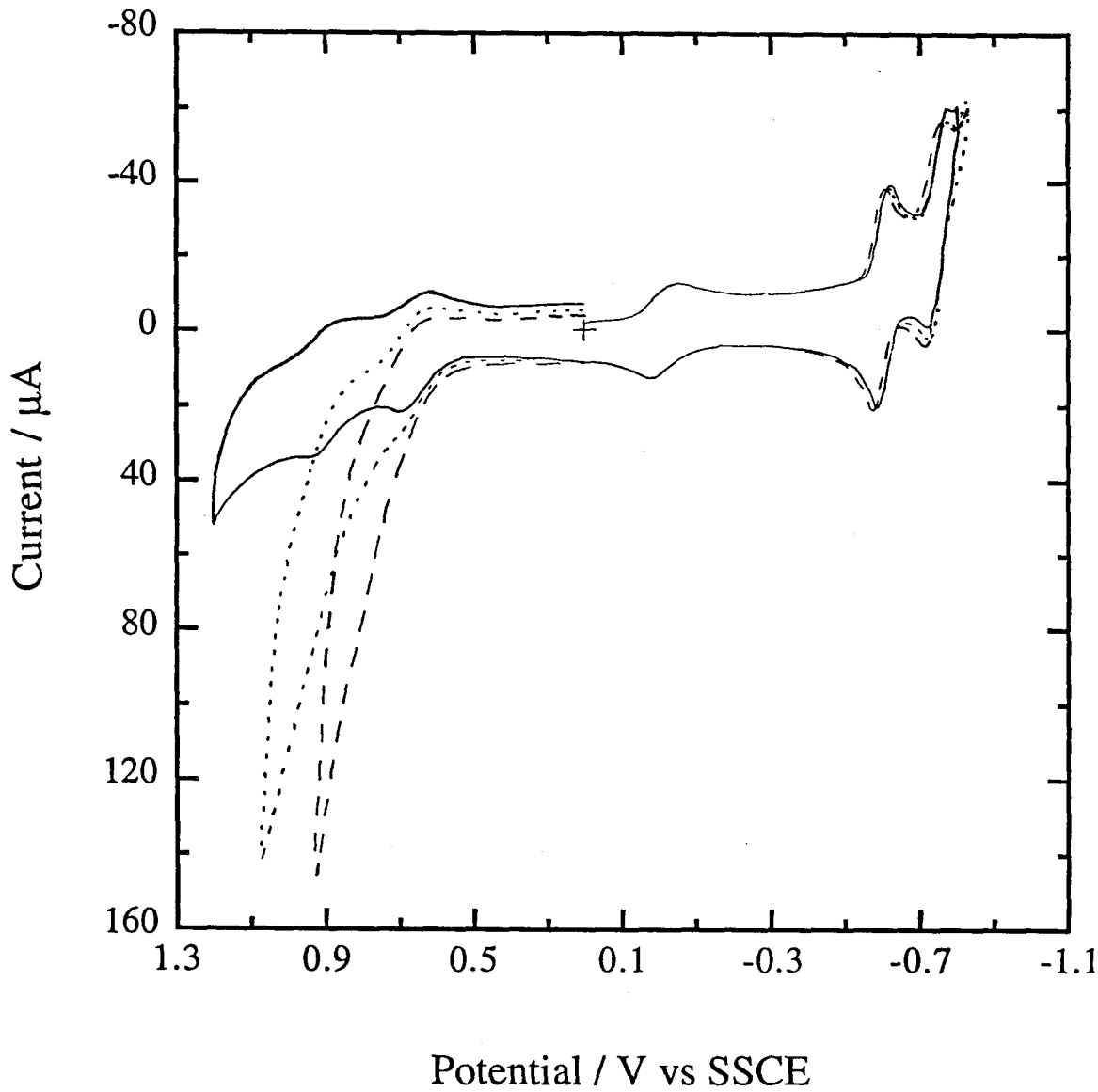

also be used to catalyze the reduction of substrates, just as the Fe-HPA was.[9,10] It seemed logical to begin this investigation by using the substrates which were catalyzed by Fe-HPA. Sodium nitrite was catalytically reduced to ammonia by Fe-HPA when the applied potential was negative enough to reduce the tungsten-oxo cage.[10] Cyclic voltammetric experiments show (Figure 4.11) that there is at least some catalysis occurring when the cage containing the ruthenium center is reduced. There also appears to be some catalysis happening at the anodic portion of the $Ru^{IV/III}$ peak, presumably oxidation of nitrite to nitrate. The larger current at the $Ru^{V/IV}$ anodic peak is due, at least in part, to direct oxidation of the substrate at the electrode (see Figure 4.12). Brief attempts to investigate the catalytic reduction of nitrite by Ru-HPA by RDE were unsuccessful because the catalytic plateau currents at the cage reduction potentials were ill-defined due to the presence of a large, sloping background current. The CV and RDE data both seem to indicate that the enhancement of the current at the tungsten-oxo waves is caused (to a greater extent) by a large increase in the background current rather than by catalytic current. The catalytic oxidation actually looks more promising, but it is doubtful that the catalytic current could be separated from the much larger current due to the direct oxidation of nitrite by the electrode, which begins at a potential only 50 mV more positive. The results when the substrate is hydrogen peroxide are similar to sodium nitrite. An increase in the tungsten-oxo cage peak currents occurs only at high substrate concentration and appears to be at least partially due to an increase in the background current. A catalytic current is also observed positive of the $Ru^{V/IV}$ anodic peak, but it occurs at about the same potential as the uncatalyzed oxidation of hydrogen peroxide at the EPG electrode. Three other substrates were also used to test the catalytic activity of Ru-HPA, but were found to be inert or nearly so. The compounds included: hydrogen, sodium chlorate, and carbon monoxide.

Figure 4.11 A cyclic voltammogram of 0.50 mM $Cs_4PRu(OH_2)W_{11}O_{39}$ in a pH = 2.0, 0.3 M sodium sulfate buffer in the absence (——) and presence (· · · · · = 0.5 mM) and (– – – = 1.5 mM) of sodium nitrite. The scan rate was 50 mV s^{-1}.

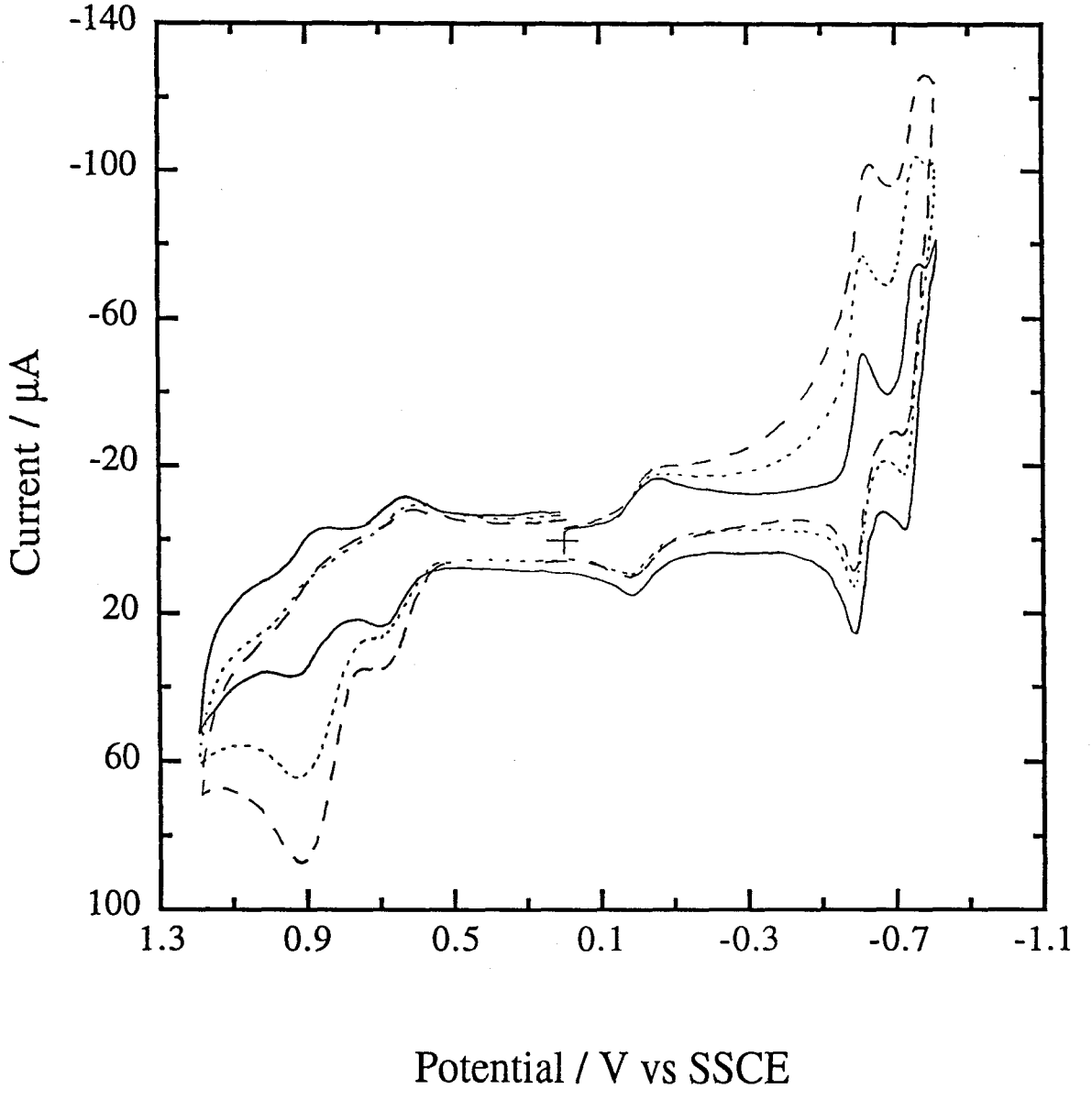

Figure 4.12 A cyclic voltammogram of pure pH = 2.0, 0.3 M sodium sulfate buffer in the absence (——) and presence (– – –) of 1.0 mM sodium nitrite. The scan rate was 50 mV s^{-1}.

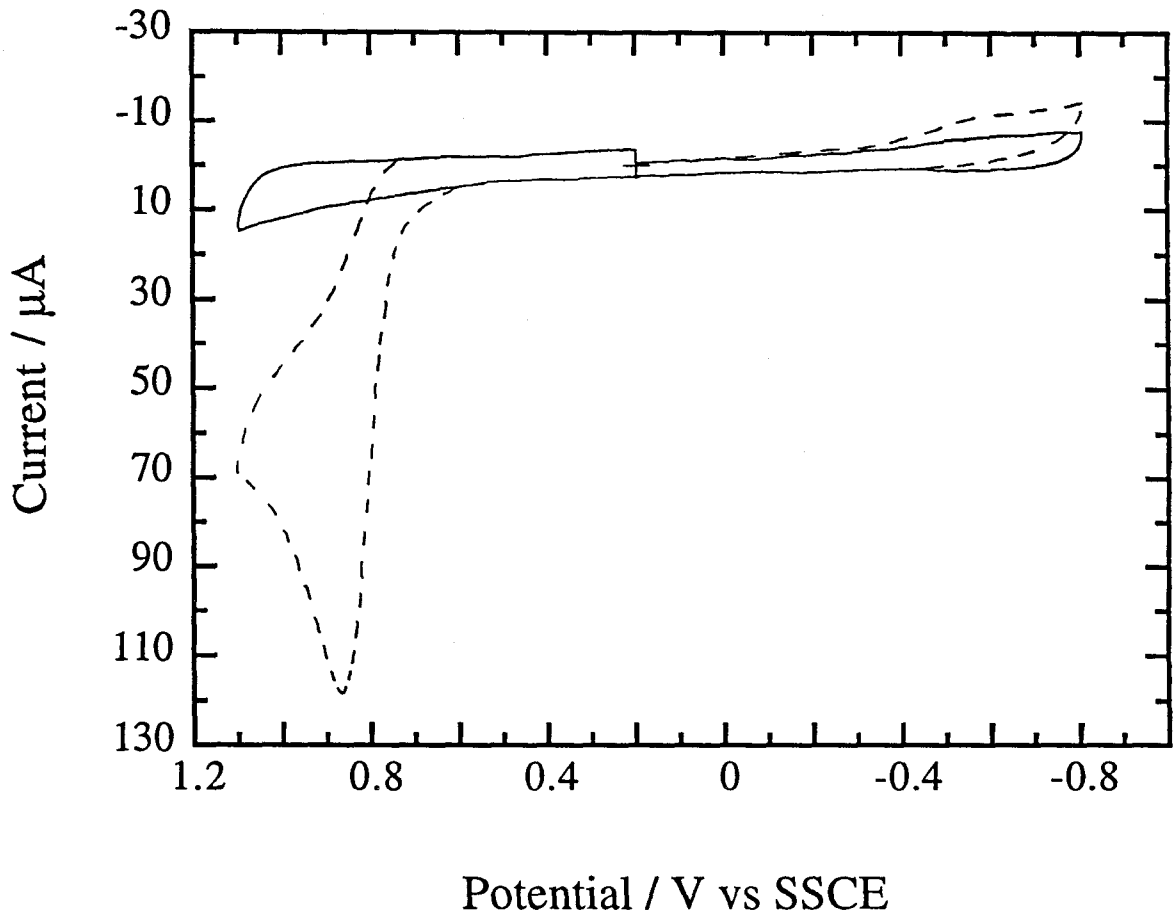

4.4 *Discussion*

4.4.1 Catalysis of the Oxidation of Alcohols

It is quite unfortunate that the ruthenium-substituted heteropolytungstate anion does not perform catalytic oxidations of alcoholic substrates anywhere near as well as we had hoped. The oxidation of benzyl alcohol is slow (about 30 M^{-1} s^{-1}) and rate constants for the catalysis reactions with other alcohols get progressively smaller. The only trait that the catalyst has that was expected is its variation in reactivity toward various alcohols. The catalytic rate of alcohol oxidation by Ru-HPA is methyl < primary < secondary < benzylic, just as it is with other ruthenium catalysts.[12b,22] To decide whether the benzyl alcohol rate constant that we measured is unusually low or not, a compilation of rate constants for the catalytic oxidation of benzyl alcohol by various ruthenium-oxo complexes was made (Table 4.3). The oxoruthenium (V) species are the most useful for a direct comparison to the Ru-HPA data. Unfortunately, complexes of this type are fairly rare,[23] so there are not a lot to survey. Most Ru^{V}=O catalysts react with benzyl alcohol with a rate constant in the 100-200 M^{-1} s^{-1} range. These rate constants are only a factor of three to seven greater than Ru-HPA, so the cage seems to have only a slight negative effect on the rate of benzyl alcohol oxidation when compared to the macrocyclic amine ligands listed in Table 4.3. Only the Ru^{V}=O complex Che *et al.*[24] synthesized which employs the N,N'-dimethyl-N,N'-bis(2-pyridylmethyl)ethylene-diamine ligand shows the vigorous catalytic activity ($k = 8.4 \times 10^4$ M^{-1} s^{-1}) that we expected from a Ru^{V}=O compound. Unfortunately, Che does not attempt to explain why this particular ligand makes the ruthenium center such an efficient catalytic site when other similar ligands do not. Che[24] does make a convincing case that the rate of benzyl alcohol oxidation is not simply a matter of the strength of the oxidant, as a plot of log(k) versus E^{o} is not linear. Cundari and Drago[25] have tried to answer questions about the

mechanism of alcohol oxidation by ruthenium-oxo catalysts by performing a molecular orbital analysis. While their calculations were for a Ru^{IV}=O catalyst oxidizing methanol, and thus not directly applicable here, the insights into the preferred geometry of catalyst and substrate could be useful when contemplating the mechanism of alcohol oxidation by Ru^{V}=O catalysts too. Cundari and Drago studied three different geometries of catalyst/substrate interaction, all of which are pictured in Figure 4.13. The "perpendicular" approach (Figure 4.13A) was found to be the worst, there being repulsion between substrate and catalyst at all distances. Having the substrate's C-H bond approach the ruthenium-oxo bond "end-to-end" is a better scenario (Figure 4.13B): while there is a repulsion maximum at r = 1.4 Å, an energy minimum occurs at r = 1.2 Å. So if the substrate approaches the catalyst with enough energy to traverse the maximum, it will fall into an energy minimum were there is a favorable interaction between the ruthenium-oxo and the α-proton of the alcohol. The best geometry is actually the seven-coordinate "cyclic" species (Figure 4.13C). In this case, there is no energy barrier to overcome; the catalyst/alcohol complex simply gets stronger as the two species approach until the seven-coordinate intermediate is formed. While none of these calculations are valid for d^3 Ru^{V}=O catalysts, they do point out the importance that the geometry of the intermediate may have on the reaction kinetics. If the Ru^{V}=O/alcohol intermediate was to prefer the seven-coordinate geometry, or one similar, the reactivities of the catalysts in Table 4.3 and that of Ru-HPA could be rationalized. The catalyst which reacts the quickest is the one which has a small ligand (a chloride ion) *cis* to the oxo group, thus leaving plenty of space into which the seventh ligand can go. More rigid ligands, like the tetramethylcyclam macrocycle, not only force the smaller ligands into a *trans* geometry, but are also less likely to want to deform to allow a seventh ligand to be incorporated into the ruthenium center. This would perhaps force the reaction to proceed through a higher energy intermediate, such as the "end-to-end" species, and thus slow the reaction down

Figure 4.13 Various proposed[25] geometries for the initial ruthenium-oxo/methanol intermediate. A) The "perpendicular" approach. B) The "end-to-end" geometry. C) The "cyclic" seven-coordinate species.

A)

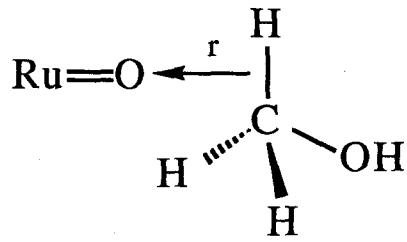

B)

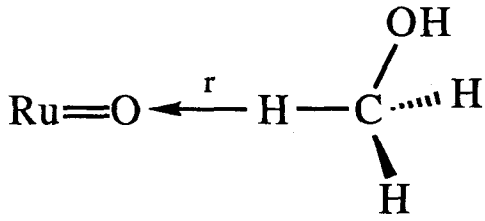

C)

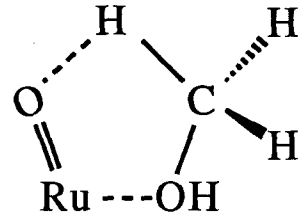

considerably. The polyoxotungstate cage would be even worse since it occupies 5/6^{ths} of the coordination sphere around the ruthenium center and is unlikely to permit a seventh ligand to bind to the metal due to steric hindrance problems with the tungsten-oxo groups nearby. Besides the possible problems in achieving the desired intermediate, there are several other reasons which could be to blame for the slow reaction kinetics. For example, if the anionic charge of the five oxides which link the metal center to the cage provides too much stabilization of the high-valent ruthenium species, the compound will not be very active. A delicate balance must be struck between metal and ligand so that the catalyst is unstable enough to want to react with the substrate presented to it, but not so reactive that it spontaneously decomposes before performing the desired oxidation. This might at least explain why the Ru-HPA reacts with alcohols about five times slower than the Ru^V catalysts studied by Wong and Che.[22,24,26-28] These catalysts are all surrounded by ligands which are either neutral or only have a 1- charge, so the Ru^V=O state has much less negative charge to balance it, and should be more likely to want to reduce its charge by reacting with the substrate than the Ru^V=O in the heteropolytungstate cage. Of course, the Ru-HPA is also the weakest oxidant of all the catalysts in Table 4.3, so it would be expected to have the smallest catalytic rate constant if all other factors were constant. But these are fairly subtle differences; the main conclusion that can be drawn from the catalytic study performed here and the ones listed in Table 4.3 is that oxoruthenium (V) catalysts are surprisingly unreactive toward organic substrates. Griffith[29] points out that not only are his Ru^V=O complexes containing α-hydroxy carboxylic acid ligands unreactive, but the same is true of the corresponding oxochromium (V) species. Obviously, a highly-oxidized metal center is not going to be much of a reactive site for catalysis if the surrounding ligand(s) prevent the proper catalyst/substrate interaction from occurring. It appears that most of the oxoruthenium (V) catalysts bound to multidentate macrocyclic ligands, such as tetramethylcyclam or the

heteropolytungstate anion, studied so far have failed this key requirement, and thus are weak catalysts even for easily oxidized substrates like benzyl alcohol.

Failure to achieve a highly reactive catalyst for benzyl alcohol oxidation only means that primary and secondary alcohols have even less of a chance of being rapidly oxidized by Ru-HPA. Indeed, the kinetic data compiled here indicate that Ru-HPA follows the normal[12b,22] trend in that the rate of alcohol oxidation goes as methyl < primary < secondary < benzylic, with tertiary alcohols generally being totally unreactive. This is a measure of the relative acidity of the α-protons of the alcohol; the more acidic the proton, the easier it is for the catalyst to break the C-H bond which initiates the oxidation of the alcohol. Thus it is disappointing, but not too surprising, that the alcohols that have real usefulness in providing electrical energy through a fuel cell (methanol and 2-propanol) react too slowly to be efficient (about 10^{-1} and 10 M^{-1} s^{-1} respectively).

4.4.2 Catalysis of the Oxidation of Non-alcoholic Substrates

The inability of Ru-HPA to enhance significantly the rate of oxidation of alcoholic substrates led to the investigation of other types of compounds as possible reactants. In an attempt to learn more about the nature of the product of the reaction of Ru^{V}-HPA with alcohols, we tested the catalyst for activity in oxidizing aldehydes such as benzaldehyde and formaldehyde. Previous oxoruthenium (V) catalysts[22,24,26-29] were all found to oxidize primary and benzylic alcohols exclusively to aldehydes, and it seems that Ru^{V}-HPA is no different as it displays little activity towards aldehyde oxidation. It is not unusual, then, that Ru-HPA exhibited even less activity when the substrate was the formate ion. In this case, no catalytic current was observed at either the Ru^{IV} or Ru^{V} potentials.

Our study was not confined to organic substrates; it included several inorganic species which were used to probe both the oxidative and reductive powers of the ruthenium-substituted heteropolytungstate anion. The oxalate anion is an interesting

compound to investigate. It can be considered the "dimer" of the formate ion, and is occasionally an important intermediate in the catalytic reduction of carbon dioxide.[30] But cyclic voltammetric data (Figure 4.8) indicate that the catalytic oxidation of oxalate by Ru^{V}-HPA, if it truly occurs, is not only slow but also proceeds at a potential which is hardly more negative than the oxidation of oxalate directly at the bare EPG electrode. The Ru^{V}=O group in the polyoxotungstate cage apparently has as much difficulty oxidizing a C-C bond as it does a C-H bond, even though this should involve a simpler (i.e., no proton transfer involved) mechanism. There is some precedent for choosing hydrazine as the next substrate, as there is a report[31] that it reacts with $[(Et_2COCO_2)_2Cr^{V}=O]^-$, but unfortunately the oxidation of hydrazine by Ru-HPA suffers from the same problems as oxalate, except that the reaction occurs at the Ru^{IV} wave instead of the Ru^{V} potential. But even at low concentrations of hydrazine where the direct oxidation of substrate at the electrode does not obscure the catalyzed reaction (Figure 4.9), the catalytic current observed is only a fraction of the uncatalyzed peak current, an observation that is indicative of a very slow catalytic reaction.

The next two substrates studied, sodium nitrite and hydrogen peroxide, offered some unique catalytic opportunities. Not only were both used in the previous work in the Anson group[9-11] in which the iron-substituted heteropolytungstate was employed as a reduction catalyst, but these substrates also offer the possibility of either being oxidized or reduced by the Ru-HPA. Sodium nitrite was the substrate which really demonstrated the usefulness of transition metal-substituted heteropolytungstates as catalysts.[10] By taking advantage of the ability of the cage to store multiple electrons, the full power of the Fe-HPA as a multielectron catalyst was shown. Although Ru-HPA appears to have some activity towards the reduction of nitrite, it is much less pronounced than the iron-based species. This is most likely due to the non-lability of the aquo group bound to the sixth ligand site of the ruthenium center compared to the iron catalyst. If the initial step

in the catalytic cycle of the Ru-HPA/nitrite system is the same as the iron mechanism (reaction 5),[10] then we would expect the ruthenium catalyst to react slower than the iron

$$2\ (H_2O)Fe^{II}\text{-HPA} + NO_2^- + 2H^+ \longrightarrow (ON)Fe^{II}\text{-HPA} + Fe^{III}\text{-HPA} + 2\ H_2O \quad (5)$$

catalyst, even though they are nearly equal in strength as reductants, because of the very slow dissociation of the water molecule bound to the ruthenium center (see Section 2.4.3). Unlike earlier inorganic substrates, nitrite is oxidized by Ru-HPA at a potential about 50 mV negative of the direct oxidation at the EPG electrode. The likelihood that this separation is sufficient to observe a clean plateau current in a RDE experiment is moot; the procedure was not even attempted because the catalytic current is small enough that further kinetic analysis seemed unwarranted.

Catalytic reduction of hydrogen peroxide by Ru-HPA is not as clear as for sodium nitrite. The mechanism for hydrogen peroxide reduction by Fe-HPA is thought to proceed through a combination of several different pathways.[9] One possible way is simply to go the same way as nitrite (reactions 6 and 7). The hydroxide radical is then

$$(H_2O)Fe^{II}\text{-HPA} + H_2O_2 \longrightarrow (H_2O_2)Fe^{II}\text{-HPA} + H_2O \quad (6)$$

$$(H_2O_2)Fe^{II}\text{-HPA} \longrightarrow (HO)Fe^{III}\text{-HPA} + \cdot OH \quad (7)$$

either reduced by another Fe^{II}-HPA and then protonated to give water, or abstracts a hydrogen atom from $PFe^{II}(OH_2)W_{11}O_{39}^{5-}$, and the catalyst then undergoes an intramolecular electron transfer followed by a protonation step to regenerate the aquoiron (III) species. It was also proposed that the hydroxyl radical could attack unreduced catalyst so as to produce an oxoiron (IV) species and regenerate starting material (reactions 8 and 9). This pathway was employed to account for the fact that the bulk

$$(H_2O)Fe^{III}\text{-HPA} + \cdot OH \longrightarrow O{=}Fe^{IV}\text{-HPA} + H_2O + H^+ \quad (8)$$

$$O{=}Fe^{IV}\text{-HPA} + H_2O_2 + H^+ \longrightarrow (H_2O)Fe^{III}\text{-HPA} + \cdot O_2H \longrightarrow H_2O_2 \quad (9)$$

electrolyses of hydrogen peroxide in the presence of Fe-HPA often consumed significantly less than the theoretical value of 2.0 electrons per H_2O_2 molecule. If

reactions (6) and (7) tend to dominate (8) and (9), then Ru-HPA is going to react more slowly than the iron heteropolyanion, just as in the nitrite experiments. Again, the slow dissociation of the initial ligand on the ruthenium center will prevent the catalysis from occurring at as high a rate as the iron did (900 M^{-1} s^{-1}).[9]

It is not too surprising that hydrogen showed no evidence of being oxidized by Ru-HPA. Hydrogen is kinetically inert and generally not reactive unless a proper catalyst is used.[32] The Ru-HPA catalyst is not well-suited for this task; the Ru=O group is of no help in this reaction; what is needed is two open coordination sites where the H_2 molecule can bind (the H_2 molecule will split either homo- or heterolytically to give two Ru-H bonds). The only way this could occur is to have two Ru^{II}-HPA molecules dissociate their bound water ligands and cooperatively attack a single hydrogen molecule. Perhaps the reaction is merely too slow to see evidence of catalysis on the timescale of the cyclic voltammetric experiment. An aqueous solution saturated with hydrogen gas only contains 0.85 mM hydrogen,[33] so unless the catalytic rate constant is extremely large, it is quite likely that no catalytic current would be observed. Sodium chlorate also appears to be inert to oxidation by our catalyst. This response is logical since the oxidation of chlorate by Ru^{V}-HPA is thermodynamically uphill [E^{o} (ClO_3^-/ClO_4^-) = 0.953 V vs. SSCE][34] by a small amount. No evidence of catalytic reduction of chlorate was observed either. Carbon monoxide is another substrate which offers the possibility of being either oxidized or reduced. The lack of catalytic current for the reduction of CO is not surprising given the difficulties encountered in reducing NO_2^- and H_2O_2. Oxidizing carbon monoxide to carbon dioxide is basically just a simple oxygen-atom transfer, a reaction at which ruthenium-oxo compounds usually excel.[5c,35-37] The only difference here is that CO is a tougher substrate to oxidize than typically tested substrates such as converting triphenylphosphine to triphenylphosphine oxide or epoxidizing an olefinic bond because the catalyst must convert a carbon-oxygen triple bond to a double

bond. Whatever the reason, Ru-HPA either has no catalytic activity towards oxidizing carbon monoxide or reacts so slowly that the catalytic current cannot be detected during the timescale of the electrochemical experiment. As with hydrogen, the reaction could be slow due to the low (~1 mM)[38] solubility of CO in aqueous solutions.

4.5 *Conclusions*

Throughout this chapter, data were presented which, when considered as a whole, indicate that the ruthenium-substituted heteropolytungstate anion $PRu^{V}(O)W_{11}O_{39}^{4-}$ is not a very good catalyst for the electrochemical oxidation of organic or inorganic substrates. Several factors most likely contribute to this unexpected inability to catalyze seemingly simple reactions. First, the anionic charge of the cage probably lends too much stability to high-valent ruthenium-oxo species, thus rendering them much less reactive than we hoped them to be. Second, the cage ties up $5/6^{ths}$ of the coordination sphere of the catalytic center, thereby severely restricting bond formation directly between ruthenium and the substrate. This is crucial, since molecular orbital calculations[25] indicate that the lowest energy intermediate in the oxidation of methanol by a Ru^{IV}=O catalyst is a seven-coordinate cyclic species. Third, steric hindrance problems around the metal may slow coordination and perhaps prevent alcohol oxidation from proceeding through the lowest energy intermediate. Depending on how far down in the lacunary ion's "hole" the ruthenium sits, its sixth coordination site may be partially shielded from the substrate in solution by the polyoxotungstate cage. Fourth, in the case of Ru-HPA acting as a reductant, the poor activity compared to the iron heteropolyanion is easily explained by the fact that the dissociation of the solvent (H_2O) molecule from Ru^{II}, which needs to occur before catalysis can begin, has been shown to be extremely slow at ambient laboratory temperature (Section 2.4.3).

Although this work lessens our enthusiasm for using ruthenium-substituted heteropolytungstate anions as catalysts, this class of compounds should not be abandoned just yet. While the chances of a mono-substituted heteropolyanion, like the one studied here, being a vigorous oxidation catalyst are very low because the substrate is prevented from directly interacting with the metal center when it is surrounding with the polyoxotungstate cage, these compounds may be useful for minor synthetic conversions, such as oxo transfers.[5c,6,35,39] A new class of transition metal-substituted heteropolyanions which has recently[40] attracted attention are multiply-substituted cage complexes. The dicopper species, $P[Cu(OH_2)]_2W_{10}O_{38}^{7-}$, has recently been synthesized.[40a] This compound has the two copper centers adjacent to one another, making it much more attractive than a single metal center catalyst. If a similar compound containing two chromium or ruthenium centers could be made, perhaps the limitations imposed by $PRu(OH_2)W_{11}O_{39}^{4-}$ could be overcome. An extremely brief attempt was made[41] to synthesize $SiRu_2W_{10}O_{38}^{6-}$, but it was not successful. However, this work was done without the knowledge that previous synthetic procedures existed,[40a] so it is possible that the problems we incurred have already been addressed. On the other hand, if this compound is similar to Ru-HPA, the synthesis may not be a straightforward extension of their work. It has been discussed here and elsewhere[5c] that the synthesis of ruthenium-substituted heteropolyanions is often quite a bit more difficult than cage complexes containing simple first row transition metals like Cu and Fe. I believe that the possibility that the disubstituted heteropolyanion (or trisubstituted analogs) could fulfill the expectations that we had for the mono-substituted Ru-HPA is strong enough that further research into this area is warranted.

References

1. Baker, L. C. W.; Baker, V. E. S.; Eriks, K.; Pope, M. T.; Shibata, M.; Rollins, O. W.; Fang, J. H.; Koh, L. L. *J. Am. Chem. Soc.* **1966,** *88,* 2329.

2. Pope, M. T. *Heteropoly and Isopoly Oxometallates*; Springer-Verlag: Berlin, 1983; p 93.

3. Weakley, T. J. R.; Malik, S. M. *J. Inorg. Nucl. Chem.* **1967,** *29,* 2935.

4. Zonnevijlle, F.; Tourné, C. M.; Tourné, G. F. *Inorg. Chem.* **1982,** *21,* 2751.

5. a) Ortéga, F.; Pope, M. T. *Ibid.* **1984,** *23,* 3292.
   b) Katsoulis, D. E.; Pope, M. T. *J. Chem. Soc., Chem. Commun.* **1986,** 1186.
   c) Rong, C.; Pope, M. T. *J. Am. Chem. Soc.* **1992,** *114,* 2932.

6. Khenkin, A. M.; Hill, C. L. *J. Am. Chem. Soc.* **1993,** *115,* 8178.

7. a) Akid, R.; Derwent, J. R. *J. Chem. Soc., Dalton Trans.* **1985,** 395.
   b) Nomiya, K.; Mizazaki, T.; Maedak, M.; Miwa, M. *Inorg. Chim. Acta* **1987,** *127,* 65.
   c) Combswalker, L. A.; Hill, C. L. *J. Am. Chem. Soc.* **1992,** *114,* 938.

8. a) Keita, B.; Nadjo, L. *J. Electroanal. Chem.* **1985,** *191,* 441.
   b) Keita, B.; Nadjo, L. *Ibid.* **1987,** *227,* 265.
   c) Keita, B.; Nadjo, L. *Ibid.* **1988,** *240,* 325.
   d) Keita, B.; Nadjo, L. *Ibid.* **1990,** *287,* 149.
   e) Keita, B.; Nadjo, L. *Electroanalysis* **1991,** *3,* 637.

9. Toth, J. E.; Melton, J. D.; Cabelli, D.; Bielski, B. H. J.; Anson, F. C. *Inorg. Chem.* **1990,** *29,* 1952.

10. Toth, J. E.; Anson, F. C. *J. Am. Chem. Soc.* **1989,** *111,* 2444.

11. Toth, J. E. Ph.D. Thesis, California Institute of Technology, 1990.

12. a) Thompson, M. S.; Meyer, T. J. *J. Am. Chem. Soc.* **1982,** *104,* 4106.
    b) Roecker, L.; Meyer, T. J. *Ibid.* **1987,** *109,* 746.
    c) Seok, W. K.; Dobson, J. C.; Meyer, T. J. *Inorg. Chem.* **1988,** *27,* 3.
    d) Seok, W. K.; Meyer, T. J. *J. Am. Chem. Soc.* **1988,** *110,* 7358.

13. a) Che, C.-M.; Wong, K.-Y. *J. Chem. Soc., Chem. Commun.* **1986,** 229.
    b) Yam, V. W.-W.; Che, C.-M.; Tang, W.-T. *Ibid.* **1988,** 100.
    c) Khan, M. M. T.; Ramachandraiah, G.; Mehta, S. H. *J. Mol. Cat.* **1989,** *50,* 123.
    d) Cundari, T. R.; Drago, R. S. *Inorg. Chem.* **1990,** *29,* 2303.
    e) Li, C.-K.; Che, C.-M.; Tong, W.-F.; Tang, W.-T.; Wong, K.-Y.; Lai, T.-F. *J. Chem. Soc., Dalton Trans.* **1992,** 2109.
    f) Dovletoglou, A.; Meyer, T. J. *J. Am. Chem. Soc.* **1994,** *116,* 215.

14. Kelson, E. P.; Henling, L. M.; Schaefer, W. P.; Labinger, J. A.; Bercaw, J. E. *Inorg. Chem.* **1993,** *32,* 2863.

15. a) Upadhyay, M. J.; Bhattacharya, P. K.; Ganeshpure, P. A. *J. Mol. Cat.* **1993,** *80,* 1.
b) Lai, Y.-K.; Wong, K.-Y. *Electrochim. Acta* **1993,** *38,* 1015.
c) Poiner, M. G.; Trudel, J.; Guay, D. *Catal. Lett.* **1993,** *21,* 99.
d) Shi, C.; Anson, F. C. *J. Electroanal. Chem.* **1994,** *362,* 273.

16. Tézé, A.; Hervé, G. *J. Inorg. Nucl. Chem.* **1977,** *39,* 999.

17. Bernhard, P.; Biner, M.; Ludi, A. *Polyhedron* **1990,** *9,* 1095.

18. Bard, A. J.; Faulkner, L. R. *Electrochemical Methods*; J. Wiley and Sons: New York, 1980; p 469.

19. Ref. 18, p 288.

20. Ref. 18, p 468.

21. Galus, Z. *Fundamentals of Electrochemical Analysis*; Reynolds, G. F., translation ed.; Ellis Horwood Limited: Chichester, England, 1976; p 325.

22. Che, C.-M.; Tang, W.-T.; Lee, W.-O.; Wong, K.-Y.; Lau, T.-C. *J. Chem. Soc., Dalton Trans.* **1992,** 1551.

23. Griffith, W. P. *Chem. Soc. Rev.* **1992,** *21,* 179.

24. Li, C.-K.; Tang, W.-T.; Che, C.-M.; Wong, K.-Y.; Wang, R.-J.; Mak, T. C. W. *J. Chem. Soc., Dalton Trans.* **1991,** 1909.

25. Cundari, T. R.; Drago, R. S. *Inorg. Chem.* **1990,** *29,* 3904.

26. Che, C.-M.; Ho, C.; Lau, T.-C. *J. Chem. Soc., Dalton Trans.* **1991,** 1259.

27. Wong, K.-Y.; Yam, V. W.-W.; Lee, W. W.-S. *Electrochim. Acta* **1992,** *37,* 2645.

28. Wong, K.-Y.; Che, C.-M.; Anson, F. C. *Inorg. Chem.* **1987,** *26,* 737.

29. a) Dengel, A. C.; Griffith, W. P.; O'Mahoney, C. A.; Williams, D. J. *J. Chem. Soc., Chem. Commun.* **1989,** 1720.
b) Dengel, A. C.; Griffith, W. P. *Inorg. Chem.* **1991,** *30,* 869.

30. *Electrochemical and Electrocatalytic Reactions of Carbon Dioxide*; Sullivan, B. P.; Krist, K.; Guard, H. E., eds.; Elsevier: Amsterdam, 1993.

31. Gould, E. S. *Acc. Chem. Res.* **1986,** *19,* 66.

32. Collman, J. P.; Wagenknecht, P. S.; Hutchison, J. E.; Lewis, N. S.; Lopez, M. A.; Guilard, R.; L'Her, M.; Bothner-By, A. A.; Mishra, P. K. *J. Am. Chem. Soc.* **1992,** *114,* 5654.

33. *Handbook of Chemistry and Physics*, 64th ed.; Weast, R. C., ed.; CRC Press, Inc.: Boca Raton, 1984; p B-96.

34. Ref. 33, p D-157.

35. Neumann, R.; Abu-Gnim, C. *J. Am. Chem. Soc.* **1990,** *112,* 6025.

36. Steckhan, E.; Kandria, C. *Synlett.* **1992,** 139.

37. Perrier, S.; Kochi, J. K. *Inorg. Chem.* **1988,** *27,* 4165.

38. Ref. 33, p B-82.

39. Mizuno, N.; Tateishi, M.; Hirose, T.; Iwamoto, M. *Chem. Lett.* **1993,** 1839.

40. a) Gomezgarcia, C. J.; Coronado, E.; Gomezromero, P.; Casanpastor, N. *Inorg. Chem.* **1993,** *32,* 89.
b) Mizuno, N.; Tateishi, M.; Hirose, T.; Iwamoto, M. *Chem. Lett.* **1993,** 2137.
c) Mizuno, N.; Tateishi, M.; Hirose, T.; Iwamoto, M. *J. Mol. Cat.* **1994,** *88,* L135.

41. Bart, J. C.; Anson, F. C., unpublished results.

42. Muller, J. G.; Acquaye, J. H.; Takeuchi, K. J. *Inorg. Chem.* **1992,** *31,* 4552.

43. Che, C.-M.; Ho, C.; Lau, T.-C. *J. Chem. Soc., Dalton Trans.* **1991,** 1901.

44. Che, C.-M.; Leung, W.-H.; Li, C.-K.; Poon, C.-K. *Ibid.* **1991,** 379.

Table 4.1 RDE data for the catalysis of various amounts of benzyl alcohol by 0.30 mM $Cs_4PRu(OH_2)W_{11}O_{39}$ in pH = 4.0, 0.2 M lithium acetate buffer. Plateau currents were sampled at E = +1.0 V vs. SSCE.

	Plateau current of $Ru^{V/IV}$ wave in μA						
$\omega^{1/2}$ ($rpm^{1/2}$)	0 mM ROH	2.9 mM ROH	5.9 mM[a] ROH	8.7 mM ROH	12 mM[a] ROH	15 mM ROH	18 mM ROH
4	4.82	8.48	16.7	15.3	19.4	20.7	22.1
5	5.48	8.77	17.5	15.5	19.8	21.1	22.5
6	6.03	9.00	17.5	15.8	20.3	21.4	22.7
7	6.72	9.39	18.3	15.9	20.5	21.7	23.0
8	7.29	9.79	18.8	16.4	20.4	22.1	23.3
9	8.06	10.2	19.3	16.6	21.3	22.4	23.5
10	8.64	10.8	19.7	17.1	21.5	23.0	23.9
11	9.54	11.2	20.5	17.5	22.0	23.4	24.3
12	10.2	11.8	21.4	18.0	22.5	24.0	24.6
15	12.1	13.0	23.0	19.2	23.7	25.0	25.6
20	15.2	15.1	25.8	21.3	26.3	27.1	28.0
30	20.3	19.3	31.6	25.5	31.5	31.8	32.7

a. Data collected on a different day than other entries. All these currents were normalized to be comparable to the others.

Figure 4.2 RDE data for the catalysis of various amounts of methanol by 0.30 mM $Cs_4PRu(OH_2)W_{11}O_{39}$ in a pH = 4.0, 0.2 M lithium acetate buffer. The plateau currents were measured at E = 1.0 V vs. SSCE.

	Plateau current for the $Ru^{V/IV}$ wave in μA				
$\omega^{1/2}$, $rpm^{1/2}$	0 mM ROH	23 mM ROH	41 mM ROH	0.1 M ROH	0.2 M ROH
4	4.60	4.53	4.75	5.43	6.15
5	5.05	5.53	5.65	6.28	6.42
6	5.82	6.16	6.20	6.81	6.84
7	6.34	6.92	6.79	7.40	7.42
8	7.02	7.67	7.41	8.03	8.09
9	7.82	8.18	8.00	8.62	8.64
10	8.48	8.88	8.62	9.23	9.28
11	9.10	9.57	9.30	9.94	9.93
12	9.78	10.2	10.0	10.6	10.6
15	11.7	12.1	11.8	12.4	12.2
20	14.3	15.2	14.6	15.1	15.0
30	19.6	20.9	19.6	20.1	20.3

Figure 4.3 The rate of benzyl alcohol oxidation by various mono- and dioxoruthenium catalysts.

Catalyst	Conditions	E vs. SSCE	k, M^{-1} s^{-1}	reference
$(L_1)_2L_2Ru^{IV}=O$	0.1 M H^+	0.88 V	2.43	12b
$(L_1)_2L_3Ru^{IV}=O$	pH=2 $NaNO_3$	1.05 V	0.58	42
$L_4L_5Ru^{IV}=O$	0.1 M H^+	1.12 V	2.23	43
$L_6Ru^{V}=O$	pH=4 LiAc	0.97 V	170	27
$L_6Ru^{V}=O$	0.1 M H^+	0.97 V	117	26
$L_7(Cl)Ru^{V}=O$	Acetonitrile	1.36 V	210	28
$L_7L_8Ru^{V}=O$	Acetonitrile	1.20 V	140	28
$L_xRu^{V}=O$	0.1 M H^+	1.00 V	120	24
$L_9(Cl)Ru^{V}=O$	0.1 M H^+	1.29 V	8.4×10^4	24
Ru^{V}-HPA	pH=4 LiAc	0.86 V	31	(this work)
$L_7Ru^{VI}(=O)_2$	0.1 M H^+	0.66 V	2.0×10^{-4}	22
$L_{10}Ru^{VI}(=O)_2$	0.1 M H^+	0.76 V	3.3×10^{-3}	22
$L_{11}Ru^{VI}(=O)_2$	0.1 M H^+	0.89 V	0.93	22
$L_{12}Ru^{VI}(=O)_2$	0.1 M H^+	0.92 V	0.69	22
$(L_o)_2Ru^{VI}(=O)_2$	0.1 M H^+	1.00 V	3.6	44
$(L_1)_2Ru^{VI}(=O)_2$	0.1 M H^+	1.01 V	20.8	22

L_1 = bipyridine
L_2 = pyridine
L_3 = triphenylphosphine
L_4 = terpyridine
L_5 = 6,6'-dichlorobipyridine
L_6 = bis(2-(2-pyridyl)ethyl)(2-hydroxy-2-(2-pyridyl)ethyl)amine
L_7 = tetramethylcyclam
L_8 = cyanate
L_x = (Unknown. Ligand not described in reference.)
L_9 = N,N'-dimethyl-N,N'-bis(2-pyridylmethyl)ethylenediamine
L_{10} = *meso*-2,3,7,11,12-pentamethyl-3,7,11,17-tetraazabicyclo[11.3.1]heptadeca-1(17),13,15-triene
L_{11} = N,N'-dimethyl-N,N'-bis(2-pyridylmethyl)propylenediamine
L_{12} = N.N'-dimethyl-6,7,8,9,10,11,17,18-octahydro-5*H*-dibenzo[*en*][1,4,8,12]-dioxadiazacyclopentadecine
L_o = 5,5'-dimethylbipyridine